INFLUENCE OF MOISTURE ON BOND STRENGTH OF ASPHALT-AGGREGATE SYSTEMS

By

Audrey R. Copeland

Dissertation

Submitted to the Faculty of the

Graduate School of Vanderbilt University

in partial fulfillment of the requirements for

the degree of

DOCTOR OF PHILOSOPHY

in

Civil Engineering

August, 2007

Nashville, Tennessee

Approved:

Professor Sankaran Mahadevan

Professor Prodyot K. Basu

Professor Sanjiv Gokhale

Professor Florence Sanchez

Professor Robert Stammer, Jr.

Dr. Jack Youtcheff

DEDICATION

To my parents, Terry and Glenda, and my brother Scott.

This body of work is also dedicated to the mentors in my life.
A little guidance goes a long way – thank you.

ACKNOWLEDGEMENTS

I would first like to thank my advisor, Dr. Sankaran Mahadevan, for his insight and guidance throughout my PhD journey. I would also like to express gratitude for my advisor at Federal Highway Administration (FHWA), Dr. Jack Youtcheff, for giving me the freedom to choose my path in the many roads of moisture damage research and supporting my decisions. A very special thank you to my committee members: Dr. Prodyot K. Basu, Dr. Sanjiv Gokhale, Dr. Florence Sanchez, and Dr. Robert Stammer, Jr. I appreciate your insight into the research process and helpful suggestions.

This research project was made possible through an Eisenhower Transportation Fellowship provided by FHWA and administered by the National Highway Institute. Being an Eisenhower Fellow has been a rare opportunity for which I am most appreciative, and the experience I have gained as a result is invaluable. Funding for my first two years as a PhD student was provided by the National Science Foundation Integrative Graduate Education and Research Traineeship (NSF IGERT) Program. I am especially grateful for this fellowship because it allowed me to quickly complete my coursework so I could concentrate on my research. Additional funding was provided by an IBM Fellowship through the Vanderbilt University School of Engineering and by the Association of Asphalt Paving Technologist (AAPT) Scholarship. I was also fortunate to receive a Vanderbilt University Graduate Student Travel Grant in addition to travel funding through the Eisenhower Fellowship; these resources allowed me to present my research at multiple international and national conferences.

I would like to acknowledge the professors and office staff at Vanderbilt University's Department of Civil and Environmental Engineering. Karen Page has been especially helpful in taking care of administrative needs and always providing me with a laugh. I would also like to thank Dr. Mark Abkowitz and Dr. Florence Sanchez, in particular, for your guidance in my quest to find a research project. I had the pleasure of forming meaningful friendships while at Vanderbilt and I would like to thank the following fellow IGERT and graduate students for their friendship: Sarynna Lopez, Ned Mitchell, Marcus Knight, Candice Griffith, Robert Guratzsch, Ramesh Rebba, and Natasha Smith.

At FHWA, I would like to express my sincere appreciation to the Pavement Materials and Construction Team at Turner Fairbank Highway Research Center (TFHRC). A very special thank you goes to Susan Needham for conducting dynamic shear rheometer experiments and Jenny Rozario for conducting pull-off tests that provided the data for Chapter III of this dissertation. Jenny has been especially supportive throughout my PhD for which I am grateful. A special thanks to Jussara Ramadan and Dr. Haleh Azari for being so kind to me and dear friends. Very special thanks to Terry Arnold; I have learned so much from you in the laboratory and commonsense wise that I bestow a quarter (or was it half?) of this dissertation to you. I would also like to thank Dr. Ernest Bastian and Dr. Aroon Shenoy; without their insight and assistance this dissertation would not be possible. I would like to thank the following individuals for their help in various aspects of this research project: Dr. Clay Ormsby, Rick Meininger, Dr. Rong Tang Liu, Kevin Connor, David Hatchett, Bill Webb, Frank Davis, Scott Parobeck, and Jianming Wei. I would also like to acknowledge the guidance

provided by Kevin Stuart in regards to moisture-induced damage research conducted at TFHRC and nationally.

A very special thank you goes to Tom Harman for supporting this project and for providing me the opportunity to speak at the Asphalt Binder Expert Task Group meeting. Your guidance in my professional career and life has been invaluable; thank you for always looking out for me. I would also like to thank Dr. Cheryl Richter for her advice and mentoring, especially during my oral defense preparations and while I was evaluating career options. Thank you to Katherine Petros for encouragement throughout my time at TFHRC.

I am very fortunate to have had the opportunity to collaborate with Dr. Tom Scarpas and Dr. Niki Kringos of Delft University of Technology (TU Delft). This project would not have been possible without the leadership of Dr. Scarpas. Your suggestions and support took this project to new heights and gave it international scope. I am most appreciative of the opportunity to spend time with the Structural Mechanics group at TU Delft. I also want to thank Niki for her immense help writing papers and who, ultimately, has become a cherished friend.

I would also like to thank the following colleagues and officemates at TFHRC for helping me keep my sanity during this time by making me coffee after late study nights, going out for lunch, and most of all, making me laugh: Mike Scott, Eric Weaver, Tom Stabile, Satish Belagutti, and Raghu Satyanarayana. I would like to especially thank Raj Dongre for making me feel at home at TFHRC from the beginning and posing thought-provoking questions regarding moisture damage research. A very special thank you goes to Mike Adams for challenging me in the gym. Your commitment to being active every

day is motivating and I doubt you realize how much your presence in the gym each afternoon meant to me.

In addition to the professional support network, there are also special close friends in my life that have found their way into my heart and have supported me through this process: Megan Woody, Terra Baranowski, Krissy Shepherd, Maureen Pratt, and Christine Rath. A very special thank you to Heather Weger; we have experienced this marathon called dissertation side by side and I couldn't ask for a better, more supportive friend as I reach the finish line.

Last, but certainly not least, I am most grateful for my family. I have exceptional grandparents: Glen and Margie Wilson and Marie Copeland. Thank you for your kind words of encouragement and supporting me as I chose what may have seemed an unconventional path. Finally, I would like to thank my parents for their unending support. I am still amazed at your selflessness in raising me to become the individual that I am. This effort and dissertation is a direct result of your commitment to being the best parents possible.

TABLE OF CONTENTS

Page

LIST OF TABLES

Page

Page

Page

LIST OF FIGURES

Page

Page

Page

Page

CHAPTER I

INTRODUCTION

1.1 Perspective and Background

There are two million miles of paved roadways in the United States (NCHRP 2004) and Hot Mix Asphalt (HMA) is used on approximately ninety-six percent of all paved surfaces. Over time, our existing highway system has been taxed due to an increased level of demand. According to the American Society of Civil Engineers (ASCE) Infrastructure Report Card (2005), the nation's highways experienced 2.85 trillion vehicle-miles in 2002. This is over four times the level of vehicle miles in 1960 and truck travel alone has increased by 231 percent since 1970 (NCHRP 2004). Due to increased demand from additional and heavier traffic loads, lack of resources for additional roadways, and user expectations regarding safety, HMA pavements must perform well for longer periods of time, especially in light of budget shortfalls to cover estimated costs for necessary development.

According to the National Cooperative Highway Research Program (NCHRP) Guide for Mechanistic-Empirical Design for New and Rehabilitated Pavement Structures (2004), the total expenditure by State highway agencies was $89.8 billion in 2000. About ten (10.5) percent was disbursed to new highway construction and over forty (42.6) percent went toward improvements of existing roadways (NCHRP 2004). However, in 1999 the capital investment by all levels of government was $59.4 billion for roads, which was well below the estimated $94 billion needed to improve the nation's

transportation infrastructure (ASCE 2005). The highways contribute to the economic growth of the nation and require a substantial investment and commitment of resources to construct and maintain. The reliable performance of HMA pavements is critical to the nation's infrastructure and economy in reducing the cost of maintaining roadways.

1.2 Problem Statement

A typical HMA pavement consists of several layers, as shown in Figure 1. Two of the most important layers are the top two layers; the wearing surface and intermediate, load bearing layer. Both of these layers utilize asphalt binder to bind aggregate together for a mixture that sustains applied loads and maintains durability. A critical property of the asphalt binder is its ability to bond to the mineral aggregate and maintain this bond (i.e. durability). Properties of this bond, however, are not well-understood. The bond may degrade at the interface between asphalt and aggregate (loss of adhesion) or within the asphalt binder (loss of cohesion) due to loading and environmental conditions.

Moisture is the major environmental condition that adversely affects asphalt concrete quality and primarily results in bond strength degradation. Moisture-induced damage within HMA pavements is a national issue that decreases the lifespan of the nation's highways (St. Martin, et al. 2003). Moisture damage is caused by distress mechanisms induced by the presence or infiltration of moisture and manifests itself in a phenomenon referred to as stripping, where the asphalt binder is "stripped" from the aggregate. In 2002, a survey of state highway agencies, Federal Highway Administration (FHWA) federal lands offices, and selected Canadian provinces revealed that forty-five out of fifty-five agencies responding acknowledged a moisture-related problem in their

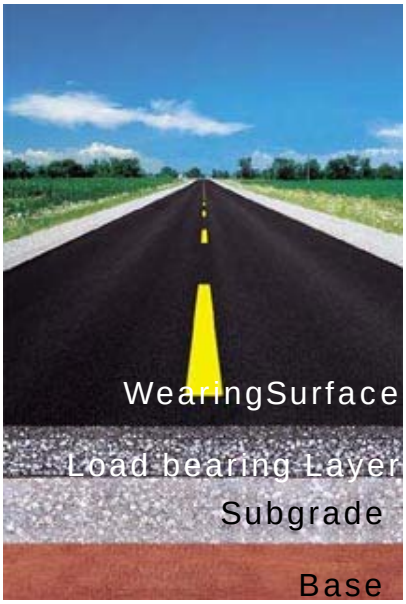

Figure 1. Layers of Asphalt Road ("Anatomy of a Road")

HMA pavements (Hicks, et al. 2003). Of the fifty-five agencies, eighty-seven percent test HMA mixtures for moisture sensitivity.

The test method specified by most State Departments of Transportation (DOTs) and adopted in the Superpave® volumetric mixture design system is outlined in the American Association of State Highway and Transportation Officials (AASHTO) document T 283 *Resistance of Compacted Asphalt Mixtures to Moisture-Induced Damage*. This test method expresses a compacted asphalt mixture's sensitivity to moisture as the ratio of moisture-conditioned strength to dry strength expressed as a numerical index. The use of a numerical index does not predict the likelihood of moisture-induced damage; rather the index heuristically provides a deterministic indication of moisture sensitivity. Also, AASHTO T 283 captures several behaviors in one test method creating difficulty in distinguishing the actual mechanism (i.e. loss of

cohesion within binder or loss of adhesion between asphalt and aggregate) that contribute to moisture damage. This highlights the need for experimental methods that can evaluate the asphalt mixture components and analysis procedures that reliably predict performance expectations under varying moisture-conditioning scenarios.

Past research and practice has shown that empirical tests alone do not accurately predict performance. A systematic method, utilizing empirical test methods as well as computational models, is needed to predict the onset and progress of moisture damage in asphalt mixtures. The durability of an asphalt mixture is compromised when the stresses imparted due to moisture combined with traffic loading exceed the strength of the bond between asphalt and aggregate. A critical parameter is knowledge of the bond strength of asphalt binder, mastic, and between asphalt and aggregate and the loss of bond strength in the presence of water. A test procedure called the pull-off test method used in the coatings industry is modified and pursued in this study to measure the tensile bond strength properties of asphalt materials and evaluate the effect of moisture conditioning on bond strength. There is limited research on the use of the pull-off test in the asphalt industry; however the modified pull-off test method has potential for routine use to evaluate bond strength characteristics of asphalt materials.

1.3 Objectives

The FHWA Office of Research and Development has established two overarching objectives to address moisture damage in asphalt mixtures:

- Advance understanding of the fundamental mechanisms of moisture damage, and

- Develop test procedures and models that enable prediction of moisture damage in asphalt mixtures.

The study in this dissertation is intended to address the second objective and provide insight for the first objective. The research pursues the following objectives:

1. Determine feasibility of the modified pull-off method as a test procedure to measure bond strength of asphalt materials and analyze effect of moisture conditioning on bond strength of asphalt materials.
2. Illustrate how bond strength measurements from the test procedure in objective one may be correlated to a model that simulates moisture transport processes to quantify moisture induced-damage in asphalt-aggregate mixtures.
3. Use the damage parameter developed in objective 2 to introduce the concept of a risk-based framework to address moisture-induced damage in design of asphalt mixtures and outline the procedure for a reliability analysis method to quantify damage between asphalt and aggregate as a result of moisture.

1.4 Research Approach

There are three major components of this dissertation research: (i) analysis of bond strength of asphalt materials and effect of moisture on bond strength, and (ii) development of the moisture-induced damage parameter identified in (i) using a combined experimental-numerical model, and (iii) conceptual development of a risk assessment framework and development of specific performance criterion related to moisture-induced damage in asphalt mixtures.

The following tasks were completed to address each component which in turn addresses a specific objective:

(i) analysis of factors influencing the bond strength of asphalt binder and mastic to determine usefulness of the modified pull-off test method to measure bond strength of asphalt binders and mastics;

(ii) use of the modified pull-off test to evaluate bond strength and influence of moisture on bond strength between asphalt and aggregate;

(iii) development of a damage parameter that quantifies loss of bond strength (i.e. damage) at asphalt-aggregate interface as a function of moisture content at the mastic-aggregate interface.

(iv) development of a risk assessment framework and application of reliability analysis concepts to predict moisture-induced damage at mastic-aggregate interface;

The materials used in this study include both binders and aggregates used in highway construction applications. Specific materials are from the Strategic Highway Research Program (SHRP) Materials Reference Library (MRL) (Jones 1993, Robl, et al. 1991) and the FHWA polymer-modified binder study (Stuart and Mogawer 2002, Stuart, et al. 2002, Stuart and Youtcheff 2002). These materials were chosen because of their availability, their use in previous research studies, and their relevance to projects in the United States.

1.5 Dissertation Structure

This dissertation is organized into eight chapters. Chapter I provides background information on the need for durable asphalt mixtures, the research objectives and approach and dissertation structure. Chapter II is a literature review that defines moisture damage and reviews the processes that lead to moisture damage. The most common test methods to evaluate moisture susceptibility of compacted asphalt mixtures are discussed and a test method to measure bond strength at the asphalt-aggregate interface is introduced. Available moisture damage models are identified and the most promising computational model (Kringos and Scarpas 2005a, Kringos and Scarpas 2005b) developed at Delft University of Technology (TU Delft) that simulates moisture-induced damage in an asphalt mixture is discussed.

Chapter III presents an in-depth statistical analysis of pull-off test results on polymer-modified asphalt binders and mastics. The effect of mineral filler, moisture conditioning and aging is evaluated. The ability of the pull-off test to rank binders and mastics according to their resistance to moisture-induced damage is determined. Chapter IV utilizes the modified pull-off test to study the effect of moisture and aggregate on the development and degradation of bond strength. The influence of aggregate type combined with moisture conditioning is considered. Chapter V evaluates bond strength at the asphalt-aggregate interface as a function of moisture content obtained from diffusion simulations performed by TU Delft. From this combination of experimental and numerical results, a moisture-induced damage parameter is developed.

Chapter VI introduces the concept of a risk assessment framework to address moisture susceptibility of asphalt mixtures. A performance criterion is identified which

can be used in a reliability analysis to determine the probability of damage at the asphalt-aggregate interface. In addition, system reliability analysis concepts are introduced for the evaluation of multiple failure modes due to moisture-induced damage.

Finally, Chapter VII concludes the dissertation by providing a concise summary of results and conclusions, the significance and applications of the research and identifies future work. Appendix A provides the data for Chapter III and Appendix B provides data for Chapter IV. Appendix C provides a modified procedure for the pull-off test method based on the standard method (ASTM 1995) for the pull-off test.

CHAPTER II

LITERATURE REVIEW

2.1 Introduction

This chapter provides a literature review on moisture damage in HMA, the processes contributing to moisture damage and efforts to mitigate and predict moisture damage in asphalt mixtures. The objectives of this chapter are to:

1. Define moisture damage and identify the two primary failure modes related to moisture damage,
2. Review state-of-the-practice in determining moisture susceptibility of asphalt mixtures,
3. Discuss previous research and theory for the measurement of bond strength of asphalt materials, and
4. Reference the TU Delft model for simulating damage due to moisture and introduce reliability engineering concepts that can be utilized to predict moisture-induced damage at the asphalt-aggregate interface.

2.2 Asphalt Mixture Terminology

Pavements designed using HMA are referred to as flexible pavements and HMA is classified as a bituminous mixture. HMA consists mainly of aggregate (approximately eighty-five percent by volume), asphalt binder, additives, and air. According to the American Society of Testing and Materials (ASTM) Designation D 8, *Standard*

Terminology Relating to Materials for Roads and Pavements (1997), bitumen is defined as a class of black or dark-colored cementitious substances, natural or manufactured, composed principally of high molecular weight hydrocarbons. Asphalt is a dark brown to black cementitious material in which the predominating constituents are bitumen that occur in nature or are obtained in petroleum processing (ASTM 1997).

Bituminous mixture is a general term for *asphalt mixture* and they are used interchangeably. The top wearing surface and the load bearing layer of a flexible pavement are constructed with compacted asphalt mixture. Asphalt *binder* describes the principal binding agent in HMA and includes the asphalt cement and any added materials used to modify the original asphalt properties (i.e. modifiers). *Aggregate* is the general term for granular material of mineral composition such as sand, gravel and crushed stone. Aggregate can be classified as coarse or fine. The term *mastic* represents the combination of asphalt binder and mineral fillers (e.g. fine aggregate and/or hydrated lime).

2.3 Definition of Moisture Damage

Asphalt pavement failures are typically classified as stability (load) or durability related failures. Moisture damage is signified by loss of strength or durability in an asphalt pavement due to the effects of moisture and may be measured by the asphalt mixture's loss of mechanical properties (Little and Jones 2003). The integrity of an asphalt concrete pavement depends on the bond between aggregate and asphalt cement. Moisture in the form of liquid or vapor can degrade this bond and lead to the first stage of failure which is deterioration of the asphalt-aggregate bond or "stripping" followed by the

second stage which is premature failure of the pavement structure. Kiggundu and Roberts (1988) define stripping (moisture-induced damage) as:

> "The progressive functional deterioration of a pavement mixture by loss of the adhesive bond between the asphalt cement and the aggregate surface and/or loss of the cohesive resistance within the asphalt cement principally from the action of water."

Stripping typically begins at the bottom of the compacted bituminous layer where tensile stresses are greatest due to cyclic traffic loading. The stripping then progresses upward to the surface. The surface layer can be replaced; however stripping in the load bearing layer does not provide support so the effective compacted bituminous layer thickness is decreased. This may lead to pavement cracking and surface rutting and to loss of serviceability (Lottman, et al. 1974). According to Kandhal and Rickards (2002), there are four "essential ingredients" that encourage stripping: presence of water, high air void content, high temperature, and high stress.

2.4 Moisture-Induced Damage Processes

Moisture damage is a complex process that is influenced by material factors, their combinations, construction, and external effects such as environment and loading (Solaimanian, et al. 2003). These factors influence physical properties of an asphalt mixture such as air void content, mechanical strength, and stiffness. When moisture is introduced and transported through the mixture and individual materials, deterioration may occur in the form of detachment, displacement, spontaneous emulsification, pore pressure or hydraulic scour (Kiggundu and Roberts 1988, Terrel and Al-Swailmi 1994).

As a result, major pavement failure modes may occur such as cracking and permanent deformation. Figure 2 provides an overview of the moisture damage process in asphalt mixtures.

2.4.1 Transport Processes

How water enters an asphalt mixture and movement of moisture through the asphalt mixture is an important consideration. Water may enter a pavement layer from the top (road surface), bottom, and sides. Run-off water primarily can enter the road surface via surface cracks. Water can enter from the side and bottom from a high water table in the cut areas or from seepage. According to Kandhal (1992), the most common water movement is upward from under the pavement by capillary action. This is due to

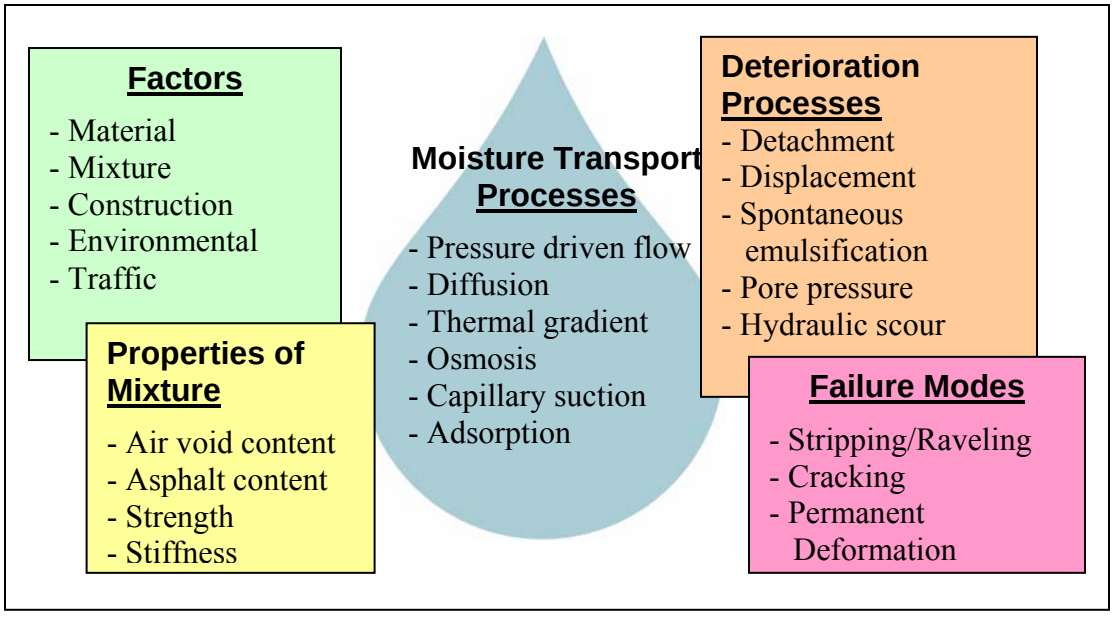

Figure 2. Factors Influencing Moisture Damage Process in Asphalt Pavements

poor subbases or subgrades that lack proper characteristics such as sufficient permeability that can lead to improper drainage. Thus, the subsurface is saturated with moisture that can migrate upwards to the asphalt-aggregate mixture.

Once water is present, there are three ways water may influence an asphalt mixture: (i) a flow field, (ii) static water, and (iii) water present in aggregates (Kringos 2005). If a flow field is present, water may wash away the mastic in a process termed "advective transport" (Kringos and Scarpas 2005a), weaken the binder, and eventually attack the bond between asphalt and aggregate. Static moisture may weaken the binder and attack the bond between asphalt and aggregate. Wet aggregates become an issue if the aggregates are not thoroughly dried during mixture production. The moisture within the wet aggregate may weaken the aggregate or move towards the asphalt-aggregate interface and weaken the bond between asphalt and aggregate. The two primary modes of failure are softening of the binder which results in cohesive failure and loss of bond strength between asphalt binder and aggregate referred to as adhesive failure.

Claisse (2005) describes the primary transport processes through concrete which are used to develop the three primary moisture transport processes through compacted asphalt mixtures: pressure-driven flow, diffusion, and thermal migration. Diffusion occurs when particles of two or more substances intermingle as the molecules move from regions of higher to lower concentration. In other words, ions will migrate between solutions until they both achieve the same concentration. Thus, diffusion is driven by concentration gradients. Moisture diffusion can also occur in a gas when the concentration of water vapor is higher in one region than another. This allows movement of water through unsaturated compacted bituminous mixtures. Moisture typically

reduces the stiffness of the binder and mastic through diffusion which may lead to cohesive failure.

In a solid, water moves from hot or warm regions to cold regions and the rate at which water moves is determined by the solid's permeability. Similarly, in a saturated mixture, ions will also move from hot towards a cold area. An ion that is moving rapidly in hot water has a greater probability of migrating through the asphalt mixture. This is an important consideration considering the highly dependent nature of asphalt mixture properties on temperature.

There are also internal asphalt mixture processes that affect the transport processes: adsorption, capillary suction, and osmosis. Adsorption is used to describe any process that binds an ion (temporarily or permanently) to the asphalt mixture and prevents the ion from moving. Adsorption may be a result of a chemical process or physical surface effects. Capillary suction occurs when water is drawn into the fine voids in compacted mixtures with wet surfaces. Capillary suction is due to surface tensions and mixtures with finer pore structures experience higher capillary suction pressures. In dense graded mixtures this may be compensated by the limitation of flow due to impermeability. Water may move in both vertical directions, up and down, due to gravity or capillary suction. Osmosis depends on a semi-permeable membrane in which water may pass but material dissolved in the water cannot pass through easily. This causes a flow from the weak solution to the stronger solution. Water will pass through asphalt by osmosis and can eventually reach the aggregate surface causing stripping of the asphalt from the aggregate.

2.4.2 Moisture-Induced Damage Mechanisms

Two primary mechanisms are associated with moisture damage in asphalt pavements: loss of cohesion and loss of adhesion (Terrel and Al-Swailmi 1994). Cohesion refers to the interaction between the asphalt mastic and water; moisture may weaken the asphalt binder, which can lead to severe loss of durability and strength. Adhesion as a failure mechanism relates to the degradation of the bond between the aggregate and the asphalt. Although degradation of the aggregate or weak aggregates may damage an asphalt mixture moisture-related failure due to aggregate strength loss is rare, according to Stuart (1990).

2.4.2.1 Loss of Cohesion

Cohesion is defined as the intermolecular force that holds molecules in a solid or liquid together. At the macro level of a compacted bituminous mixture, cohesive forces constitute the integrity of the material. At the micro level, considering asphalt film surrounding aggregate, cohesion may be defined as deformation under load that occurs at a distance from the aggregate substrate and beyond the influence of mechanical interlock and molecular orientation (Terrel and Al-Swailmi 1990). Cohesive forces develop in the mastic and are influenced by the viscosity of the asphalt binder. The viscosity of asphalt binder is dependent on temperature and cohesive forces developed in the asphalt mixture are inversely proportional to temperature.

Loss of cohesion due to moisture typically occurs in the asphalt mastic. Water can affect cohesion in various ways such as deterioration of the mastic due to saturation and void swelling. Water may behave like a solvent in asphalt and result in reduced strength and increased permanent deformation. Asphalts that retain the most amount of

water have been shown to accumulate damage at a more rapid pace (Cheng, et al. 2002a). In the extreme case, the presence of water (saturation) can result in bituminous emulsion: a suspension of minute globules of bituminous materials in water (ASTM 1997). A greater tendency is the occurrence of an inverted emulsion where water becomes suspended within the asphalt binder in spheres (Miknis, et al. 2005).

2.4.2.2 Loss of Adhesion

Adhesion is the molecular force of attraction in the area of contact between unlike bodies that acts to hold them together. Loss of adhesion may be used to refer to the amount of energy required to break the bond between asphalt and aggregate (Kanitpong and Bahia 2003). Seven factors are identified that affect adhesion of asphalt to aggregate:

1) Surface tension (i.e. surface free energy) of the asphalt and the aggregate
2) Chemical composition of the asphalt and aggregate
3) Viscosity of the asphalt
4) Surface texture of the aggregate
5) Porosity of the aggregate
6) Cleanliness of the aggregate
7) Moisture content and temperature of aggregate during mixing with asphalt cement (Terrel and Al-Swailmi 1990).

There are four prevalent theories in the literature to describe the adhesive bond between asphalt binder and aggregate: (i) molecular orientation (Mack 1957), (ii) chemical bonding (Petersen, et al. 1982), (iii) surface energy (Ishai and Craus 1977, Thelen 1958), and (iv) degree of mechanical interlock (Rice 1958). These theories each

individually explain some aspect of adhesion but do not completely capture the mechanism.

Molecular theory involves the orientation of asphalt molecules in relation to the aggregate surface charges and depends on the dipole moment between liquid binder and aggregate. Asphalt consists of a combination of polar (Lifshitz-van der Waals) and non-polar (Lewis acid and base) molecules where the polar molecules are dispersed in a non-polar fluid. The bonding of acidic asphalt molecules to base molecules of aggregate is a primary form of adhesion for compacted bituminous mixtures (D'Angelo and Anderson 2003). Depending on the surface composition of the aggregate, the aggregate may readily attract dipolar water molecules over acidic asphalt molecules.

The chemical interaction between the asphalt binder and the aggregate is critical in understanding the capability of compacted bituminous mixtures to resist moisture damage. Curtis, Ensley et al (1993) measured the energy of adsorption and indicated that physisorption rather than chemisorption occurs during bonding of asphalt and aggregate. Physisorption is due to interactions between surface energy components: electrostatic, dipole-dipole and Van der Waals. Aggregate chemistry was shown to be more influential than asphalt composition for adhesion near the interface and sensitivity to moisture (Curtis, et al. 1993).

Aggregates may be classified as hydrophilic or hydrophobic. Hydrophilic aggregates such as siliceous aggregates (e.g. granite) tend to strip easier than hydrophobic aggregates such as limestone. Some aggregates may display both characteristics so there has been further classification depending on the aggregate's surface charge; electronegative or electropositive (Stuart 1990). Although aggregates may be classified

as poor, fair and good performers in regards to stripping (Scholz, et al. 1994), acceptable bituminous mixtures have been made with each type of aggregate. This is notable considering that a State DOT may not have many choices for aggregate type due to availability and cost constraints. The chemical properties of asphalts and modified asphalts and their interaction with aggregates in the presence of moisture have been extensively investigated through a project still in progress at Western Research Institute (WRI) titled *Fundamental Properties of Asphalts and Modified Asphalts* (Robertson, et al. 2001, WRI 2004).

For an effective bond with aggregate, the asphalt binder should coat or "wet" the aggregate. The wetting ability of asphalt, or any liquid, for that matter, is a function of its surface energies. The surface free energy of a solid (or liquid) is a measure of the energy that is necessary to form a unit area of new surface of that solid. Recently, the ability to accurately determine surface free energy of asphalt binders and aggregates (Bhasin and Little 2006, Cheng, et al. 2001, 2002a, Hefer, et al. 2005) has been developed based on the Good-van Oss-Chaudhury theory. Based on the molecular forces (discussed in the previous paragraph) acting on the solid's surface, the surface free energy, γ^{total}, of a material is determined by combining the polar and nonpolar components as follows:

$$\gamma^{total} = \gamma^{LW} + 2\sqrt{\gamma^{+}\gamma^{-}} \tag{2-1}$$

where γ^{LW} is the Liftshtiz-van der Waals component, γ^{+} is the Lewis acid component, and γ^{-} is the Lewis base component. Several methods have been used to determine surface free energy of asphalt materials, such as Atomic Force Microscopy (Pauli, et al. 2003), Nuclear Magnetic Resonance Imaging (Miknis, et al. 2005), Inverse Gas Chromotography (Hefer 2007) and contact angle measurements (Cheng, et al. 2001,

Cheng, et al. 2002(a), Elphingstone 1997). The surface free energy of a solid cannot be directly determined, however based on experimental contact angle measurements between the solid and liquids with known surface free energy values, the work of adhesion between the liquid and solid may be determined and the surface free energy of the solid can be calculated.

The work of adhesion between a solid, *X*, with an unknown surface free energy, and a probe liquid or vapor, *P*, is calculated from experimentally measured parameters contact angle, θ, and equilibrium spreading pressure, π_e, and is related to the surface free energy as follows (Bhasin, et al. 2006):

$$2\sqrt{\gamma_X^{LW}\gamma_P^{LW}} + 2\sqrt{\gamma_X^{+}\gamma_P^{-}} + 2\sqrt{\gamma_X^{-}\gamma_P^{+}} = \pi_e + \gamma_P^{total}(1+\cos\theta) \qquad (2\text{-}2)$$

Asphalt binder is a low-energy surface and the equilibrium spreading pressure, π_e, becomes negligible and is set to zero so that only the contact angle is measured. Aggregate is a high-energy surface where the contact angle is set to zero and the spreading pressure is determined experimentally. Contact angles or equilibrium spreading pressures must be determined for three different probe materials to generate three equations that are solved simultaneously for the surface energy components of the solid (Bhasin, et al. 2006).

The surface free energy values for asphalt, γ_A, and aggregate, γ_S, are used to calculate the total adhesive bond energy, ΔG_{AS}, as follows (Bhasin, et al. 2006):

$$\Delta G_{AS} = \frac{dU_S}{dA} = \gamma_A + \gamma_S - \gamma_{AS} \qquad (2\text{-}3)$$

where γ_{AS} is the interfacial surface energy between asphalt and aggregate. Referring to equation 2-2, the work of adhesion between the two materials is (Bhasin, et al. 2006):

$$\Delta G_{AS} = 2\sqrt{\gamma_A^{LW}\gamma_S^{LW}} + 2\sqrt{\gamma_A^{+}\gamma_S^{-}} + 2\sqrt{\gamma_A^{-}\gamma_S^{+}} \quad (2\text{-}4)$$

allowing for calculation of the *dry* adhesive bond energy between asphalt and aggregate based on the surface free energy components of the asphalt and aggregate. Combining equations 2-3 and 2-4, the interfacial surface free energy is expressed (Bhasin, et al. 2006):

$$\gamma_{AS} = \gamma_A + \gamma_S - 2\sqrt{\gamma_A^{LW}\gamma_S^{LW}} - 2\sqrt{\gamma_A^{+}\gamma_S^{-}} - 2\sqrt{\gamma_A^{-}\gamma_S^{+}} \; . \quad (2\text{-}5)$$

An advanced method for determining thermodynamic equilibrium adhesion (i.e. bond strength) between asphalt-aggregate pairs in the presence of water has been developed (Cheng, et al. 2001, Cheng, et al. 2002b, Elphingstone 1997, Zollinger 2005). The interfacial surface energy of the asphalt-aggregate system in the presence of water is determined based on the individual surface energies of the components. Water, denoted '*W*', can displace asphalt binder from the aggregate surface and the work of debonding of asphalt from aggregate by water, ΔG_{ASW}, may be determined (Bhasin, et al. 2007):

$$\Delta G_{WAS} = \gamma_{AW} + \gamma_{SW} - \gamma_{AS} \quad (2\text{-}6)$$

The interfacial surface free energy, γ_{AS}, in equation 2-5 is used to determine the energy required to displace a unit of area of the asphalt-aggregate interface by water creating a unit area of asphalt-water interface (*AW*) and aggregate-water interface (*SW*).

The magnitude of ΔG_{WAS} may be used to determine the potential for water to displace asphalt from the aggregate interface. A larger magnitude indicates a larger

reduction in free energy and implies a greater potential for water to displace asphalt at the aggregate surface (Bhasin, et al. 2006). Both ΔG_{AS} and ΔG_{WAS} are used to evaluate moisture sensitivity of materials and predict moisture damage in asphalt mixtures (Bhasin, et al. 2007, Bhasin, et al. 2006, Cheng, et al. 2002b, Masad, et al. 2006, Zollinger 2005).

The thermodynamic equilibrium bond strength is only one component of the actual bond strength between asphalt and aggregate. Bond strength at the asphalt-aggregate interface is a function of not only interfacial forces, but also the mechanical properties of the interfacial zone and the bulk phases of the components. Equation 2-3 and 2-6 do not account for the influence of the viscoelastic nature of the asphalt binder on the adhesive energy. In addition, the plastic work by the binder in the asphalt-aggregate system may be orders of magnitude higher than G_{WAS} at the interface. The stress necessary to detach asphalt film from a substrate is a function of material properties such as bulk modulus, film thickness, elastic energy due to stored strain energy, work expended in plastic deformation and interfacial work of adhesion.

The mechanical interlock or bond strength of asphalt and aggregate mainly depends on the physical properties of the aggregate. These properties include: surface area and texture, surface coatings, particle size and porosity or absorption (Terrel and Al-Swailmi 1994). A stronger bond between asphalt and aggregate is created with a rough, porous aggregate with large surface area. According to Kandhal (1994) "…physicochemical surface properties of mineral aggregate are more important for moisture induced stripping as compared to the properties of the asphalt binder."

2.5 Distress Mechanisms in Asphalt Pavements Due to Moisture

In Chapter I, moisture damage was recognized as a national problem that contributes to early failure of flexible pavements. Moisture-induced damage may result in cracking, permanent deformation, raveling (i.e. loss of surface material), and localized failures (i.e. potholes). Knowledge of various pavement distress types is essential to identify the causes of failure. The Distress Identification Manual for the Long-Term Pavement Performance Project (LTPP) groups each distress into one of the following categories:

A. Cracking,

B. Potholes,

C. Surface Deformation,

D. Surface Defects, and

E. Miscellaneous Distresses (Miller, et al. 1993).

Damage to the bituminous pavement as a result of moisture is a primary distress mode that accelerates degradation and premature failure of the mixture in tandem with distresses in each of the above categories. For example, moisture may degrade the adhesive bond at the aggregate-asphalt interface, which under applied load can lead to cracking as a result of tensile stress. In turn, cracks in the pavement facilitate the entry of moisture into the bituminous mixture. Moisture can also affect the cohesive bond within the asphalt mastic and weaken the asphalt binder, which can lead to permanent deformation.

There are three main distress modes used in the analysis and design of flexible pavements: fatigue cracking, thermal cracking, and permanent deformation. This section

defines distress mechanisms and the three main failure mechanisms and provides information on the cause and resulting problems of the distresses as they specifically relate to moisture damage.

2.5.1 Stripping and Raveling

Tunnicliff and Root (1984) define stripping in asphalt pavements as the displacement of asphalt cement film from aggregate surfaces by water. Stripping typically begins at the bottom of the compacted bituminous layer, shown in Figure 3, where the tensile stresses are the greatest due to cyclic loading. The stripping then progresses upward to the surface. Stripping that occurs on the surface of a pavement is referred to as raveling. Raveling is the wearing away of the asphalt pavement surface caused by the dislodging of aggregates due to stripping (Huang 1993).

Figure 3. Stripping at Bottom of Hole (Washington 2005)

Stripping can occur due to many causes including improper material selection, poor mixture design and construction, and the presence of water in the mixture or pavement layers. Stripping is difficult to detect since it often begins in the bottom of the bituminous layer and manifests itself as other distress mechanisms such as fatigue

cracking due to a loss of structural support, longitudinal cracking, and permanent deformation.

2.5.2 Fatigue Cracking

Fatigue cracking is considered a major structural distress of pavements and is a load-associated distress mechanism. Fatigue cracking is a chain of interconnected cracks caused by failure of asphalt surface or stabilized base under cyclic traffic loading (Huang 1993). "Bottom-up" cracking begins at the bottom of the asphalt surface where the tensile stress or strain is highest under the wheel load. The cracking then propagates upwards toward the surface where longitudinal cracks appear. Longitudinal cracks run parallel to the pavement's centerline and are indicative of the beginning of fatigue cracking. Due to repetitive loading the cracks connect and develop a pattern that resembles the skin pattern on an alligator and is termed "alligator cracking". In the case of thick pavements, the cracks may propagate at the surface and migrate downwards which is referred to as "top-down" cracking. Excessive or severe alligator cracking can lead to potholes. Potholes occur when there is a hole left after interconnected cracks create a small piece of pavement that is broken from the pavement surface (Figure 4). Potholes may also be formed during freeze-thaw cycling or localized disintegration within the bituminous pavement layer (Huang 1993).

Figure 4. Pothole from Fatigue Cracking (Washington 2005)

Fatigue cracking occurs due to a loss of structural support. Moisture has an effect on the structure of the pavement in two possible locations: at the subgrade or base layers and within the compacted bituminous layer. The subgrade or base layers can lose support due to poor drainage and during the thawing process. Stripping may occur as a result of high tensile stresses in the bottom of the bituminous layer. The stripped area will not provide any support so the effective compacted bituminous layer thickness is decreased. Further, fatigue cracking allows moisture infiltration, which can lead to further damage and the onset of other distress mechanisms.

2.5.3 Thermal Cracking

Thermal cracking is not associated with loading and occurs due to low-temperature shrinkage or hardening of the compacted bituminous mixture. The change in temperature results in cyclic stresses and strains that cause longitudinal and transverse cracking at the asphalt surface (Figure 5). Transverse cracks are perpendicular to the pavement's centerline.

Kim, Roque et al. (1994) determined the low-temperature properties of field samples (i.e. cores) at two different moisture levels. They found that changes in the moisture state in an asphalt mixture had a significant impact on low-temperature properties of the asphalt mixtures. Thus, moisture most likely may have an impact on the thermal-cracking performance of asphalt pavement.

Figure 5. Fatigue Cracking from Frost Action (Washington 2005)

2.5.4 Permanent Deformation

Permanent deformation occurs in the pavement layers or subgrade as a result of consolidation or movement of the materials due to traffic loads (Huang 1993). Permanent deformation manifests itself as depressions in the pavement. Rutting is the depression of the surface of the pavement in the wheel paths. Rutting is caused by inadequate compaction (i.e. too low or high air void content) or movement of the pavement layers and can also occur due to plastic flow of asphalt in hot or weakened (i.e. less stiff) conditions. Loss of adhesive and cohesive strength within the asphalt mixture due to moisture can facilitate permanent movement under traffic loading.

2.6 Test Methods to Assess Moisture Susceptibility

In a survey conducted in 2002 including fifty State DOTs and the District of Columbia, three FHWA Federal Land offices, and one Canadian province, eighty-seven percent of the agencies report testing for moisture susceptibility (Hicks, et al. 2003). Most user agencies, sixty-two percent, conduct moisture sensitivity test as part of their asphalt mixture design process.

The tests for determining moisture sensitivity of asphalt-aggregate mixtures can be classified into two broad categories: tests performed on loose mixtures and those performed on compacted specimens. The following test methods are national standards:

- AASHTO T 165/ASTM D 1075 *Effect of Water on Compressive Strength of Bituminous Mixtures*
- AASHTO T 283/ASTM D 4867 *Resistance of Compacted Asphalt Mixtures to Moisture-Induced Damage*
- ASTM D 3625 *Effect of Water on Bituminous-Coated Aggregate using Boiling Water*
- ASTM D 4867 *Effect of Moisture on Asphalt Concrete Paving Mixtures*
- AASHTO T 324 *Hamburg Wheel-Track Testing of Compacted Hot-Mix Asphalt.*

The first tests introduced considered uncompacted mixtures and included the boiling water test (ASTM D 3625) and static-immersion test (AASHTO T 182; no longer a national standard). These tests were purely subjective and did not relate to field performance (Kandhal 1992). Subsequently the immersion-compression test (AASHTO

T165 or ASTM D1075) was introduced to include the effects of compaction and was the first test to become an American Society of Testing and Materials (ASTM) standard.

In the late nineteen-seventies and early eighties, Lottman developed the test that currently has the widest acceptance in the paving industry, AASHTO T 283 (also known as ASTM D 4867). The majority of user agencies, eighty-two percent, use AASHTO T 283 for moisture damage evaluation. However, a major concern regarding AASHTO T 283 was the fact that it did not capture the combined effect of moisture and dynamic loading due to traffic. In the 1990's tests that capture the effects of traffic loading such as the Hamburg Wheel-Tracking Device (HWTD) were introduced (Solaimanian, et al. 2003). Approximately four percent of agencies surveyed use a wheel-tracking test such as the HWTD (Hicks, et al. 2003). In the following subsections, AASHTO T 283 is discussed since it is the most common test used to determine moisture sensitivity, the HWTD is discussed because results from the HWTD test are used in Chapter III to correlate bond strength results of asphalt binders to asphalt mixture performance, and background information is provided on the modified pull-off test method for evaluating moisture sensitivity of asphalt binders.

Numerous other tests have been developed to evaluate moisture sensitivity of loose or compacted mixtures with the goal of identifying mixtures at risk to water damage, compare mixtures composed of different aggregate quantities and types, and assess effectiveness of antistripping additives. A thorough review regarding test methods to predict moisture sensitivity of HMA pavements may be found in Solaimanian et al. (2003). The most commonly used tests are subjective and are not designed to predict performance (i.e. estimate the life of the pavement), may not be applicable to a wide-

range of materials and conditions (Terrel and Al-Swailmi 1994), do not distinguish between different failure modes and cannot be combined with developing models to quantify moisture-induced damage.

2.6.1 Modified Lottman Procedure (AASHTO T 283)

The modified Lottman procedure, AASHTO T 283, measures the indirect tensile strength of a compacted asphalt mixture specimen, Figure 6, and the tensile strength of a moisture-conditioned specimen and calculates the Tensile Strength Ratio (*TSR*) between the specimens.

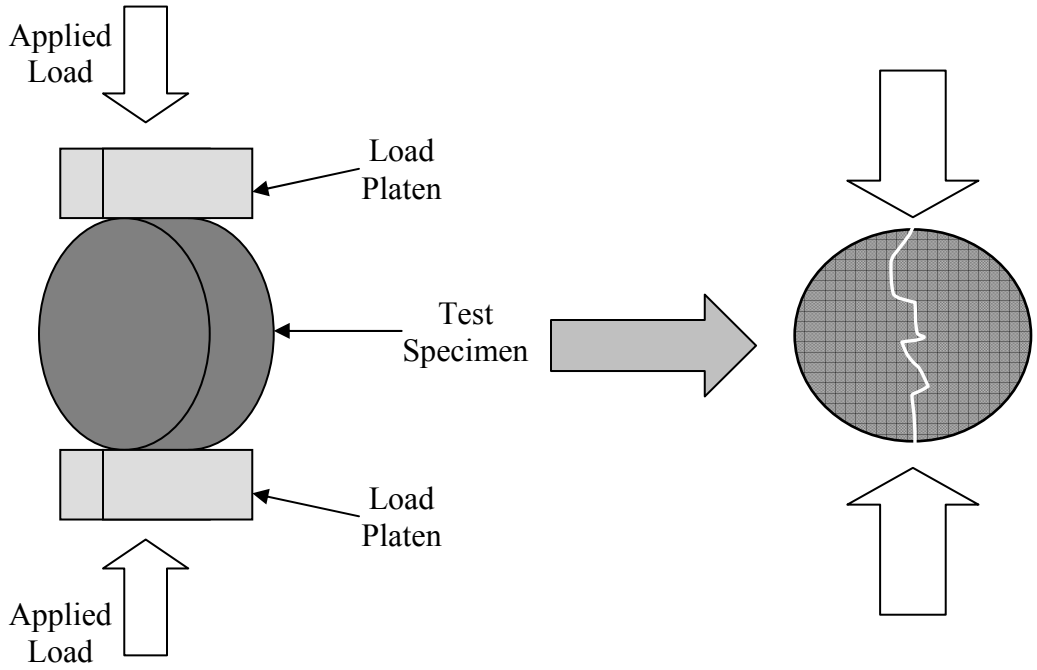

Figure 6. Schematic of Indirect Tensile Test Illustrating Experiment Set-up (left) and Location of Failure (right)

AASHTO T 283 allows specimens that are compacted using Marshall Apparatus, California Kneading Compactor, Superpave Gyratory Compactor, or U.S. Corps of Engineers Gyratory Testing Machine. Field mixed, laboratory compacted and field mixed, field compacted specimens may also be tested. Six samples, 100 mm (4 in) diameter by 63.5 ± 2.5 mm (2.5 ± 0.1 in.) height or 150 mm (6 in) diameter by 95 ± 5 mm (3.75 ± 0.2 in.) height are required. After mixing, the mixture is short-term aged by cooling at room temperature for two hours and then cured in an oven at 60° C (140° F) for sixteen hours. The specimens are brought to compaction temperature for two hours and then compacted to 7.0 ± 0.5 percent air voids. After removal from the mold, the specimens are stored for twenty-four hours at room temperature. The maximum specific gravity, thickness, diameter, and bulk specific gravity of each specimen is determined. The volume and percentage of air voids is calculated and the specimens are sorted into two groups (with approximately equal average air void contents) of three specimens each.

Group one is considered unconditioned and are wrapped in plastic and immersed in water at a temperature of 25° C (77° F) for two hours prior to testing. Group two specimens are conditioned by partial vacuuming saturation at 13 – 67 kPa absolute pressure (10-26 in. of Mercury partial pressure) for five minutes. The samples are then soaked (without vacuum) for five to ten minutes and the degree of saturation is determined. If the degree of saturation is below seventy percent, the process is repeated. If the degree of saturation is above eighty percent the sample is considered damaged and discarded. The samples are then placed in plastic bags with 10 mL (0.338 ounces) of water and frozen at –18° C (0° F) for at least sixteen hours. The specimens are then put in a water bath at 60° C (140° F) and the plastic wrap is immediately removed and they are

allowed to soak for twenty-four hours. The samples are then soaked at 25° C (77° F) for two hours prior to testing.

The Indirect Tensile Test (IDT) is used to obtain the tensile stress characteristics of a compacted bituminous mixture before and after moisture conditioning. The indirect tensile strength is the maximum stress from a diametral vertical force that a sample can endure. The tensile strength of a mixture is an important property since the bottom of the compacted mixture layer is repeatedly subjected to tensile stresses as a wheel load passes over. The estimated maximum tensile strength is determined using the following equation:

$$S_t = \frac{2000P}{\pi t d} \tag{2-7}$$

where S_t = tensile strength (kPa),

P = maximum load required to fail sample (N),

t = specimen thickness (mm),

d = specimen diameter (mm),

or in U.S. Customary units

$$S_t = \frac{2P}{\pi t d} \tag{2-8}$$

where S_t = tensile strength (psi),

P = maximum load required to fail sample (lbs),

t = specimen thickness (in.),

d = specimen diameter (in.).

The moisture susceptibility or stripping potential is determined by calculating the tensile strength ratio (*TSR*) using the tensile strength of an unconditioned sample and a conditioned or wet sample. The retained *TSR* is calculated:

$$TSR = \frac{S_{t,wet}}{S_{t,dry}} \tag{2-9}$$

where TSR = tensile strength ratio,

$S_{t,dry}$ = average tensile strength of conditioned samples (kPa or psi), and

$S_{t,wet}$ = average tensile strength of unconditioned samples (kPa or psi).

The minimum *TSR* value allowed is 0.70, however it is recommended to use a minimum value of 0.80. The samples are visually observed for damage and rated from "0" to "5" ("5" is the most stripped).

NCHRP Project 9-13 (Epps, et al. 2000), titled "*Evaluation of Water Sensitivity Tests*" focused on the effectiveness of AASHTO T 283 and its compatibility with the Superpave® volumetric mixture design system. The investigators suggested improvements to the conditioning procedure, which resulted in the most recent standardized version of AASHTO T 283. As a result of NCHRP Project 9-13, AASHTO T 283 remains the most useful test method to predict moisture sensitivity before construction as compared to other available procedures. However, the test is empirical, known to provide false negatives or positives, and there is concern regarding its ability to predict moisture susceptibility with confidence (Solaimanian, et al. 2003).

There are limitations in using AASHTO T 283 alone in determining moisture susceptibility. For example, uncertainty in the quality of mixing and construction processes, such as in-place asphalt content and field-compacted mixture characteristics

such as density are not considered. Further, AASHTO T 283 does not couple moisture sensitivity of the mixture with climate and traffic to predict pavement performance for a particular mixture design (Epps, et al. 2000). Using test methods that evaluate compacted asphalt mixtures, such as AASHTO T 283, it is difficult to indicate which material component of the asphalt mixture contributes to damage.

2.6.2 Hamburg Wheel-Tracking Device (AASHTO T 324-04)

Test methods have been developed that combine moisture with cyclic traffic loading such as the Hamburg Wheel Tracking Device (HWTD) shown in Figure 7. The HWTD includes cyclic loading conditions and saturation of compacted asphalt mixtures. The HWTD is used to predict permanent deformation potential and moisture damage of HMA. The samples used for the test are Linear Kneading compacted slabs and are typically 260 mm (10.25 in.) wide, 320 mm (12.5 in.) long and 38 mm (1.5 in.) to 100 mm (4 in.) thick. Two Superpave Gyratory Compacted (SGC) samples (150 mm (6 in.) in diameter) may also be used that have been compacted in accordance with AASHTO 312 *Standard Method of Test for Preparing and Determining the Density of the HMA Specimens by Means of the Superpave Gyratory Compactor*. The sample is compacted to 7.0 ± 2.0 percent air voids or some other designated air void content. The samples are submerged in water at 50^{o} C (122^{o} F), but the temperature can be specified within a range from 25^{o} C to 70^{o} C (77^{o} F to 158^{o} F). A steel wheel 47 mm (1.85 in.) wide is rolled across the surface of each submerged sample at a load of 705 N (158 lbs). The wheel passes over each sample fifty times per minute at a maximum velocity of 34 cm/sec (1.1 ft/sec) in the center of the sample. Each sample is loaded for 20,000 passes or until the

average linear variable displacement transducer (LVDT) displacement is 40.90 mm (1.6 in.). The test takes approximately six and a half hours (Aschenbrener 1995).

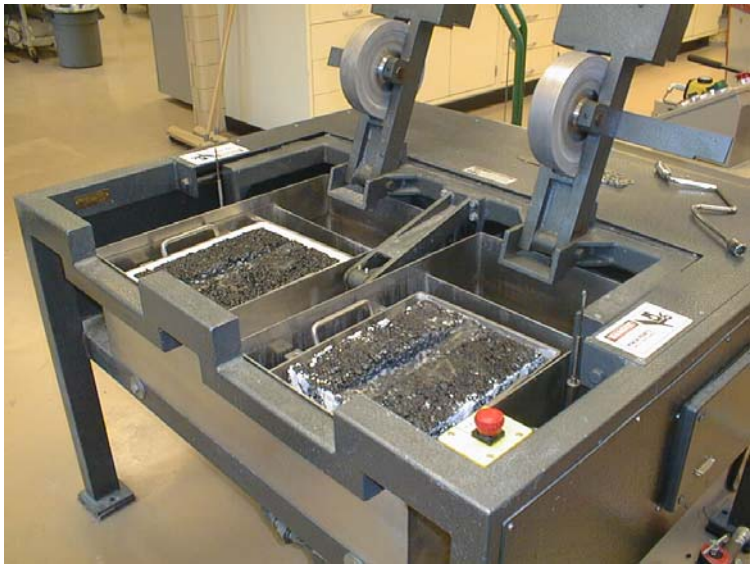

Figure 7. Hamburg Wheel-Tracking Device

The rut depth (i.e. deformation) is plotted versus the number of passes and the results usually show a curve with two distinct steady-state portions, see Figure 8. The first portion denotes the creep (i.e. rutting) slope and the second portion begins when there is a sudden increase in the rate of deformation. This coincides with stripping of the asphalt binder from the aggregate and is considered the stripping slope. The stripping inflection point is the number of passes at the intersection of the creep slope and the stripping slope and is calculated by

$$Stripping\ Inflection\ Point\ (SIP) = \frac{Intercept\ (second\ portion) - Intercept\ (first\ portion)}{Slope\ (first\ portion) - Slope\ (second\ portion)} \quad (2\text{-}10)$$

where all parameters are expressed in "passes". The rutting slope is the inverse of the rate of deformation in the linear region of the deformation curve before stripping begins to occur. The rutting slope relates the plastic flow of the material under load to rutting depth. The stripping slope is the inverse of the rate of deformation in the linear region of the deformation curve after stripping begins and until the end of the test. The number of passes for each 1 mm (0.04 in) of deformation from stripping is determined. The stripping slope relates the plastic flow to the degree of moisture damage. The stripping inflection point is related to the resistance of HMA to moisture damage (Aschenbrener 1995).

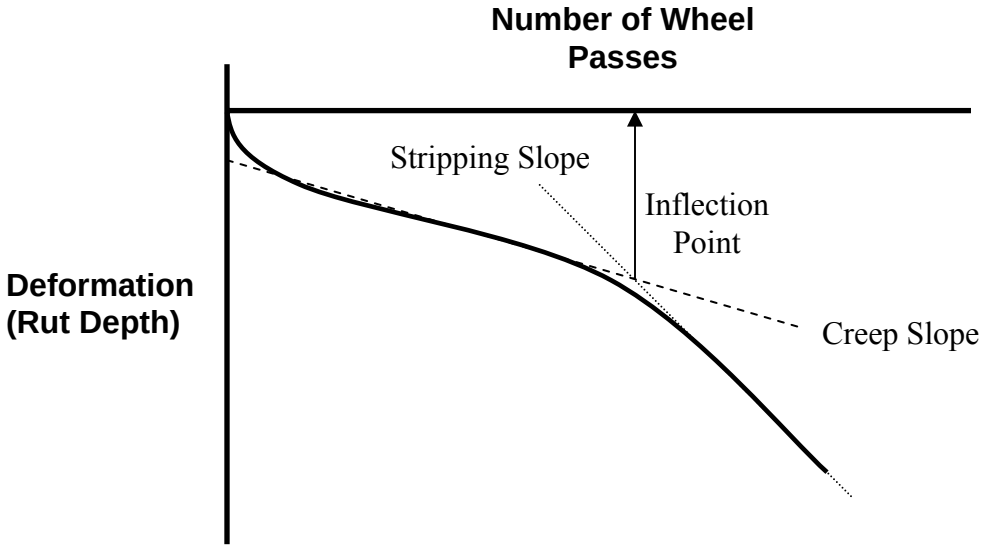

Figure 8. Hamburg Wheel-Tracking Device Test Results

Aschenbrener (1995) discovered there is good correlation between stripping observed in the laboratory HWTD tests and field pavements with known moisture

damage. In addition the stripping inflection point relates known stripping performance. For well performing pavements, the stripping inflection point was above 10,000 wheel passes. The advantages of this method are that the results are sensitive to aggregate properties, aging, asphalt source, and additives. However, for some mixtures the test is too severe.

Aschenbrener recommends that test temperature should be selected depending on the project's climate (i.e. highest temperature pavement will experience). Unfortunately, recommended values for specific climates as well as traffic conditions are not available. With the advent of the mechanistic-empirical design methodology, a disadvantage of this method is that the HWTD method does not provide a fundamental property measure that can be utilized in models (Solaimanian, et al. 2003).

2.6.3 Modified Pull-off Test Method

A critical parameter to the moisture-induced damage process is knowledge of the bond strength between asphalt and aggregate and loss of bond strength in the presence of moisture. To date, a method to accurately determine mechanical bond strength between asphalt binder and aggregate has not been established. In the coatings and adhesive industry, several test methods have been developed to determine the mechanical strength of an adhesive joint. A compilation and discussion of available methods is provided in Kanitpong and Bahia (2003). The pull-off test method specified in ASTM D 4541 *Pull-off Strength of Coatings using Portable Adhesion Testers* has been identified as a promising procedure for determining adhesion (i.e. bond strength) of asphalt materials

(Copeland, et al. 2007, Kanitpong and Bahia 2005, Kanitpong and Bahia 2003, Nguyen, et al. 1996, Youtcheff and Aurilio 1997).

The device used to conduct the pull-off strength test is the Pneumatic Adhesion Tensile Testing Instrument (PATTI) shown in Figure 9, which was developed at the National Institute of Standards and Technology (NIST). Using the PATTI, researchers noted that for dry specimens, cohesive failure within the asphalt binder occurred. However, for moisture-conditioned specimens, the mode of failure changed from cohesive to mixed mode or adhesive failure (Kanitpong and Bahia 2005, Youtcheff and Aurilio 1997). The hypothesis is that moisture decreases the tensile strength of asphalt at the asphalt-substrate interface.

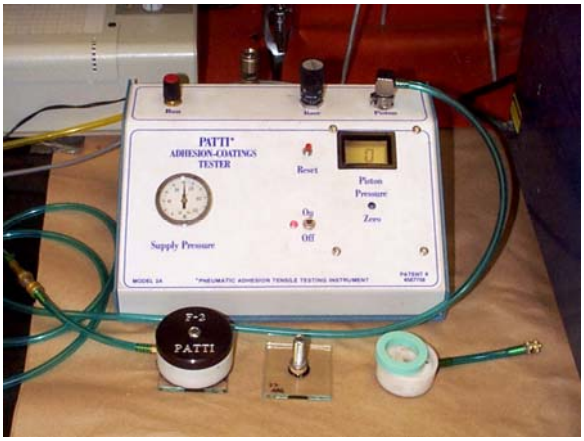

Figure 9. Photograph of Pneumatic Adhesion Tensile Testing Instrument (PATTI) and Associated Equipment

Youtcheff and Aurilio (1997) developed a procedure for evaluating moisture sensitivity of asphalt binders using the modified pull-off test method. They considered several operational parameters for development of a protocol for a rapid, inexpensive,

reproducible evaluation of moisture sensitivity of asphalt binders. These parameters included: temperature, type of porous stub, and trimming the asphalt binder around the stub. As a result, they standardized the materials used to conduct the test, sample preparation, procedure and testing.

Binders of various SHRP performance grades were used to evaluate the relationship between binder stiffness and moisture susceptibility. SHRP core asphalts of different grades applied to soda glass substrates were evaluated. The authors determined that asphalt film thickness, loading rate, test temperature, soak time, grade, and aging all have significant effects on the pull-off tensile strength (*POTS*) value. The pull-off strength decreases as soak time increases.

Based on the degradation of pull-off strength as soak time increases, Youtcheff and Aurilio (1997) developed the following exponential model that describes loss of pull-off strength of an unaged, unmodified binder with soak time in water:

$$S_i = m1 + m2 * (1 - \exp(-m3 * t_i)) \tag{2-11}$$

where S_i is the pull-off strength at time i; t_i is the soak time, and $m1$, $m2$ and $m3$ are regression coefficients. A moisture sensitivity profile is defined by the following three features:

- Cohesive strength of asphalt binder, St_o,
- The rate of loss of pull-off strength, and
- The pull-off strength at equilibrium, St_{eq}.

Each parameter of the model given by Equation 2-11 relates to the features of the moisture sensitivity profile. Parameter $m1$ is equivalent to St_o; $m2$ is the difference

between St_o and St_{eq}; and $m3$ is the regression slope that relates to the rate of loss (Youtcheff and Aurilio 1997).

For aged binders, the authors found that the pull-off strength increased in the dry condition and after twenty-four hours soak time, but did not follow the same trend as the unaged binders. Thus, equation 2-8 is not valid for aged binders. A concern with the pull-off test is the repeatability of the test method due to the lack of control over certain variables during specimen preparation such as film thickness and temperature.

Kanitpong and Bahia (2005) used the modified pull-off test to measure adhesive strength of asphalt-aggregate combinations and, in combination with cohesive strength measurements, predicted mixture performance in the laboratory. They evaluated effects of different aggregate substrates in asphalt mixtures, the use of additive, polymer modification of the binder and conditioning time in the water bath on the pull-off strength of an asphalt binder. They found that all factors had a significant effect on the pull-off strength. In fact, it appears that the binder type and aggregate type have a far more significant effect on the *POTS* than does the interaction between asphalt and aggregate. The effect of the binder in combination with water conditioning also has a significant effect on *POTS*.

In regards to the aggregate substrate, there was a significant decrease in pull-off strength for granite surfaces as compared to limestone surface (Kanitpong and Bahia 2005). Aggregate type appears to influence bond strength. The authors also related the adhesive and cohesive properties of the binder to moisture-conditioned hot mix asphalt mixtures using the indirect tensile strength test and a combined function that accounts for cohesive (using tack test with Dynamic Shear Rheometer) and adhesive (using the pull-

off test method) strength (Kanitpong and Bahia 2003). The cohesive and adhesive properties of the binders were further related to mixture performance using results of the Hamburg Wheel Tracking Device (HWTD) and the simple performance test (Kanitpong and Bahia 2005).

2.6.3.1 Test Methodology

The maximum adhesive strength of binder is defined as the average stress, σ_{avg}, which can be applied in normal direction to the surface without damaging the material,

$$\sigma_{avg} = \frac{F}{A} \tag{2-12}$$

where F is the pull-off force which can be applied by a pull-stub adhered to the binder and A is the cross sectional area of the pull-stub. The force necessary to pull asphalt from aggregate depends on the strength of adhesion (i.e. bond) between the two materials and the asphalt's ability to resist stretching. In Equation 2-12 the stress distribution in area A is assumed to be uniform (Soltesz, et al. 1992). However, stresses induced in the binder layer during the pull-off test are much more complicated. This is due to the fact that asphalt binder has a different modulus than the pull-stub and the aggregate substrate. The tensile stresses are non-uniform, the stress state is not uniaxial (in fact, it is triaxial) and shear stresses may be present.

The procedure developed by Youtcheff and Aurilio (1997) was followed in this study to prepare the test specimens. A porous, ceramic stub that allows water to migrate consistently through the asphalt film is applied to the pull-stub using two-part epoxy glue. A small sample of asphalt (< 10 grams) is mixed with one percent (by weight) 200 μm glass beads to ensure uniform film thickness. The sample is heated to about 100^{o} C (212^{o}

F) using a hot plate. The sample is then applied to the ceramic and the pull-stub is pressed onto a substrate by the test operator. The specimens are cured at room temperature, about 22° C (71.6° F), for twenty-four hours.

The geometry of the pull-off test is shown below in Figure 10. Considering only the part of the substrate in contact with binder, we can equate the radius of the loading fixture, *R*, to the contact radius of the binder with the stone substrate. The thickness of the binder before testing is *h*. If we apply an external tension, force *P*, along the longitudinal axis of the loading fixture, the binder should contract laterally along the air-binder interface and the adhesive thickness increases to $h + \Delta h$. Eventually failure will occur at the weakest link. The pull-off test measures the tensile stress at failure and bond strength is defined as the mean Pull-Off Tensile Stress (*POTS*) at failure.

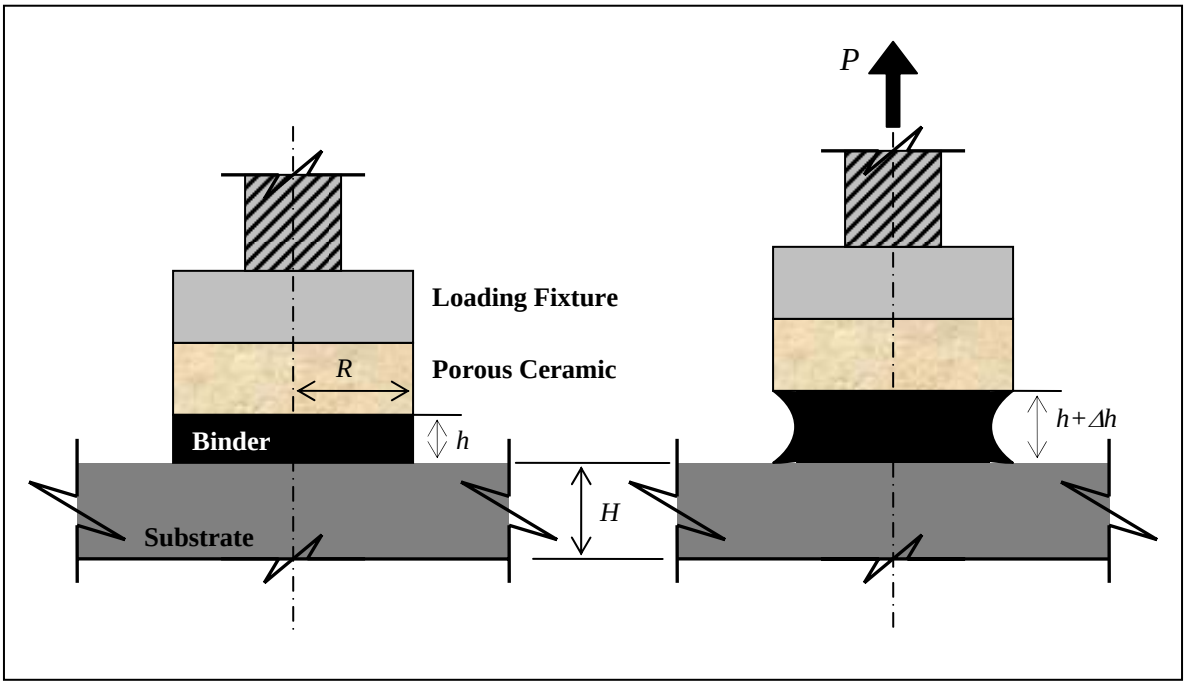

Figure 10. Schematic of Pull-off Test of an Asphalt-Aggregate Butt Joint

Dry specimens (i.e. zero hours soak time) are tested immediately after curing. Specimens that are moisture conditioned are immersed in distilled water at 25° C (77° F), withdrawn from the water bath at a given time, and immediately tested. Using the PATTI device and a chart recorder, the burst pressure (*BP*) under constant load rate necessary to debond each specimen at room temperature is measured. Figure 11 shows a cross-section schematic of the pull-off test piston attached to the pull-stub. The *POTS* in psi for each specimen is determined as follows:

$$POTS = \frac{(BP \times A_g) - C}{A_{ps}} \tag{2-13}$$

where A_g = contact area of the gasket with the reaction plate (sq in)

C = piston constant (lbs.)

A_{ps} = area of the pull-stub (sq in)

BP = burst pressure (psig).

The modified pull-off test method provides a value for the maximum strength the asphalt-substrate bond can tolerate. In addition, the pull-off test provides information for the loss of strength over time due to moisture.

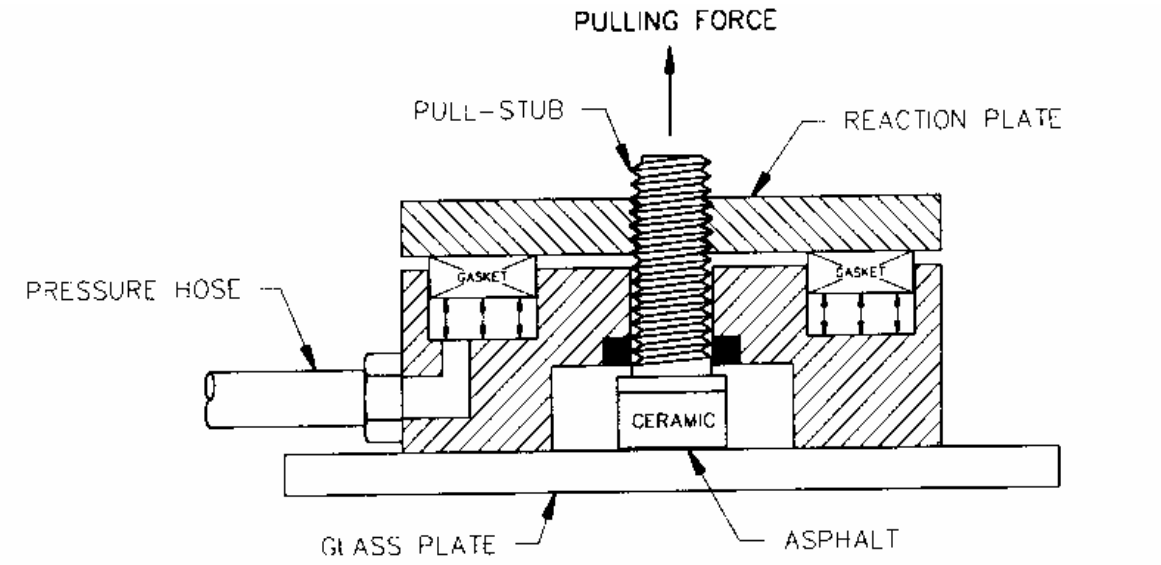

Figure 11. Cross-section of Piston Attached to Pull-stub Used in Pull-off Test Method (Youtcheff and Aurilio 1997)

2.7 Modeling Approaches to Predict Moisture Damage in Asphalt Mixtures

Quantitative models exist for the distress mechanisms that affect asphalt pavements such as cracking and permanent deformation. In particular, the use of advanced mechanics (e.g. continuum damage) has been used to characterize moisture damage of asphalt mixtures (Birgisson, et al. 2003, 2004, Cheng, et al. 2002a, Kim, et al. 2004). There has been doubt cast on the use of a single parameter (e.g. tensile strength, resilient modulus) to evaluate moisture damage. A unified framework is needed that considers changes in influential mixture properties to estimate the effects of moisture damage in bituminous mixtures (Birgisson, et al. 2004). Using an HMA fracture mechanics model developed at the University of Florida Birgisson, Roque et al (2004) showed that moisture damage impacted the fracture resistance of mixtures and a performance-based fracture criterion, the energy ratio (ER) can be used to quantify the

effects of moisture damage on the fracture resistance of bituminous mixtures. By measuring the creep, resilient modulus, and strength of the compacted mixture, the energy ratio can be calculated which can then be used in combination with a fatigue model to evaluate the effects of moisture damage on the fracture resistance of compacted bituminous mixtures.

An adhesion failure model (Cheng, et al. 2003) has been developed that considers the surface energy of adhesion between two materials (asphalt and aggregate) in contact with a third material (water). The model was developed to analyze the adhesive fracture between asphalt and aggregate in the presence of moisture. The model is based on the fundamental theories of Schapery's Law of Fracture Mechanics for Viscoelastic Media and Surface Energy Theory. Using Schapery's Law, the authors show that the surface energy of an asphalt aggregate system is related to the fracture characteristics of the asphalt. Surface energies are used to compute the adhesive bond energy of asphalt binder and aggregate and the cohesive bond energy of asphalt binder (Bhasin, et al. 2006, Cheng 2002, Cheng, et al. 2002b, Elphingstone 1997, Hefer, et al. 2006, Zollinger 2005). The adhesive strength between the two materials is affected by their surface energies, the surface texture of the aggregate, and presence of water.

At Delft University of Technology (TU Delft), an analysis model has been developed to approximate the physical and mechanical aspects of moisture damage to asphalt materials (Kringos 2007). The finite element tool, RoAM (Raveling of Asphalt Mixes), is a sub-system of the finite element system CAPA-3D (Scarpas 2000) and has been developed in order to simulate the progressive development of damage in asphalt mixtures at the micro level due to the combined action of moisture and traffic loading,

Figure 12. Moisture diffusion and washing away of the mastic film (mastic erosion) are identified as the primary physical moisture-induced damage processes. In Kringos (2007), the governing equations and finite element formulas to simulate these processes are derived. RoAM simulates water damage mechanisms (diffusion, advective transport) that occur in a bituminous mixture exposed to constant flow of water through the mixture (Kringos and Scarpas 2005a). Advective transport occurs on a macroscopic level and is the "washing away" of the outer layers of the mastic film (i.e. mastic erosion) exposed to the water flow field. This occurs in areas that experience heavy rainfall where open-graded asphalt mixtures are used to facilitate the drainage of water from the surface.

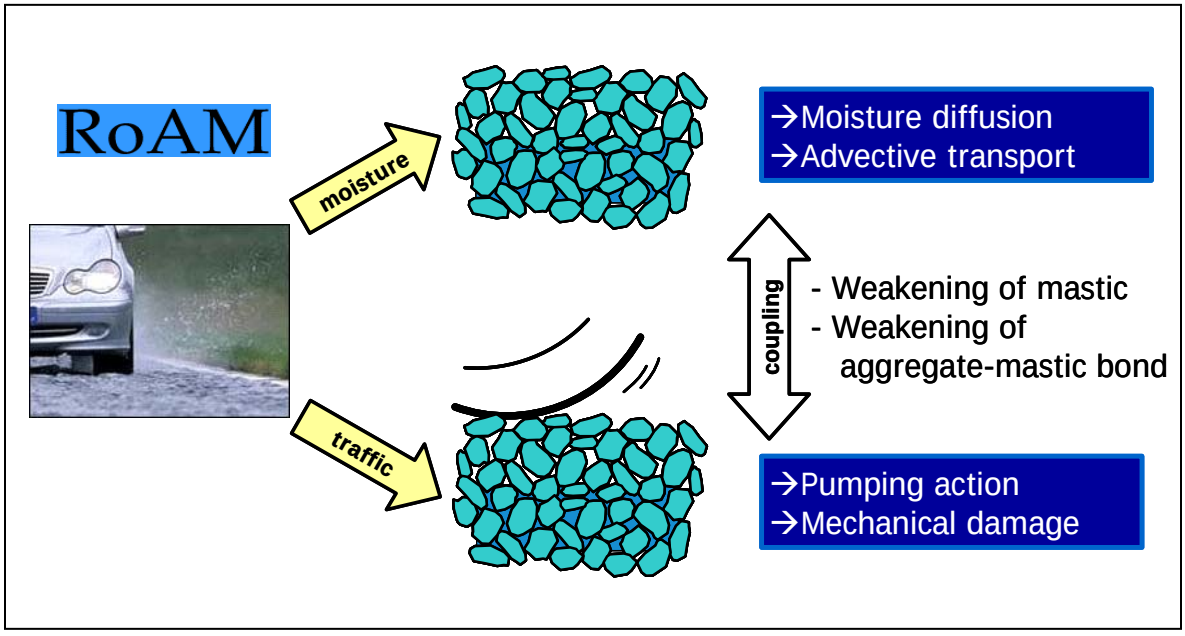

Figure 12. Approach to Moisture-induced Damage Modeling (from Kringos 2007)

Asphalt mixtures not exposed to a water flow field will not experience erosion but still remain susceptible to raveling or stripping. Diffusion is a microscopic or molecular phenomenon where the water diffuses through the mastic layers until the moisture disperses the asphalt mastic or reaches the interface of the mastic with the aggregate. In RoAM, the transport of moisture due to diffusion through asphalt mastic and/or aggregate is simulated based on Fick's Law. Diffusion of water through the mastic reduces the cohesive strength within the mastic and leads to dispersion or a loss of concentration in the mastic. Eventually, moisture reaches the interface between asphalt binder and aggregate and this can lead to an adhesive failure at the asphalt-aggregate interface.

For long-term behavior of the asphalt mixture in a pavement, both moisture-induced and mechanically-induced damage impact the overall damage development. For this reason, a combined mechanical-moisture induced damage model is necessary. Fluid flow equations of water through an asphalt mixture system are coupled with constitutive equations that model the mechanical response of the asphalt mixture. In Kringos and Scarpas (2005(b)), the performance index of a progressively damaging asphalt mixture and interrelation between mechanical and moisture induced damage has been postulated as

$$\mathbf{S} = \left(1 - \xi_d\right)\left(1 - \xi_m\right)\mathbf{S}_0 \tag{2-14}$$

where ξ_m is the physical damage parameter due to diffusion and advective transport of moisture, ξ_d is the mechanical damage parameter due to pumping action and mechanical loading, and $\mathbf{S}_0$ is the strength before damage. After simulating the physical moisture-induced damage processes, the material characteristics are updated and then

communicated to CAPA-3D. The mechanical damage processes and material response for the given time are simulated using CAPA-3D. The damaged material properties and water pressure due to traffic loading are input back into RoAM and the process is repeated until the end of the designated simulation time (Kringos 2007).

2.8 Conclusion

In this chapter moisture-induced damage was defined, the processes that contribute to damage and distress mechanisms that result from moisture-induced damage were discussed. The most common moisture susceptibility test, AASHTO T 283, measures the indirect tensile strength of a compacted asphalt mixture before and after moisture conditioning, but does not distinguish between cohesive and adhesive failure and does not provide information on the strength of the bond near the asphalt-aggregate interface.

Based on information from the literature review, the two primary failure modes that occur in an asphalt mixture as a result of moisture are identified as cohesive failure within the asphalt binder and adhesive failure between binder and aggregate. An important parameter to the two common modes of failure is bond strength between asphalt and aggregate. In addition to tensile stresses due to moisture ingression in asphalt mixture components, traffic loading induces tensile stresses within the mixture so a method to quantify bond strength directly between asphalt and aggregate by direct tension is necessary.

The modified pull-off test method has been shown to effectively measure bond strength and the loss of bond strength due to moisture between asphalt and various substrates. For glass substrates, the pull-off test can distinguish between cohesive failure

within the asphalt binder and adhesive failure at the interface after moisture conditioning. The modified pull-off test method has the potential to routinely be used to compare materials and their resistance to moisture. The mechanical bond strength as measured by the pull-off test provides a value for maximum fracture strength which may be used along with moisture-related parameters to quantify damage at the asphalt-aggregate interface.

A single test method cannot satisfactorily predict moisture-induced damage and is not applicable to a wide-range of materials and conditions. The design of an asphalt mixture to mitigate moisture-induced damage should be approached in a systematic manner with a combination of objective methods such as empirical procedures that quantify physical, mechanical and chemical properties and computational methods that model material response. In order to predict moisture-induced damage for many scenarios, these objective methods are within a larger framework that is based on risk and reliability principles.

CHAPTER III

FACTORS INFLUENCING BOND STRENGTH OF POLYMER MODIFIED ASPHALT BINDERS AND MASTICS[i]

3.1 Introduction

Moisture damage occurs in asphalt mixtures due to a combination of mechanical loading and moisture. There are three mechanisms in which moisture degrades a mixture: (1) loss of cohesion within the asphalt mastic; (2) failure of the adhesive bond between aggregate and asphalt (referred to as stripping); and (3) degradation of the aggregate. Loss of cohesive or adhesive (i.e. bond) strength results in weakening of the asphalt matrix, which may lead to loss of stiffness and strength. As a result of matrix strength loss, moisture damage can manifest itself through permanent deformation (i.e. rutting) as well as cracking.

In Chapter II, it was acknowledged that there is not an accepted test to determine the bond strength of asphalt binders and the influence of moisture on bond strength of asphalt materials. In fact, Superpave® binder specifications do not include a method to evaluate adhesive characteristics of asphalt binders. A modified version of the pull-off test method has been used in the asphalt research industry to measure adhesive properties of asphalt binders and evaluate their ability to resist moisture (Kanitpong and Bahia 2005, Kanitpong and Bahia 2003, Nguyen, et al. 1996, Youtcheff and Aurilio 1997).

[i] Parts of this chapter are from "Moisture Sensitivity of Modified Asphalt Binders" by Audrey Copeland and Jack Youtcheff, accepted for publication in *Transportation Research Record: The Journal of the Transportation Research Board*, 2007.

Asphalt binders are commonly modified to improve binder properties and performance. For example, polymers have been used to extend the high- and low-temperature grade range for asphalts or address specific service conditions such as high volume traffic loading (Bahia, et al. 2001). As part of the National Cooperative Highway Research Project (NCHRP) 90-07 "Understanding the Performance of Modified Asphalt Binders in Mixtures", the performance of mixtures containing polymer-modified asphalt binders with the same Superpave® Performance Grade (PG), but with different chemistries due to mode of modification, was evaluated. These binders present a unique opportunity to evaluate adhesive characteristics without influence of varying PGs.

The objectives of this chapter are to determine influence of modification, moisture conditioning, and aging on bond strength of asphalt binders and mastics using the pull-off test. The influence of each factor is determined by statistically analyzing available pull-off data. Using results of the statistical analysis, the following questions are also addressed:

1) Is the pull-off test repeatable for modified asphalt binders and mastics?
2) Can the pull-off test distinguish between binders and mastics with different modifications?
3) Does the pull-off test provide meaningful results?

3.2 Experiment Details

3.2.1 Bond Strength Definition and Experimental Factors

The adhesive characteristics of asphalt binder and mastic were determined by measuring the maximum tensile strength of binder and mastic applied to a substrate.

Bond strength is defined as the mean tensile stress at failure and designated as Pull-Off Tensile Strength (*POTS*). The effects of moisture conditioning, modification (i.e. binder type), and aging on the bond strength of asphalt binder and mastic were evaluated. Moisture conditioned samples were soaked for four, eight, and twenty-four hours. Eleven different binders were tested and six of those eleven binders were combined with mineral filler to make mastic. Binder and mastic properties are discussed below in the section titled "Materials".

The influence of aging on binder is determined by aging binders in a Pressure-Aging Vessel (PAV) for thirty and forty hours. The PAV-aging standard practice protocol involves the exposure of the asphalt binder to a temperature of 100^{o} C (212^{o} F) for 20 hours (AASHTO 2002). The binder after this laboratory aging condition is presumed to represent the aging conditions that occur in the pavement after seven to ten years of service. In order to understand how the binder would perform after extended years of service beyond seven to ten years, laboratory PAV-aging conditions were altered to arbitrarily chosen thirty hours and forty hours of aging time. Binders aged for thirty hours (PAV 30) were tested in the dry condition. Binders aged for forty hours (PAV 40) were tested dry and select binders were tested after moisture conditioning.

3.2.2 Materials

Three unmodified asphalt binders with different performance grades (PG) and eight modified binders with the same PG were tested. Their description is given in Table 1 and Superpave® PG descriptions are provided in Table 2. The binders were graded at Turner-Fairbank Highway Research Center (TFHRC) and the base binder was

determined to be a PG54-33. The numbers 54-33 indicate the maximum, 54, and minimum (-33) temperatures in degrees Celsius that the binder specification tests are run at. According to the Superpave® grading system where the binders are graded within six temperature degree differences, the binder is designated as a PG52-28. This means the binder is specified to perform in conditions where the average seven day maximum pavement design temperature is less than fifty-two degrees Celsius and the minimum pavement design temperature is negative twenty-eight degrees Celsius. The grade provided by the supplier, however, was PG52-34. The polymer-modifed binders were obtained by modifying a PG52-28, a PG64-28 binder or a combination of the two to achieve the target grade, PG70-28. The term "grafted" designates that the polymers are chemically reacted with the asphalt binder (Stuart and Youtcheff 2002).

Six of the eleven binders were chosen to make mastic: three unmodified and three modified. The six binders are: PG54-28, PG64-28, PG70-28, Airblown, Elvaloy, and EVA-g. Two aggregates were chosen from the Strategic Highway Research Program (SHRP) Materials Library, Limestone labeled RD and Lithonia Granite labeled RA, and were combined with asphalt binders to make mastic. RD Limestone has low absorption properties and is generally considered to perform well under moisture conditions. RA Lithonia Granite is considered a stripping aggregate (Robl, et al. 1991). However, these properties do not necessarily apply to material classified as filler. An additional aggregate, Diabase from Sterling, Virginia, was also used to make mastics.

The fine aggregate material for each filler that passes the #200 sieve (75 μm) was combined with the asphalt binders at two different levels: six and thirty-one percent by weight. Six and thirty-one percent represent two extreme amounts of filler present in

binders. About thirty percent is recognized as the average level observed in asphalt mixtures (Shenoy 2001). To prepare the mastic, the aggregate was combined with the binder by heating the binder sample in a beaker on a hot plate with a temperature ranging from 45 to 70^{o} C (113 to 158^{o} F) and adding the aggregate. The mixture was stirred until the aggregate was distributed with the binder (Ogunsola, et al.).

Table 1. Descriptions of Asphalt Binders (Stuart and Mogawer 2002)

Name of Asphalt	Percent Polymer	PG of Base Asphalt	Description Provided by Source	Trade Name	Source
Unmodified Asphalts	0	Not Applicable	PG52-34, PG64-28, PG70-22	Not Applicable	Citgo Asphalt Refining Co.
Air-blown Asphalt	0	52-34	Air-blown Asphalt without Catalyst	Not Applicable	Trumbull and Owens Corning
Elvaloy	2.2	50% 52-34 50% 64-28	Ethylene Terpolymer	Elvaloy	DuPont
SBS Linear	3.75	58.9% 52-34 41.1% 64-28	Styrene-Butadiene-Styrene	Dexco Vector 2518	TexPar Labs and Johns Manville
SBS Linear Grafted	3.75	58.9% 52-34 41.1% 64-28	Styrene-Butadiene-Styrene and 0.05% Additive	Dexco Vector 2518	TexPar Labs and Johns Manville
SBS Radial Grafted	3.25	58.9% 52-34 41.1% 64-28	Styrene-Butadiene-Styrene and 0.05% Additive	Shell 1184	TexPar Labs and Johns Manville
EVA	5.5	52-34	Ethylene Vinyl Acetate	Exxon Polybilt 152	TexPar Labs and Johns Manville
EVA Grafted	5.5	52-34	Ethylene Vinyl Acetate and 1.35% Additive	Exxon Polybilt 152	TexPar Labs and Johns Manville
ESI	5.0	52-34	Ethylene Styrene Interpolymer	ESI	Dow and PRI

Table 2. Performance Grades of Asphalt Binders (Stuart and Mogawer 2002)

Trade Name:	**PG 52 Unmodified**	**PG 64 Unmodified**	**PG 70 Unmodified**	**Air-blown Asphalt**	**Elvaloy**	**EVA**
PG[a]:	52-28	64-28	70-28	70-28	70-28	70-28
Continuous PG[b]:	54-33	67-28	71-28	74-28	76-31	70-31
PG from supplier[c]:	52-34	64-28	70-22	73-28	74-29	73-31
Original Asphalt Binder Temperature at a $\|G^*\|/\sin\delta$ of 1.00 kPa and 10 rad/s, ^oC	55	67	73	74	76	70
RTFO Residue Temperature at a $\|G^*\|/\sin\delta$ of 2.20 kPa and 10 rad/s, ^oC	54	67	71	74	77	75
RTFO/PAV Residue Temperature at a $\|G^*\|\sin\delta$ of 5000 kPa and 10 rad/s, ^oC	8.1	20	24	21	14	13
BBR Temperature at a Creep Stiffness of 300 MPa and 60 s, $^oC + 10^oC$	-33	-28	-28	-29	-31	-31
BBR Temperature at an m-value of 0.30 and 60 s, $^oC + 10^oC$	-36	-30	-29	-28	-33	-31
Critical Cracking Temperature from the BBR and Direct Tension, ^oC	-35	-28	-27	-28	-34	-31

Trade Name:	**EVA Grafted**	**SBS Linear**	**SBS Linear Grafted**	**SBS Radial Grafted**	**ESI**
PG[a]:	70-28	70-28	70-28	70-28	70-28
Continuous PG[b]:	73-31	72-31	72-33	71-32	76-31
PG from supplier[c]:	75-31	72-28	74-29	73-28	Unknown
Original Asphalt Binder Temperature at a $\|G^*\|/\sin\delta$ of 1.00 kPa and 10 rad/s, ^oC	76	75	75	74	77
RTFO Residue Temperature at a $\|G^*\|/\sin\delta$ of 2.20 kPa and 10 rad/s, ^oC	73	72	72	71	76
RTFO/PAV Residue Temperature at a $\|G^*\|\sin\delta$ of 5000 kPa and 10 rad/s, ^oC	14	18	15	16	9.2
BBR Temperature at a Creep Stiffness of 300 MPa and 60 s, $^oC + 10^oC$	-32	-32	-33	-32	-31
BBR Temperature at an m-value of 0.30 and 60 s, $^oC + 10^oC$	-31	-31	-34	-32	-31
Critical Cracking Temperature from the BBR and Direct Tension, ^oC	-33	-33	-34	-34	-29

[a]Superpave® Performance Grade designation
[b]Measured Performance Grade
[c]Performance Grade provided by binder supplier

3.2.3 Specimen Preparation and Test Procedure

The procedure developed by Youtcheff and Aurilio (1997) was followed to prepare the test specimens. A porous, ceramic stub that allows water to migrate consistently through to the asphalt film is applied to the pull-stub using two-part epoxy glue. A small sample of asphalt (< 10 grams) is mixed with one percent (by weight) 200 μm glass beads to ensure uniform film thickness. The sample is heated to about 100° C (212° F) using a hot plate. The sample is then applied to the ceramic and the pull-stub is pressed onto a glass substrate by the test operator. Soda glass plates with dimensions of 51 x 51 x 6.35 mm (2 x 2 x ¼ in) were used as substrates. Each test specimen, was cured at room temperature, about 22° C (71.6° F), for twenty-four hours.

Dry specimens (i.e. zero hours soak time) were tested after curing. Specimens that were moisture conditioned were immersed in distilled water at 25° C (77° F), withdrawn from the water bath at four, eight, and twenty-four hours soak time, and immediately tested. Using the PATTI device and a chart recorder, the burst pressure (*BP*) necessary to debond each specimen at room temperature was measured. The *POTS* in psi for each specimen was calculated using Equation 2-13.

3.3 Results and Statistical Analysis of Pull-Off Strength Data

The mean *POTS* is the average of a minimum of four specimens and henceforth will be referred to simply as *POTS*. The results including means and coefficients of variation (*CV*) are given in Appendix A in Table A 1. A chart of the pull-off test results for binders in the dry condition and for each soak time is given in Figure 13(a). The binders were ordered from highest *POTS* to lowest *POTS* in the dry condition. The *CV*

was calculated for each sample set and combined for all binders. Table 3 lists the average *CV*s in percent for the binders and *N* is the number of specimens tested. For specimens tested dry, the *CV* is 3.29 %, which is the lowest *CV* compared to the moisture conditioning times. This implies that the pull-off test method is more precise when testing dry samples. The highest *CV* is 6.73 % after twenty-four hours of soak time. This is due to a large *CV* for SBS-radial grafted (18.87 %). The *CV* for each moisture conditioning time is within two percent of each other. When all specimens subjected to moisture conditioning are considered, the *CV* is 5.82 %. Although the number of independent variables is kept to a minimum, it may be difficult to correlate between successive tests causing reproducibility to be a concern. However, based on the individual *CV* results and average *CV* results (all less than seven percent), the pull-off test method is considered repeatable for modified asphalt binders.

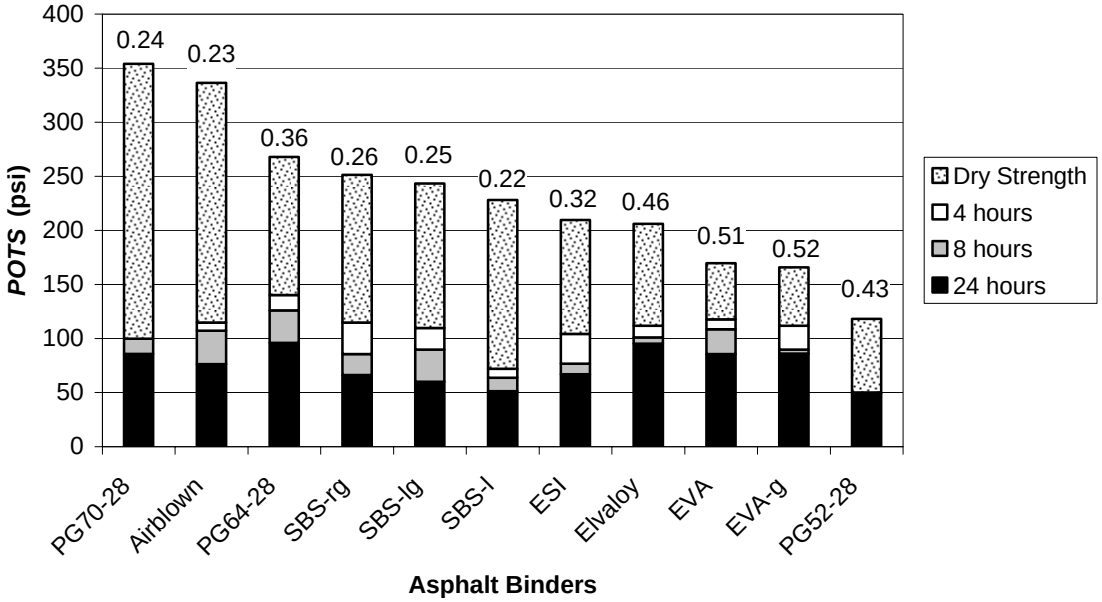

NOTE: The number at the top of each column is the ratio of $POTS_{wet}$ to $POTS_{dry}$.

(a)

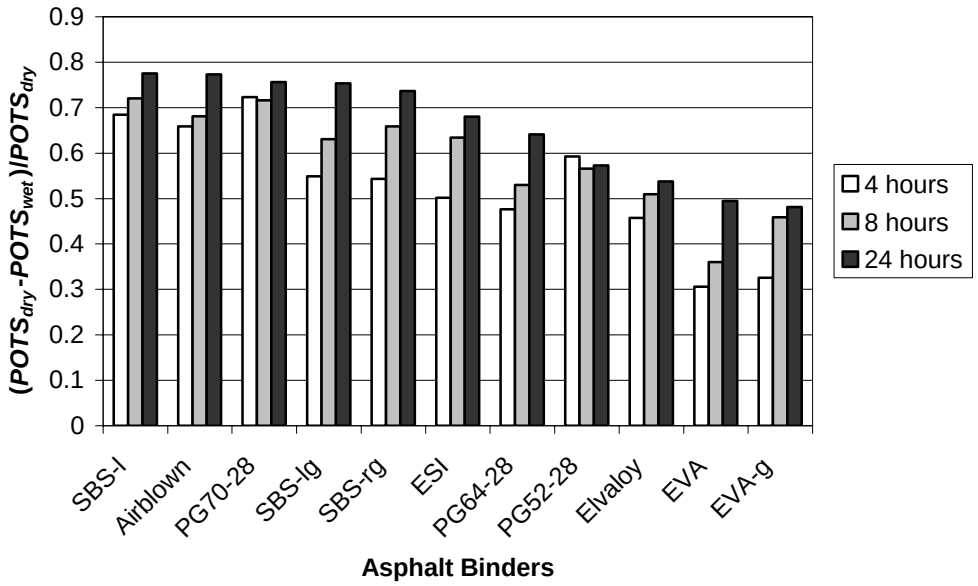

(b)

Figure 13. Pull-off Test Results Illustrating Modification and Moisture Conditioning Effects: (a) Absolute *POTS* Values; (b) Ratio Values for $(POTS_{dry}\text{-}POTS_{wet})/POTS_{dry}$

Table 3. Number of Specimens Tested (*N*) and Coefficients of Variation (*CV*) for Each Soak Time

Binder Type	**0 hours**		**4 hours**		**8 hours**		**24 hours**	
	N	*CV (%)*	*N*	*CV (%)*	*N*	*CV (%)*	*N*	*CV (%)*
Airblown	4	0.7453	4	8.2482	4	5.8662	4	6.2782
PG64-28	9	5.582	4	5.7448	4	8.5724	4	7.3657
EVA	4	2.9499	6	8.3557	4	2.6606	3	6.4291
EVA-g	4	5.7103	6	4.3958	4	2.7855	4	0
Elvaloy	5	2.7674	6	3.3656	6	7.0011	6	6.9833
ESI	13	3.1392	3	7.3204	3	3.7653	5	8.5088
PG52-28	6	3.2682	5	5.951	6	0	6	4.2361
PG70-28	4	2.5286	4	2.5707	4	10.334	4	5.2478
SBS-l	5	2.193	5	3.8036	4	7.5092	4	4.878
SBS-lg	4	4.6313	4	2.2779	4	2.7855	6	5.2705
SBS-rg	4	2.7262	4	8.2482	5	6.4305	4	18.868
Sum *N* and Average *CV* (%)	**62**	**3.29**	**51**	**5.48**	**48**	**5.25**	**50**	**6.73**

3.3.1 Statistical Analysis Methodology

The influence of each factor on *POTS* was evaluated in two parts: first, a one-way ANalysis Of VAriance (ANOVA) was carried out to determine if *POTS* values for each factor are statistically equivalent. Second, factor levels were compared using a paired Student's *t*-test to determine if pairs of *POTS* values are significantly different. A paired Student's t-test at a statistical significance level of 0.05 was chosen based on the small number of specimens (i.e. four) tested to determine *POTS*, and a paired *t*-test was used since each individual test within a sample set is run on the same material. Two assumptions are made regarding the data: (1) the data is normally distributed and (2) variances among individual results and the overall response are equal.

The influence of each factor on *POTS* is determined by performing a one-way ANOVA based on the *F*-distribution to determine if *POTS* values are statistically

equivalent. Comparing *POTS* for each factor level where μ_i is the sample mean of the *i*th conditioning level, the following hypothesis is tested:

H_o: $\mu_1 = \mu_2 = \mu_3$

H_a: The mean *POTS* differ for at least two factor levels.

The test statistic, *F*, compares the variation among the treatment means to the sampling variability within each treatment.

$$F = \frac{\text{Mean Square for Treatments } (MST)}{\text{Mean Square for Error } (MSE)} \tag{3-1}$$

The rejection region is established based on degrees of freedom. The numerator degree of freedom is:

$$\upsilon_1 = (p - 1) \tag{3-2}$$

where *p* is the number of treatments and the denominator degree of freedom is:

$$\upsilon_2 = (\eta - p) \tag{3-3}$$

where η is the number of observations. Using υ_1 and υ_2 and percentage points of the *F*-distribution at a level of $\alpha = 0.05$ (Table IX, (McClave, et al. 2001)), the value of $F_{0.05}$ was determined at which to reject H_o if *F* (calculated by one-way ANOVA) is greater than $F_{0.05}$: if $F > F_{0.05}$, reject H_o.

3.3.2 Modification Effects

If the *POTS* values for unmodified and modified binders are determined to be statistically equivalent by one-way ANOVA, this implies that no difference between binder types were observed and the pull-off test may be unable to determine the influence of modification on bond strength. For each conditioning time, the *POTS* of each binder

type is significantly different at a *p*-value of 0.0001. The *p*-value is the observed significance probability, and since the *p*-value is less than 0.05, this implies that the individual binder means do not necessarily have more variation than the overall response mean (i.e. all binder data combined) and an ANOVA model is appropriate for the data. Since the *POTS* for each binder is statistically different, the pull-off test can determine the effect of modification on bond strength as determined by the pull-off test. Based on *POTS* results, asphalt binders were then ranked from highest to lowest bond strength in the dry, as well as, wet conditions, shown in Table 4. Ranking binders based on *POTS* values or by a percent reduction in *POTS* after moisture conditioning could be a useful tool to analyze binder bond strength and distinguish between good and bad performers.

The control binder, PG70-28, had the highest *POTS* at zero hours soak time. In the dry condition, modified binders have lower *POTS* than unmodified binders. PG52-28 has the lowest *POTS* at each conditioning time. Considering moisture conditioned samples, PG64-28 has the highest *POTS* at each soak time and SBS-linear has the lowest *POTS* if PG52-28 is excluded. Considering that PG64-28 has a lower PG grade than the control and modified asphalt binders, evaluating binders based on PG does not account for adhesive behavior and the influence of moisture. Stuart et al. (2002) noted that binders having the same PG provide varying adhesive characteristics.

Pairs of binders were compared using Student's *t*-test to determine if their individual means are significantly different. Based on calculated *p*-values, the binders whose means are statistically equivalent are identified in Table 4 by shades of gray or outlined in black. To illustrate, at zero hours of soak time, there are three pairs of binders with statistically equivalent means: (i) SBS-linear grafted and SBS-radial grafted (shaded

light gray, Columns 4 and 5)), (ii) Elvaloy and ESI (shaded medium gray, Columns 7 and 8), and (iii) EVA and EVA-grafted (shaded dark gray, Columns 9 and 10). At a soak time of twenty-four hours, there are five groups of binders with statistically equivalent means: (i) PG64-28 and Elvaloy, (ii) EVA-grafted, PG70-28, and EVA, (iii) ESI and SBS-radial grafted, (iv) SBS-radial grafted and SBS-linear grafted, and (v) SBS-linear and PG52-28. Binders modified with the same polymer but in different manners (e.g. SBS-linear grafted and SBS-radial grafted or EVA and EVA-grafted) appear to be statistically equivalent. In only one occurrence (soak time = eight hours) is EVA statistically different than EVA-grafted. As soak time increases, the number of binders and groups of binders with statistically equivalent mean *POTS* values increase. This suggests that an optimal soak time exists beyond twenty-four hours which the pull-off test does not accurately measure asphalt bond strength and thus does not distinguish among asphalt binders. This "optimal" time has not yet been determined.

Table 4. Binder Rankings and Identification of Binders with Statistically Equivalent *POTS*

Soak	**Highest *POTS* to Lowest *POTS***										
Time	**1**	**2**	**3**	**4**	**5**	**6**	**7**	**8**	**9**	**10**	**11**
0	PG70-28	Airblown	PG64-28	SBS-rg	SBS-lg	SBS-l	ESI	Elvaloy	EVA	EVA-g	PG52-28
4	PG64-28	EVA	Airblown	SBS-rg	EVA-g	Elvaloy	SBS-lg	ESI	PG70-28	SBS-l	PG52-28
8	PG64-28	EVA	Airblown	Elvaloy	PG70-28	EVA-g	SBS-lg	SBS-rg	ESI	SBS-l	PG52-28
24	PG64-28	Elvaloy	EVA-g	PG70-28	EVA	Airblown	ESI	SBS-rg	SBS-lg	SBS-l	PG52-28

NOTE: Binder means that are statistically equivalent are identified by shades of gray or outlined in black.

3.3.3 Mineral Filler

The results including means and Coefficients of Variation (*CV*) of *POTS* values are given in Appendix A in Table A 2. The *CV*s for each mastic and filler amount were combined and are provided in Table A 3 for the dry condition and each moisture conditioning time. The overall *CV*s for each soak time and amount of filler are all under ten percent. Thus, the pull-off test method is considered repeatable for mastics.

The addition of mineral filler has a significant effect on the bond strength (i.e. tested in the dry condition) as evidenced by the fact that the *POTS* for mastics decreased compared to the *POTS* for binders shown in Figure 14 for all cases except Elvaloy and RD, Elvaloy and RA, and EVA-g and Diabase at six percent. To determine the effect of adding mineral filler to asphalt binder to make mastic on *POTS*, *p*-values for each pair of variables (Neat, 6% filler, and 31% filler) were calculated. The mean POTS values for filler, proportions of zero, six, and thirty-one percent were compared in order to determine if the addition of filler to the binder has a significant effect on *POTS*.

When data for all binders are combined, the addition of RD filler is significant at a level of thirty-one percent as compared to binders without filler. At six percent, the difference between the means for neat binders versus the means for binders with RD is not significant. For Diabase, six percent filler is not significantly different than zero percent filler for PG52-28 and PG64-28. Overall, the combination of all binder data shows that the mean *POTS* of six percent Diabase is not statistically different from the mean *POTS* for zero percent Diabase. The mean *POTS* values at thirty-one percent for Diabase versus neat are all statistically different. Due to the majority of the differences

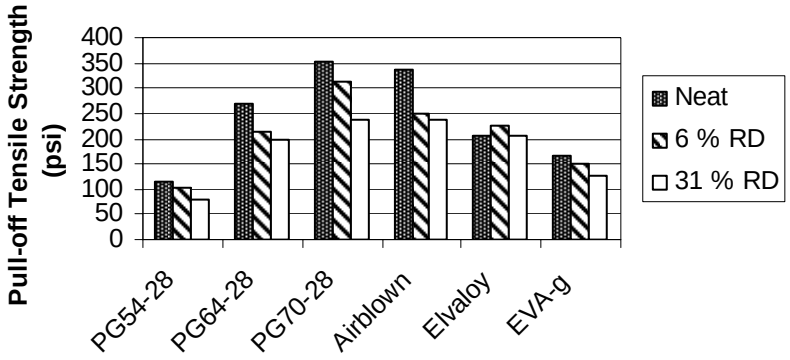

(a)

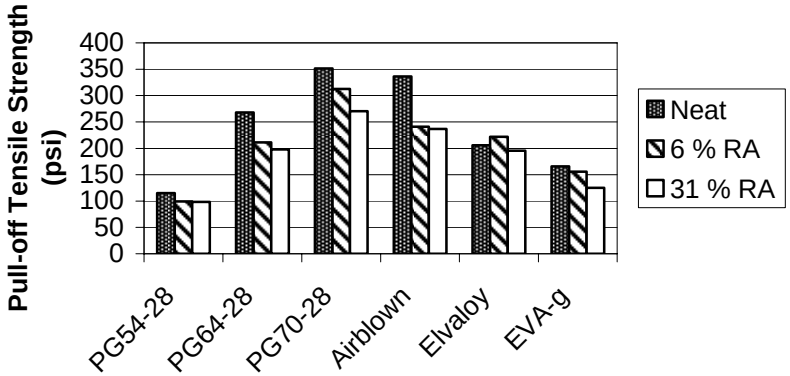

(b)

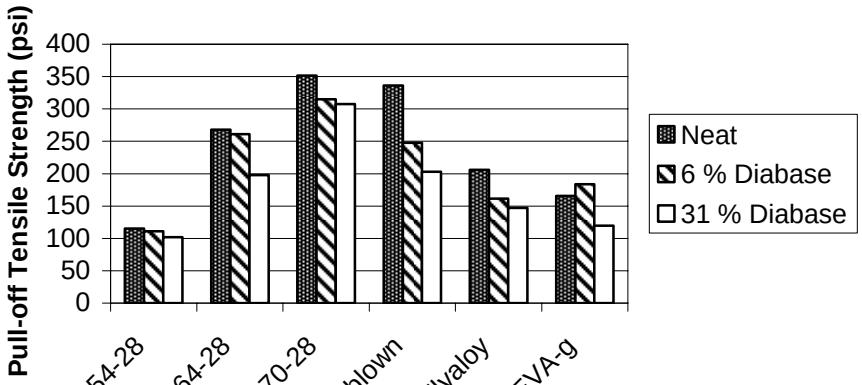

(c)

Figure 14. Pull-off Test Results Illustrating Effect of Mineral Filler on Cohesive Bond Strength: (a) Aggregate RA; (b) Aggregate RD; (c) Aggregate Diabase

in the means being significant, the addition of mineral filler to asphalt binders does have an effect on *POTS*. However, the addition of mineral filler in the amount of six percent has little affect on POTS compared to binder *POTS*. The addition of thirty-one percent mineral filler has a statistically significant effect on *POTS* compared to binder *POTS*. Table 5 gives the results for each aggregate: RD, RA, and Diabase. The results show that the addition of mineral filler to binder has a significant effect on *POTS*, in fact, the presence of mineral filler lowers *POTS* as compared to neat binders (i.e. no filler) as shown in Figure 14. This implies that the pull-off test method can distinguish between a neat binder and mastic (binder combined with mineral filler) in the dry condition. The addition of RD filler has a significant effect on the *POTS* for both six and thirty-one percent in every binder except one: Elvaloy at thirty-one percent. When the data for all binders are combined, the addition of RD is significant as compared to binders without filler. The addition of RA filler also has a significant effect on *POTS* in every case except EVA-g with six percent filler.

When data for all binders are combined, the addition of RD filler is significant at a level of thirty-one percent as compared to binders without filler. At six percent, the difference between the means for neat binders versus the means for binders with RD is not significant. For Diabase, six percent filler is not significantly different than zero percent filler for PG52-28 and PG64-28. Overall, the combination of all binder data shows that the mean *POTS* of six percent Diabase is not statistically different from the mean *POTS* for zero percent Diabase. The mean *POTS* values at thirty-one percent

Table 5. Effect of Filler and Filler Amount on Pull-off Tensile Strength

Aggregate RD							
	p-values						ANOVA
Binder Type	Neat - 6 %	Significantly Different?	Neat - 31 %	Significantly Different?	6 % - 31 %	Significantly Different?	Prob > F
Flux 6224	0.0015	yes	0	yes	0	yes	<0.0001
Base 6225	0	yes	0	yes	0.0113	yes	<0.0001
High 6226	0.0003	yes	0	yes	0	yes	<0.0001
Airblown 6227	0	yes	0	yes	0.1841	no	<0.0001
Elvaloy 6228	0.0003	yes	0.9334	no	0.0002	yes	0.0003
EVA-g 6233	0.0237	yes	0	yes	0.0039	yes	0.0003
All Binders Combined	**0.0381**	**yes**	**0.0014**	**yes**	**0.2531**	**no**	**0.0054**
Aggregate RA							
	p-values						ANOVA
Binder Type	Neat - 6 %	Significantly Different?	Neat - 31 %	Significantly Different?	6 % - 31 %	Significantly Different?	Prob > F
Flux 6224	0	yes	0	yes	0.7479	no	<0.0001
Base 6225	0	yes	0	yes	0.0406	yes	<0.0001
High 6226	0	yes	0	yes	0	yes	<0.0001
Airblown 6227	0	yes	0	yes	0.2356	no	<0.0001
Elvaloy 6228	0.0033	yes	0.0284	yes	0.0001	yes	0.0004
EVA-g 6233	0.0509	no	0	yes	0	yes	<0.0001
All Binders Combined	**0.0553**	**no**	**0.0022**	**yes**	**0.2591**	**no**	**0.0081**

Table 5. Effect of Filler and Filler Amount on Pull-off Tensile Strength (Continued)

Aggregate Diabase							
	***p*-values**						**ANOVA**
Binder Type	Neat - 6 %	Significantly Different?	Neat - 31 %	Significantly Different?	6 % - 31 %	Significantly Different?	Prob > F
Flux 6224	0.0923	no	0	yes	0.0013	yes	<0.0001
Base 6225	0.3099	no	0	yes	0	yes	<0.0001
High 6226	0	yes	0	yes	0.0809	no	<0.0001
Airblown 6227	0	yes	0	yes	0	yes	<0.0001
Elvaloy 6228	0	yes	0	yes	0.0723	no	<0.0001
EVA-g 6233	0.0206	yes	0	yes	0	yes	<0.0001
All Binders Combined	**0.0758**	**no**	**0.0007**	**yes**	**0.0853**	**no**	**0.003**

for Diabase versus neat are all statistically different. Due to the majority of the differences in the means being significant, the addition of mineral filler to asphalt binders does have an effect on *POTS*. However, the addition of mineral filler in the amount of six percent has little affect on POTS compared to binder *POTS*. The addition of thirty-one percent mineral filler has a statistically significant effect on *POTS* compared to binder *POTS*.

From the results of the paired Student's t-test, the effect of the amount (six percent versus thirty-one percent) of aggregate on *POTS* was determined. From the results above, the addition of thirty-one percent of filler by weight has a more profound effect on *POTS* than the addition of six percent filler by weight as compared to neat binders. Whether there is a significant difference between the addition of six percent

filler and thirty-one percent filler is of interest in determining the influence of mineral filler level on *POTS*. For the individual binders, the mean *POTS* for six percent filler are statistically different from the mean *POTS* for thirty-one percent filler in most cases except: Airblown and RD, Airblown and RA, PG54-28 and RA, PG70-28 and Diabase, and Elvaloy and Diabase. It is interesting to note that if all data are combined for each aggregate type, the amount of filler added (i.e. 6% vs. 31%) is not significantly different.

When the data for all binders are combined for each filler, though, the mean values are not statistically different.

3.3.3.1 Effect of Mineral Filler Type

The effect of aggregate type on *POTS* is evaluated by doing a paired *t*-test comparing the means for the addition of RA, RD, and Diabase at six and thirty-one percent respectively to each binder. Table 6 provides the *p*-values for each individual binder, the combined binder data, and the *p*-value results of a one-way ANOVA. First considering the addition of six percent aggregate by weight, for each binder and the combined binder data, RD's mean is not statistically different than RA's mean. This implies that both RA and RD have the same effect on *POTS* at a six percent filler level by weight. However, there is a significant difference between Diabase and RA and Diabase and RD for each binder except PG70-28 and Airblown. This implies that Diabase affects *POTS* differently than RA and RD does. For the binder data combined, though, there is not a significant difference between any aggregate.

In the case of the addition of thirty-one percent filler by weight, there is no significant difference between the mean *POTS* values for RA and RD except for binders PG54-28 and PG70-28. On the other hand, the differences between RA and Diabase are

significant except for PG54-28 and PG64-28 and the difference between RD and Diabase are significant except for PG64-28. Considering the combined data, there is no significant difference between filler types. From this analysis, the addition of RA versus the addition of RD to asphalt binders has an equal effect on *POTS*. This cannot be said for the addition of RA versus Diabase or the addition of RD versus Diabase. Using the limited amount of binders tested, the addition of Diabase to asphalt binders is assumed to have a different effect on *POTS* as compared to the addition of RD or the addition of RA. The pull-off test method is able to distinguish between neat (i.e. no filler) binder and mastic; however the pull-off test method may not be able to distinguish between filler types.

Table 6. Effect of Aggregate Type on *POTS* of Asphalt Binder

6% Filler							
	***p* -values**						**ANOVA**
Binder Type	RA - RD	Significantly Different?	RA - Diabase	Significantly Different?	RD - Diabase	Significantly Different?	Prob > F
Flux 6224	0.0578	no	0.0002	yes	0.0152	yes	0.0009
Base 6225	0.3078	no	0	yes	0	yes	<0.0001
High 6226	0.6687	no	0.3994	no	0.6687	no	0.6871
Airblown 6227	0.1483	no	0.3067	no	0.5787	no	0.3223
Elvaloy 6228	0.6835	no	0	yes	0	yes	<0.0001
EVA-g 6233	0.3864	no	0.0071	yes	0.0007	yes	0.0022
All Binders Combined	**0.9522**	**no**	**0.8457**	**no**	**0.7922**	**no**	**0.9628**
31% Filler							
	***p* -values**						**ANOVA**
Binder Type	RA - RD	Significantly Different?	RA - Diabase	Significantly Different?	RD - Diabase	Significantly Different?	Prob > F
Flux 6224	0	yes	0.2833	no	0	yes	<0.0001
Base 6225	1	no	1	no	1	no	1
High 6226	0.0003	yes	0.0001	yes	0	yes	<0.0001
Airblown 6227	0.7345	no	0.0016	yes	0.0005	yes	0.0011
Elvaloy 6228	0.0911	no	0	yes	0	yes	<0.0001
EVA-g 6233	0.1418	no	0.0406	yes	0.0028	yes	0.0098
All Binders Combined	**0.9819**	**no**	**0.6589**	**no**	**0.6326**	**no**	**0.8679**

3.3.3.2 Qualitative Analysis

The mastics followed a distinct trend when tested dry (i.e. zero hours). Table 7 gives the ranking of the mastics according to $POTS_{dry}$. PG70-28 forms the upper bound, ranked one, in six out of seven treatments whereas PG52-28 always forms a lower bound, ranked six. With the addition of fine aggregate mineral filler RA and RD, the binders maintain a similar ranking as they do with no modification (neat). From highest *POTS* to lowest *POTS* the following trend is established:

PG70-28 > Airblown > Elvaloy > PG64-28 > EVA-g > PG52-28.

For diabase filler the trend is similar with PG52-28 forming a lower bound for *POTS* and PG70-28 forming an upper bound. Airblown and PG64-28 appear to group together in the ranking as does EVA-g and Elvaloy.

As a further step the binders were then ordered from highest to lowest $POTS_{dry}$, the column labeled "neat" in Table 8, and the filler treatments were evaluated from highest $POTS_{dry}$ to lowest $POTS_{dry}$ for each binder. A trend is noticed with PG52-28 forming an upper bound followed by the aggregates at an amount of six percent and then finally thirty-one percent. There does not appear to be a way to distinguish between the types of aggregates except on the lower end which is as follows: 31 % RD > 31 % RA > 31 % Diabase (DIA).

Table 7. Rankings of Mastics in Dry Condition for each Filler Amount and Type from Highest $POTS_{dry}$ (1) to Lowest $POTS_{dry}$ (6)

Mastic	Neat	6% RD	31% RD	6% RA	31% RA	6% Dia base	31% Diabase
PG70-28	1	1	2	1	1	1	1
Airblown	2	2	1	2	2	3	2
Elvaloy	4	3	3	3	4	5	4
PG64-28	3	4	4	4	3	2	3
EVA-g	5	5	5	5	5	4	5
PG52-28	6	6	6	6	6	6	6

Table 8. Rankings of Mastics in Dry Condition from Highest $POTS_{dry}$ to Lowest $POTS_{dry}$.

Mastic	Highest Mean *POTS* Value → Lowest Mean *POTS* Value						
PG70-28	Neat	6% DIA	6% RD	6% RA	31% DIA	31% RA	31% RD
Airblown	Neat	6% RD	6% DIA	6% RA	31% RD	31% RA	31% DIA
Elvaloy	6% RD	6% RA	31% RD	Neat	31% RA	6% DIA	31% DIA
PG64-28	Neat	6% DIA	6% RD	6% RA	31% RD*	31% RA*	31% DIA
EVA-g	6% DIA	Neat	6% RA	6% RD	31% RD	31% RA	31% DIA
PG52-28	Neat	6% DIA	6% RD	31% DIA	6% RA	31% RA	31% RD

* Same ranking

3.3.4 Moisture Influence

Moisture lowers bond strength of asphalt binders. Referring again to Figure 13(a), for all binders, moisture conditioning decreased *POTS*. The ratio of *POTS* after twenty-four hours soak time ($POTS_{wet}$) to dry condition *POTS* ($POTS_{dry}$) is provided at the top of each bar in Figure 13(a). For those binders with high $POTS_{dry}$, such as Airblown and PG70-22, the ratio of $POTS_{dry}$ to $POTS_{wet}$ is less than that for binders with low $POTS_{dry}$ (e.g. EVA-grafted and Elvaloy). A higher $POTS_{dry}$ does not necessarily imply greater moisture resistance. From highest to lowest ratio of $POTS_{wet}$ to $POTS_{dry}$, the binders rank as follows: EVA-grafted > EVA > Elvaloy > PG52-28 > PG64-28 > ESI > SBS-radial grafted > SBS-linear grafted > PG70-28 > Airblown > SBS-linear.

After twenty-four hours soak time, each binder lost about half or more of its initial bond strength as shown in Figure 13(a). After some time, water is believed to be reaching the interface of the asphalt and glass by entering from the sides of the specimen as well as from the ceramic disc. Thus, twenty-four hours soak time may be too severe when glass substrates are used. The pull-off test captures the effect of moisture conditioning on the bond strength of asphalt binders; however uncertainty in bond strength measurement increases as a function of soak time and, as noted above, a threshold soak time for evaluating bond strength may exist. Therefore, the influence of soak time on bond strength was evaluated.

The influence of soak time on *POTS* is evaluated in two parts: first, a one-way ANOVA was carried out to ensure that the *POTS* for each binder after four, eight and twenty-four hours of soak time are different. Second, each pair of soak times (e.g. four and eight hours, eight and twenty-four hours) were compared using Student's *t*-test to

determine if individual soak times provide different results. Results are given in Table 9(a).

Table 9. Results of Statistical Analysis to Determine Moisture Influence on POTS: (a) One-Way ANOVA [Null Hypothesis (H_o) is *POTS* measured at 4, 8 and 24 Hours Soak Times are Equivalent]; (b) Student's t-test [Comparing Individual *POTS* for Each Pair of Soak Times]

(a)

Binder Type	υ_1	υ_2	$F_{0.05}$	F	**Reject H_o?**
PG54-28	2	14	3.74	3.5304	No
PG64-28	2	9	4.26	26.4365	Yes
PG70-28	2	9	4.26	5.0395	Yes
Airblown	2	9	4.26	32.8701	Yes
Elvaloy	2	15	3.68	11.8846	Yes
SBS-lg	2	11	3.98	390.8053	Yes
SBS-l	2	10	4.10	40.8265	Yes
SBS-rg	2	10	4.10	27.8233	Yes
EVA	2	10	4.10	18.0512	Yes
EVA-g	2	11	3.98	78.6535	Yes
Esi	2	8	4.46	40.3185	Yes

(b)

Binder Type	***p*-values**					
	4 & 8 hours	**Significantly different?**	**4 & 24 hours**	**Significantly different?**	**8 & 24 hours**	**Significantly different?**
PG52-28	0.0623	no	0.1689	no	0.5707	no
PG64-28	0.1138	no	0.0001	yes	0.0027	yes
PG70-28	0.6358	no	0.0452	yes	0.0186	yes
Airblown	0.1176	no	0	yes	0	yes
Elvaloy	0.0052	yes	0.0001	yes	0.1056	no
SBS-lg	0.0002	yes	0	yes	0	yes
SBS-l	0.0075	yes	0	yes	0.0005	yes
SBS-rg	0.0003	yes	0	yes	0.0059	yes
EVA	0.0648	no	0	yes	0.0009	yes
EVA-g	0	yes	0	yes	0.3428	no
Esi	0	yes	0	yes	0.0471	yes
All Binders	**0.0830**	**no**	**0.0001**	**yes**	**0.0373**	**yes**

For ten out of eleven (ninety-one percent) binders, we reject the null hypothesis that the *POTS* values corresponding to moisture conditioning time are equal. The pull-off test is able to determine the influence of soak time on bond strength of asphalt binders. In Table 9(b) the results of Student's *t*-test to compare *POTS* for pairs of moisture conditioning times are given. For more than half of the binders, the *POTS* at four hours is not statistically different than the *POTS* for eight hours. However, comparing *POTS* for eight and twenty-four hours, only three out of eleven (approximately twenty-seven percent) binders were not statistically different. If all binders are combined, the *POTS* at four hours is not statistically different than *POTS* at eight hours. The *POTS* for twenty-four hours, however, is statistically different than *POTS* at four and eight hours. Based on these results, a soak time greater than eight hours, but less than twenty-four hours (e.g. twelve hours) is recommended.

3.3.4.1 Mastics

Moisture conditioning decreases the *POTS* of mastics. Figure 15 shows the percent difference in *POTS* for specimens tested after twenty-four hours of moisture conditioning, $POTS_{wet}$, versus the *POTS* for specimens tested dry, $POTS_{dry}$, for each mineral filler type. After twenty-four hours of moisture conditioning, there is a percent loss in *POTS* (i.e. bond strength). Considering each aggregate type and soak time, the addition of mineral filler in the amount of six and thirty-one percent was compared to neat binder, as in Table A-4. Individual binders showed significantly different *p*-values; however, for all binders combined, the addition of six percent and thirty-one percent mineral filler was not significantly different than neat binders in all cases except six

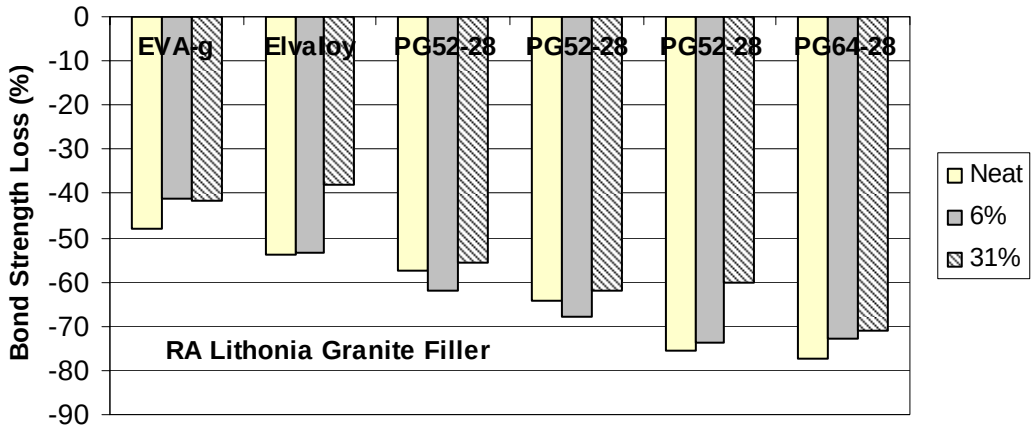

(a)

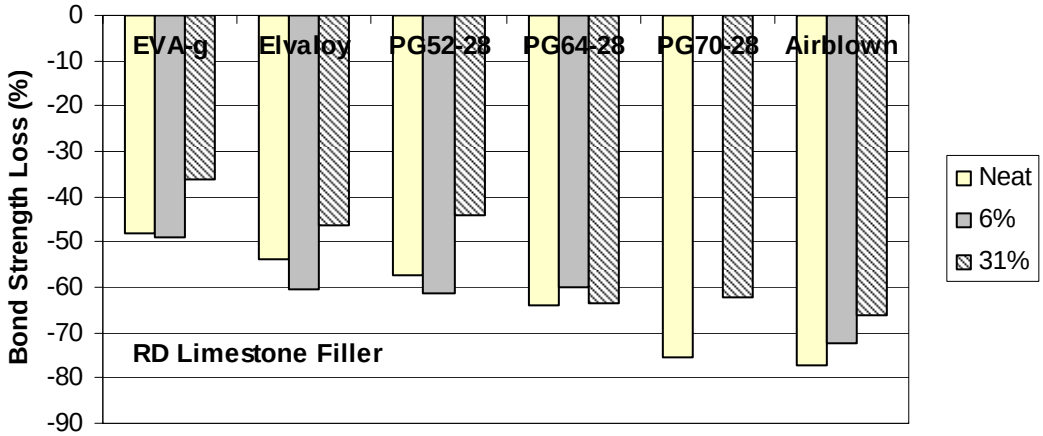

(b)

Figure 15. Percent Difference between $POTS_{wet}$ and $POTS_{dry}$ for Mastics
(a) RA Lithonia Granite
(b) RD Limestone
(c) Diabase

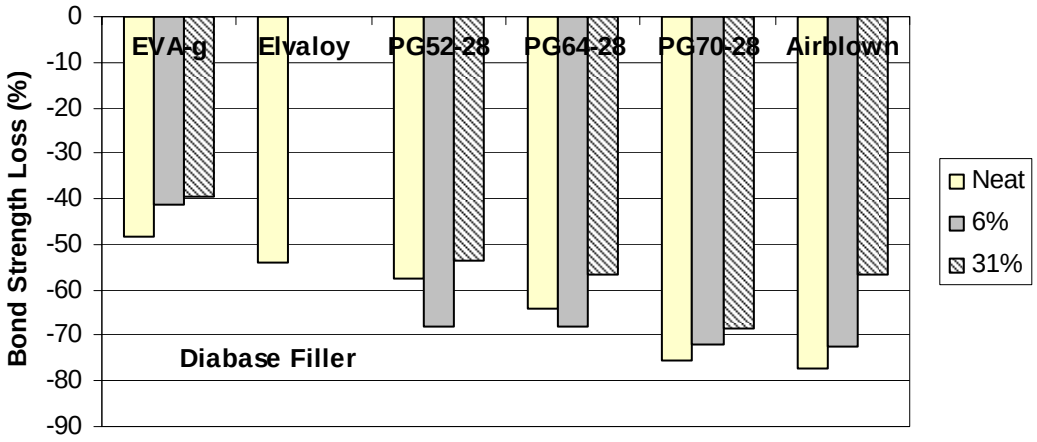

(c)

Figure 17. Percent Difference between $POTS_{wet}$ and $POTS_{dry}$ for Mastics (continued)
(a) RA Lithonia Granite
(b) RD Limestone
(c) Diabase

percent RA and RD at four hours of soak time. The addition of mineral filler appears to lower the *POTS* in the moisture condition, as well.

After moisture conditioning, according to the overall statistical results (Tables A-5 through A-8) for each moisture conditioning time and filler amount, there is not a significant difference between each filler type. Due to the fact that after moisture conditioning there is not a significant difference between the amount and type of filler, moisture conditioning is a more influential factor on bond strength than the addition of mineral filler.

3.3.5 Aging Effects

Figure 16 illustrates the effect of aging on $POTS_{dry}$ of asphalt binders. Aging data is provided in Appendix A in Table A 11 and Table A 12. PAV aging increases the *POTS* as compared to non-aged binders. Aging appears to have the greatest effect on asphalt binders with lower performance grade (e.g. PG64-28 and PG52-28). By calculating percent increase in *POTS* for aged versus non-aged binders and taking the average over all asphalt binders, the increase in *POTS* is more than thirty percent. The observed significance level from a one-way ANOVA analysis, provided in the last column of Table 7, confirm that *POTS* for each amount of aging is statistically different, thus, indicating that aging significantly influences *POTS* of binders.

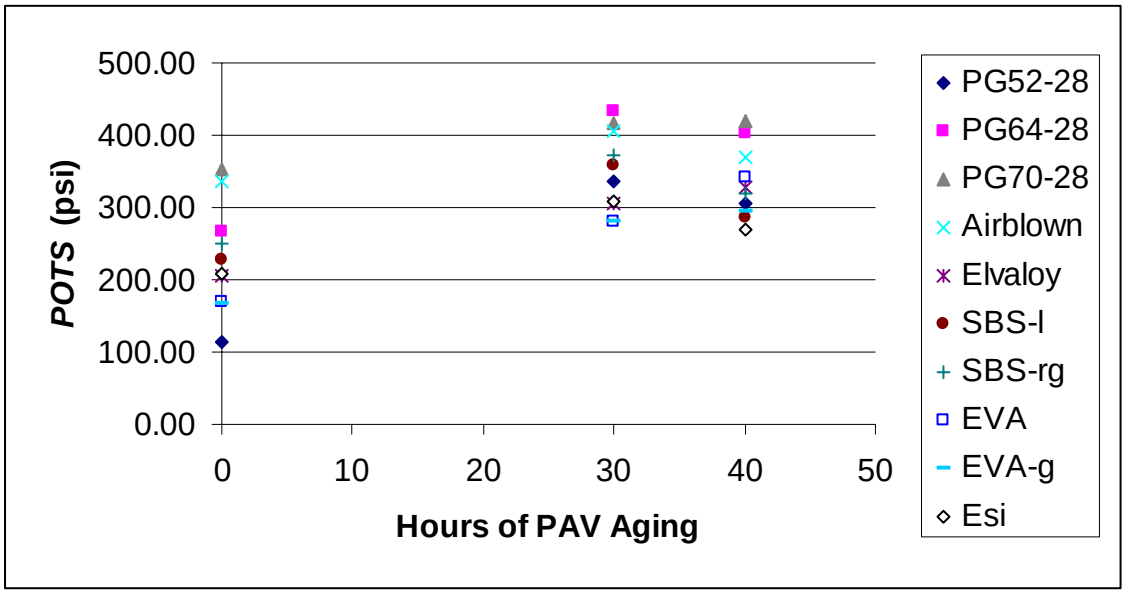

Figure 16. Influence of Laboratory Long-Time Aging on *POTS* of Asphalt Binders in Dry Condition

Using Student's *t*-test, a comparison was performed and the observed significance level (*p*-values) for each pair of independent variables is given in Table 10(a). According to the *p*-values, aging has a significant effect on *POTS* of binders as compared to no aging. However, there is no significant difference between the *POTS* for laboratory long-term aged binders for thirty hours and forty hours (i.e. PAV 30 and PAV 40).

3.3.5.1 Aging and Moisture Effects

Six of the eleven modified binders that were subjected to PAV 40 aging were subsequently submerged in a water bath for four, eight, and twenty-four hours soak time. The results are provided in Appendix A in Table A 12. Previous sections have shown that moisture conditioning decreases *POTS* and laboratory aging increases *POTS* of binders. Aging combined with moisture damage decreases *POTS* compared with no aging and no exposure to moisture of all binders tested. For four (PG64-28, PG70-28, SBS-linear, and SBS-linear grafted) out of six binders tested, moisture conditioning combined with laboratory aging decreased the *POTS* more than moisture conditioning alone. To confirm that moisture conditioning is a greater influence on *POTS* than aging, a Student's *t*-test compared the *POTS* values of unaged, moisture conditioned samples ($POTS_{wet\ on\ unaged}$) to laboratory aged, moisture conditioned samples ($POTS_{wet\ on\ aged}$). According to data shown in Table 10(b), for three out of six binders, the effect of moisture conditioning was not significantly different than the effect of moisture conditioning on *POTS* and aging. More importantly, for all data combined, the *p*-value for moisture conditioning compared to moisture conditioning combined with aging is

Table 10. Results of Student's *t*-test and One-way ANOVA to Determine Aging Influence on POTS: (a) Unaged Binder versus Laboratory Long-Term Aged Binders [PAV 30 and PAV 40]; (b) Unaged, Moisture Conditioned Binders Compared to Laboratory Aged, Moisture Conditioned Binders Soaked for Twenty-four Hours [PAV 40]

(a)

Binder Type	*p*-values			One-way ANOVA
	Unaged & PAV 30	Unaged & PAV 40	PAV 30 & PAV 40	Prob > *F*
PG54-28	0	0	0	<0.0001
PG64-28	0	0	0.0094	<0.0001
PG70-28	0.0083	0.0060	0.9633	0.0094
Airblown	0.0014	0.0460	0.0512	0.0046
Elvaloy	0	0	0.0616	<0.0001
SBS – lg	0	0	0.0240	<0.0001
SBS-l	0	0	0	<0.0001
SBS-rg	0	0	0	<0.0001
EVA	0	0	0.0026	<0.0001
EVA-g	0	0	0.0789	<0.0001
Esi	0.0002	0.0054	0.0355	0.0006
All Binders Combined	0	0	0.3164	<0.0001

(b)

Binder Type	$POTS_{wet\ on\ unaged}$ versus $POTS_{wet\ on\ aged}$	
	p-value	Significantly Different?
PG54-28	0.0022	yes
PG64-28*	0.0054	yes
PG70-28**	0.9635	no
Elvaloy	<0.0001	yes
SBS-lg*	1.0	no
SBS-l	0.2037	no
All Binders Combined	**0.3788**	**NO**

* Number of specimens tested (*N*) at twenty-four hours soak time is 2.
** Number of specimens tested (*N*) at twenty-four hours soak time is 1.

0.3788 and implies that they are not significantly different. Therefore, moisture conditioning is a dominant factor compared to aging.

3.4 Bond Strength and Resistance to Permanent Deformation

The strength of asphalt binders and mastics in the dry condition measured by the pull-off test can be related to binder and mastic resistance to permanent deformation as measured by the stiffness properties of the asphalt binder or mastic. The stiffness of asphalt binder is a function of its cohesive properties. Thus, a relationship between dry tensile strength as determined by the pull-off test and binder stiffness is hypothesized to exist.

At moderate temperature (i.e. ambient temperature), binders display elastic behavior as well as viscous. The stiffness of a binder is a function of the viscous and elastic components, see Figure 17, and quantified by the complex modulus, G^*, and phase angle, δ. Binder stiffnesses were measured using AASHTO TP 5 *Determining Rheological Properties of Asphalt Binder Using Dynamic Shear Rheometer* (DSR). The DSR uses a thin sample of asphalt binder placed between two plates. The lower plate is fixed and the upper plate oscillates back and forth at 1.59 Hz (10 rad/s). This value for frequency was chosen because it simulates shearing action corresponding to traffic at a speed of 90 km/hour (55 mph). Using the following equations G^* is calculated:

$$\tau_{max} = \frac{2T}{\pi r^3} \qquad \gamma_{max} = \frac{\theta r}{h} \qquad G^* = \frac{\tau_{max}}{\gamma_{max}} \tag{3-4}$$

where T: maximum applied torque

r: radius

γ_{max}: maximum resulting shear strain

θ: deflection angle

h: specimen height.

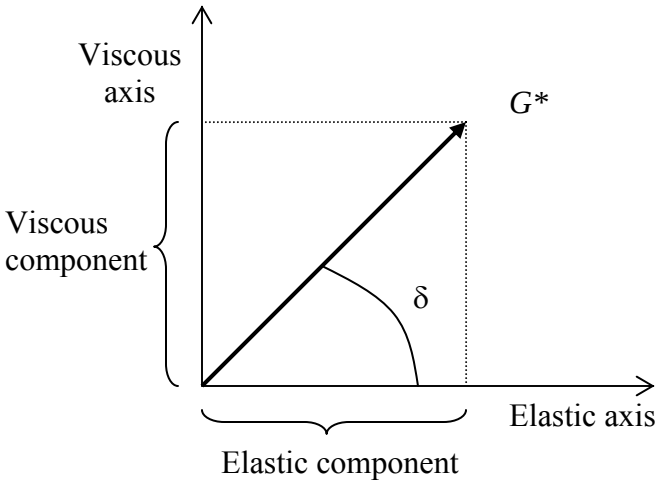

Figure 17. Complex Shear Modulus and Components Illustration

The phase angle, δ, is the lag in time (expressed in rad) between the maximum applied shear stress and the maximum resulting shear strain.

Data were generated for 19° C (66° F) and 25° C (77° F) using a time sweep at a frequency of 10 radian/s and is given in Appendix A in Table A 13. The two temperatures were chosen because pull-off testing occurs at room temperature which is between 19° (66° F) and 25° C (77° F). The specified Superpave® binder parameter is the complex modulus, |G*|, divided by sinδ, where δ is the phase angle. |G*|/sinδ was determined on original (i.e. unaged) material. The parameter |G*|/sinδ is used to grade asphalt binders according to their resistance to permanent deformation at high temperatures. The $POTS_{dry}$ was plotted versus |G*|/sinδ and is shown in Figure 18.

There is a linear relationship between $POTS_{dry}$ and permanent deformation as measured by |G*|/sinδ. For both 19° C (66° F) and 25° C (77° F), the R^2 value is equal to 0.7.

Binders' resistance to permanent deformation was generated using the DSR including |G*|/sinδ after aging binders thirty and forty hours in the PAV. The rheological data are first determined on Rolling Thin Film Oven Tested (RTFOT)-aged material and these are then used for determination of the temperature T_R at which |G*|/sinδ = 2.2 kPa. Next the rheological properties of the PAV-aged material at twenty, thirty and forty hours of aging are determined at this temperature of T_R. The data is given in Appendix A in Table 14 and is plotted against $POTS_{dry}$ for each binder shown in Figure 19(a) and Figure 19(*b)*. In both cases a linear relationship with R^2 equal to 0.77 is shown.

Absolute values were used instead of normalized values and are considered appropriate because it is theorized that a relationship exists between cohesive strength as measure by POTS and stiffness as measure by |*G**|/sinδ. Unfortunately data are unavailable to determine if there is a correlation that uses |*G**|/sinδ for the modified or aged binder that is normalized by the value of |*G**|/sinδ for the unmodified binder. The unmodified binders with varying grades were combined to create modified binders with the same PG grade, and those unmodified binders were unavailable for generation of rheological data. Second, if the rheological data is normalized, then the *POTS* data must also be normalized. The unmodified binders were unavailable for generation of *POTS* data for the same reason.

As expected, there is no linear relationship between $POTS_{wet}$ and resistance to permanent deformation (linear R^2 values were all less than 0.30) as determined using this data set. The standard binder specifications do not evaluate the bond strength of binders

before or after moisture conditioning. In order to properly evaluate moisture sensitivity of asphalt binders, a binder test that measures and evaluates adhesive strength is necessary.

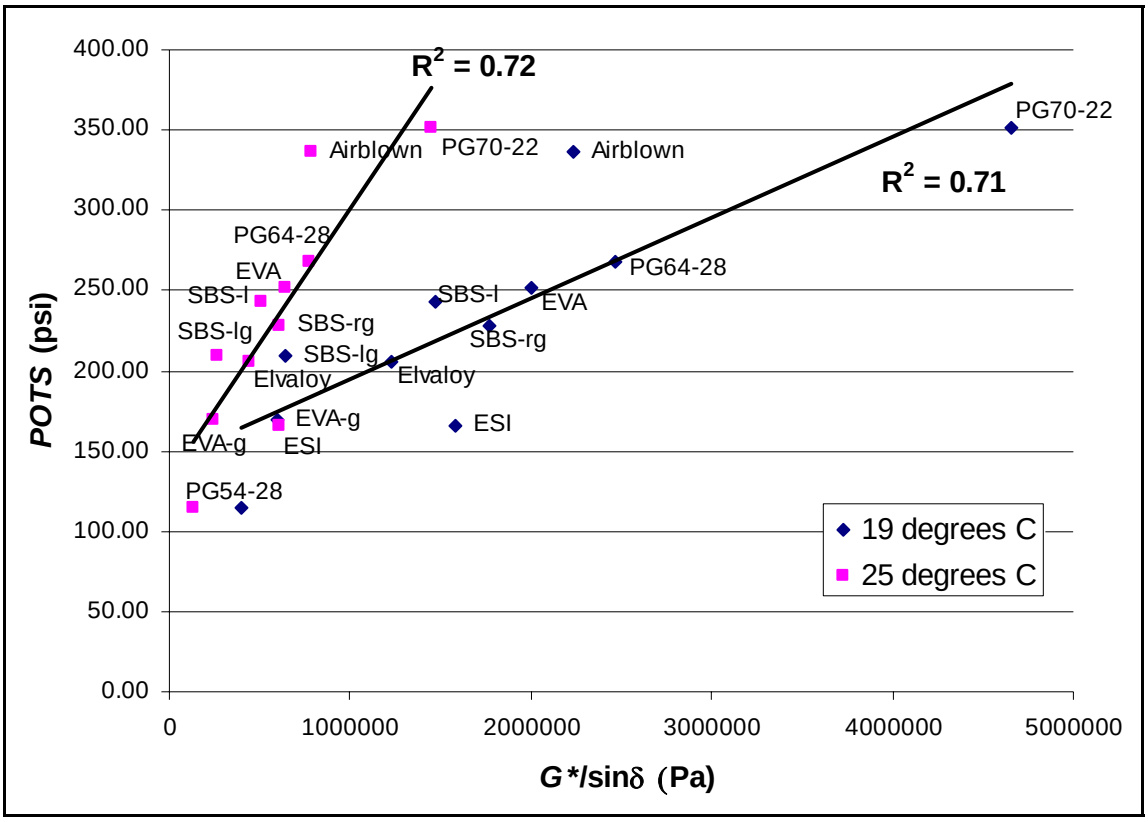

Figure 18. Relationship between *POTS* and G*/sinδ for Asphalt Binders.

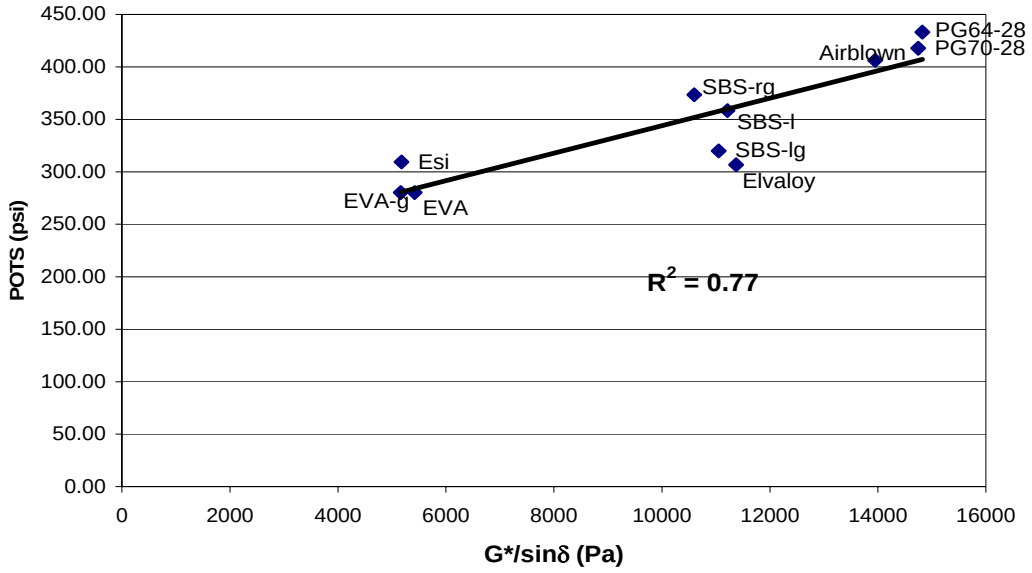

(a)

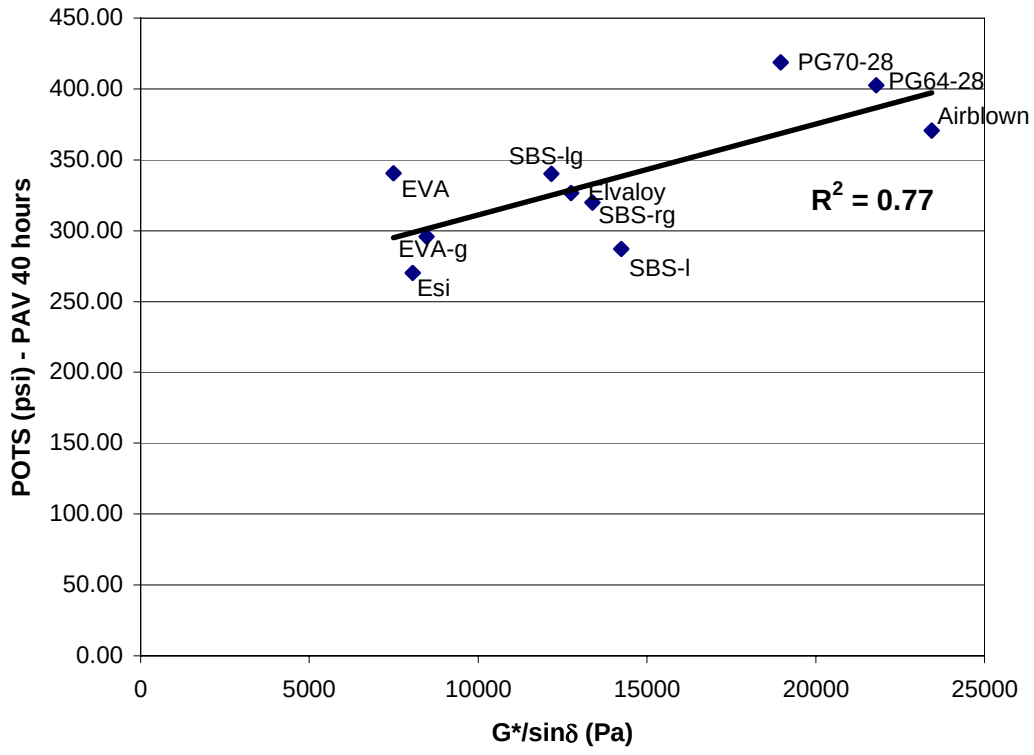

(b)

Figure 19. Relationship between $POTS_{dry}$ and G*/sinδ for Long-term Laboratory Aged Asphalt Binders: (a) PAV 30 hours; (b) PAV 40 hours

3.5 Comparison of *POTS* Results to Mixture Rutting Performance and Moisture Sensitivity

The rankings in Table 4 are not known to correspond to actual pavement stripping performance. Instead the binder rankings are strictly in regards to their ability to retain bond strength after moisture conditioning. Data from previous studies (Stuart 2002, Stuart and Mogawer 2002, Stuart, et al. 2002, Stuart and Youtcheff 2002) conducted at TFHRC to understand the performance of modified asphalt binders in laboratory mixtures was compared to *POTS* results for asphalt binders. Performance of asphalt mixtures was evaluated based on mixture resistance to permanent deformation and moisture sensitivity (Stuart and Mogawer 2002, Stuart, et al. 2002). Mixture resistance to permanent deformation has been determined using the following methods:

1.) Measuring $|G^*|/\sin\delta$ at 50^o C (122^o F) using the Superpave Shear Tester (SST) Frequency Sweep at Constant Height (FSCH),
2.) Cumulative permanent shear strain at 50^o C (122^o F) using the SST Repeated Shear at Constant Height (RSCH),
3.) Rut depths from the French Pavement Rut Tester (French PRT) at 70^o C (158^o F), and
4.) Creep slopes from the Hamburg Wheel-Tracking Device (HWTD) at 58^o C (136^o F).

For each method listed above, the results were plotted against *POTS* in the dry condition, however, no relationship was found between the method results and *POTS*. Due to the difference in test temperature between mixture performance tests ($50+^o$ C) and pull-off tests (25^o C) it is difficult to compare the results.

Moisture sensitivity of asphalt mixtures was measured by determining the number of wheel passes at five and ten mm rut depth. Mixtures are deemed sensitive to moisture if they experience greater than 10 mm rut depth after 20,000 wheel passes. A plot of the results of rut depth versus wheel passes measured at 58° C (136° F) is given in Figure A 1. The HWTD determined that Elvaloy was the only mixture that was not susceptible to moisture damage (i.e. less than 10 mm rut depth after 20,000 wheel passes) and Styrene-Butadiene-Styrene mixtures were most susceptible to moisture damage. Qualitatively this corresponds to results obtained by the pull-off test. Elvaloy had the second highest $POTS_{wet}$ after twenty-four hours soak time and third highest ratio of all binders. Excluding PG52-28, binders modified with SBS had the lowest $POTS_{wet}$ after twenty-four hours soak time. In addition, SBS-linear had the lowest $POTS_{wet}$ to $POTS_{dry}$ ratio and SBS-linear grafted and SBS-radial grafted had the lowest ratio for polymer-modified binders.

3.6 Conclusion

The pull-off test was found to be a repeatable method for measuring the bond strength of asphalt binders and mastics adhered to glass substrates and for assessing the effects of moisture on bond strength. Moisture decreases the adhesive properties of binders and mastics, and in this study is the most influential factor on bond strength. The pull-off test distinguished among binders that have the same PG but varying chemical properties due to modification and was able to rank binders and mastics according to how they may perform. Contrary to original thought, modification does not always increase binders' *POTS* after moisture conditioning. Thus, modification may not also increase a

binder's resistance to moisture damage. The addition of mineral filler to make mastics decreases the *POTS*. However there was no significant difference between filler types. Diabase filler, however, influenced *POTS* differently than RA or RD according to individual paired *t*-tests. Long-term laboratory aging increases cohesive strength of binders; however, long-term aging does not necessarily increase *POTS* after moisture conditioning.

A relationship exists between asphalt binder stiffness as determined by binder resistance to permanent deformation, $|G^*|/\sin\delta$, and cohesive bond strength ($POTS_{dry}$) of binders as measured by the pull-off test. However, no relationship exists between binder resistance to permanent deformation and bond strength after moisture conditioning ($POTS_{wet}$). Measures of binder stiffness do not reasonably relate to or predict adhesive characteristics of binder; and cannot be used to evaluate moisture resistance. The $POTS_{wet}$ results after twenty-four hours soak time ranked similar to results from the HWTD where Elvaloy ranked high in terms of resistance to moisture and SBS mixtures ranked lower.

Considering the results of this research, the pull-off test appears to be a promising method for measuring the bond strength of asphalt binders to determine moisture resistance. However, sources of variation include application of loading fixture to substrate (currently operator dependent), asphalt film thickness, and consistent curing and testing temperatures. In addition, aggregate material (i.e. rocks) is suggested for use as substrates rather than glass given that the properties of aggregates in asphalt mixture influence bond strength of binders. A key feature of the pull-off test is its ability to

quickly measure bond strength degradation after moisture conditioning to provide information regarding bond strength loss over time.

CHAPTER IV

THE USE OF THE PNEUMATIC ADHESION TEST TO DETERMINE BOND STRENGTH BETWEEN ASPHALT AND AGGREGATE

4.1 Introduction

The main failure modes related to moisture damage have been identified as (i) loss of adhesion between asphalt and aggregate, (ii) loss of cohesion within the asphalt mastic, or (iii) a combination of (i) and (ii). A critical parameter relevant to each failure mode is the mechanical (i.e. bond) strength between asphalt and aggregate, especially the loss of bond strength in the presence of water. During the Strategic Highway Research Program (SHRP) A-369 *Binder Characterization and Evaluation* project, aggregate surface was concluded to play a major role in bond strength and should be accounted for in any test that measures bond strength.

In Chapter IV, the bond strengths of asphalt binders and mastics were evaluated under direct tension using the modified pull-off test method. The pull-off test has been determined to be a quick, reliable method for measuring bond strength of asphalt binders and mastics (Copeland, et al. 2007, Youtcheff and Aurilio 1997). Further, the pull-off test can evaluate the effect of moisture on the bond strength of asphalt materials. The procedure quantitatively measures the bond strength of asphalt binders or mastics applied to a glass substrate using the Pneumatic Adhesion Tensile Testing Instrument (PATTI). Since aggregate properties play a major role in bond strength development, this chapter modifies the procedure developed in Youtcheff and Aurilio (1997) by replacing the glass

substrate with an aggregate substrate. Due to the simplicity of the PATTI device and its ability to isolate failure near the interfacial region between adhesive and substrate, the pull-off test has the potential for routine use to measure mechanical bond strength of asphalt binders applied to an aggregate substrate.

The goal of this chapter is to determine suitability of the pull-off test for use in determining pull-off (i.e. bond) strength of asphalt binders adhered to aggregate substrates. The specific objectives are:

1) Develop the methodology to replace glass substrates with aggregate substrates for the modified pull-off test method.
2) Evaluate the effect of curing and moisture on adhesion between asphalt binder and aggregate substrate.

These objectives are accomplished by: (i) defining how bond strength is determined between asphalt binder and aggregate, (ii) replacing glass substrates with aggregate substrates; (iii) characterizing aggregate substrate surface; (iv) establishing bond strength in unconditioned (i.e. undamaged) state and influence of cure time on bond strength, and (v) determining influence of moisture conditioning on bond strength between asphalt binder and aggregate.

4.2 Bond Strength of Asphalt-Aggregate Systems

The role of asphalt binder in an asphalt mixture is to uniformly coat the aggregate and bind the aggregate together. Essentially, asphalt binder behaves as an adhesive. Therefore, the theory of adhesion is applied to study Hot Mix Asphalt (HMA) bond strength (Bhasin, et al. 2006, Cheng, et al. 2001, Curtis, et al. 1993, Elphingstone 1997,

Harvey and Cebon 2003, Kanitpong and Bahia 2003). Consider two aggregates coated with a thin film of asphalt binder and attached to each other by the asphalt film as shown in Figure 20.

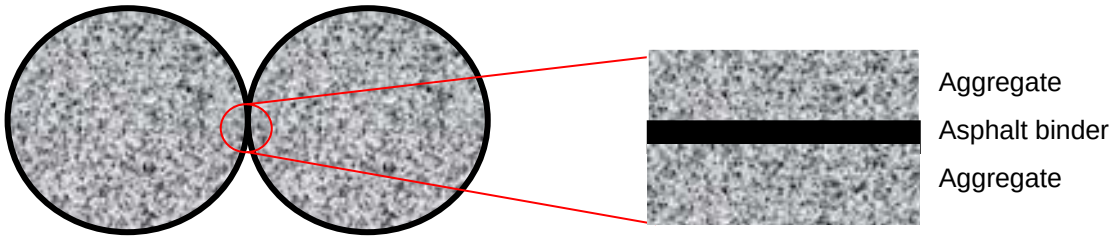

Figure 20. Asphalt-coated Aggregate Idealized as an Adhesive Joint

The bond between asphalt and aggregate can be idealized as an adhesive joint, and more specifically, a butt joint, where the binder is the adhesive and the aggregate is the adherend (Harvey and Cebon 2003). Failure can occur within the asphalt binder (loss of cohesion) or near the interface between the asphalt binder and aggregate (loss of adhesion, called stripping). In the PATTI device used here, The pull-off strength is determined by measuring the maximum tensile force that a surface area can bear before asphalt binder is separated from aggregate.

4.3 Experiment Details

The pull-off test is now modified so that aggregate substrates may be used and operator variability is removed. An experiment is designed to determine the bond strength between asphalt-aggregate pairs in the dry condition and after moisture conditioning. The experimental design is shown in Figure 21.

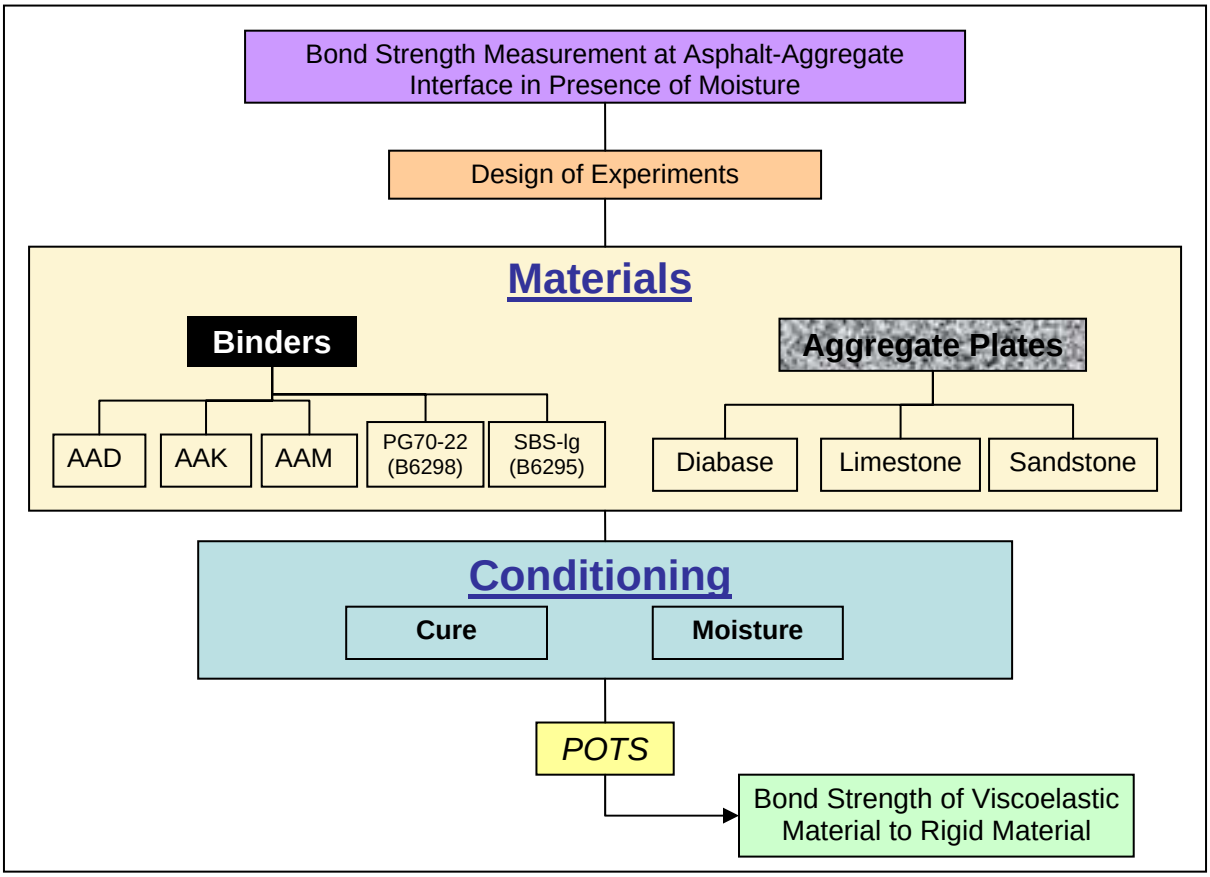

Figure 21. Experimental Design for Bond Strength Measurement between Asphalt Materials and Aggregate Substrate.

4.3.1 Materials

Four SHRP Materials Reference Library (MRL) binders (Jones 1993) were chosen: AAD, AAG, AAK and AAM. In addition, two binders used in FHWA's Accelerated Loading Facility (ALF) project were chosen: an unmodified PG 70-22 designated Control and a polymer modified Styrene-Butadiene-Styrene Linear Grafted (SBS-lg). The source and SHRP Performance Grade (PG) for each asphalt are provided in Table 11.

Table 11. Asphalt Binder Properties

Asphalt	Source	SHRP Grade
AAD-1	California Coastal	PG58-28
AAK-1	California Valley	PG64-10
AAM-1	West Texas Int.	PG64-16
Control (B6298)	Citgo Asphalt Refining Co.	PG70-22
SBS Linear Grafted (B6295)	TexPar Labs and Johns Manville	PG70-22

Three different stone types were obtained from regional quarries: diabase from Sterling, VA, limestone from Frederick, MD and Keystone sandstone from MD. More information on the aggregates is provided in Section 4.3.1.2 below.

4.3.1.1 Replacing Glass Substrates with Aggregate Substrates

To correctly determine bond strength between an asphalt binder and aggregate, an aggregate substrate or a substrate that has similar properties to aggregates should be used.

The use of stone substrates with the pull-off test was explored. The substrate used in the pull-off test method must have a flat surface large enough to accommodate and permit alignment of the loading fixture and rigid enough to support the counter force. The loading fixture has a diameter of 1 ¾ in (4.4 cm) so the substrate must be large enough to permit adequate clearance for placing the loading fixture.

To prepare aggregate plates, large hand boulders were obtained from quarries that provided each aggregate type. The boulders were cut into cubes using a large water-cooled saw and a smaller water-cooled saw with a 33 cm (13 in) diamond tipped blade. The sides of the cube were cut until they were determined to be perpendicular using a square. At this point, each cube's height varied, but its width and length were measured and cut to approximately 55 mm x 55 mm (2.17 in x 2.17 in). The height of the cube was then marked and cut every 12.7 mm (1/2 in) on center so the result is several plates of approximate dimensions slightly smaller than 55 mm x 55 mm x 12.7 mm (2.17 in x 2.17 in x ½ in).

In order to confidently compare specimens, the aggregate substrates must have precise geometries. After the cutting process, each specimen's geometry was measured using a method known as dimensional analysis to evaluate precision of the cutting process. The length, width and height were each measured in four different places using calipers for a total of twelve measurements per plate. The value for a specimen's length, width or height used for subsequent analyses is the average of the four measurements. The dimensions of each specimen are provided in Appendix B in Table B 1 and Table B 2. The average length, width and height, standard deviation and coefficient of variation (CV) for all diabase and limestone square plates combined are given in Table 12 and

Table 13. The height (i.e. thickness) of the specimens has the highest CV of 11.3 percent for diabase and 6.57 percent for limestone. The tolerance for all specimens is within one-third of an inch. The size of the saw presented difficulties in obtaining more precise heights.

Table 12. Dimensional Analysis Results for Square Diabase Plates

Sample ID	Length (mm)	Average Length (mm)	Width (mm)	Average Width (mm)	Height (mm)	Avgerage Height (mm)	Average Volume (cm^3)	M_{dry} (g)
Average	56.48	56.48	55.41	55.41	10.31	10.31	32.23	95.10
Std. Dev.	1.055	1.043	2.120	2.126	1.177	1.165	3.687	10.971
CV (%)	1.87	1.85	3.83	3.84	11.42	11.30	11.44	11.54
Minimum (mm)	53.96	54.04	50.55	50.89	6.82	7.33		
Maximum (mm)	58.21	57.86	59.91	59.73	13.68	13.39		
Difference (mm)	4.25	3.82	9.36	8.84	6.86	6.06		
Difference (in.)	0.17	0.15	0.37	0.35	0.27	0.24		

Table 13. Dimensional Analysis Results for Square Limestone Plates

	Length (mm)	Average Length (mm)	Width (mm)	Average Width (mm)	Height (mm)	Average Height (mm)	Average Volume (cm^3)
Average	56.82	56.82	55.64	55.64	7.02	7.02	22.20
Std. Dev.	0.672	0.691	0.567	0.597	0.456	0.461	1.430
CV (%)	1.18	1.22	1.02	1.07	6.49	6.57	6.44
Minimum (mm)	55.34	55.47	55.22	55.33	6.29	6.38	
Maximum (mm)	57.58	57.29	57.09	56.85	7.71	7.60	
Difference (mm)	2.24	1.82	1.87	1.52	1.42	1.22	
Difference (in.)	0.09	0.07	0.07	0.06	0.06	0.05	

Subsequently, a tile saw was obtained that permits water-cooled cutting of specimens, Figure 22. Cylindrical specimens were obtained using a coring device to save time. Coring the boulders, which requires only one cut, saves times as opposed to cutting the boulders into a cube which requires making six cuts. A device to hold the cylinder was designed for the tile saw that held specimen in place and allowed for more precise cutting. At the other side of the specimen a vacuum was applied to prevent the specimen from breaking off towards the end of the cutting process.

Using the improved cutting procedure with the coring device and tile saw, there is significant improvement in the precision of the geometry of the aggregate substrates. Each substrate is 7 cm (2 ¾") in diameter and its thickness can be varied depending on test requirements. Specimens were cut to a thickness of 6.35 mm (¼").

Figure 22. Tile Saw for Cutting Aggregate Plates

After conducting a pull-off test, a residual layer of asphalt is left on the stone plate in the area where the loading fixture was applied. Due to the amount of testing required,

rock plates should be reused. This layer of asphalt must be removed for further testing with the stone plate. There are several options for removing the residual asphalt from the surface. Previously in the pull-off test method, glass plates are put in an oxidizing oven and heated to 482^{o} C (900^{o} F) to melt the asphalt off. The plates are then cleaned with soap and glass cleaner, rinsed with distilled water and quickly rinsed with acetone to facilitate the drying process. Heating the substrates to remove the asphalt film is a quick, convenient method; however, due to the high temperature from the oxidizing oven the stones' nature may change including cracks occurring at the surface. In fact, upon placing several diabase stone substrates in the oxidizing oven, they were observed to change color from gray to dull brown. Another possibility for removing the residual asphalt is to use chemicals that dissolve asphalt.

Two methods, heat and chemical, were explored to remove residual asphalt from the stone substrate. Binders AAD and AAM were used to determine the effects of heat versus chemical cleaning of the rock substrates. Each binder was tested on rock substrates before cleaning (to establish a baseline) and after oven and chemical cleaning. The heat method involved placing the stone substrate in an oxidizing oven that reaches 482^{o} C (900^{o} F). During the heating process, the asphalt becomes a powdery substance which is then removed from the substrate using compressed air. The samples are then placed in an oven at 60^{o} C (140^{o} F) until further testing. During the chemical method, first the tested specimens were placed in a freezer to harden the layer of asphalt. The raised, hardened asphalt layer was then removed using a plastic knife so as not to scratch the surface. Each plate was rinsed with trichloroethylene until the asphalt layer on the specimen was removed and the solution ran clear. The specimens were then rinsed with

distilled water and acetone to facilitate the drying process. The specimens were kept in an oven overnight at 110° C (230° F) and then placed in a 60° C (140° F) oven until further testing. Due to the limited number of samples available to be subjected to the heat of the oven, only three specimens were tested for oven cleaning, except for AAM where the samples were tested three times for a total of nine tests.

In Table 14, the results of a statistical analysis used to determine if either cleaning method (heat or chemical) is different than the baseline results is provided. A one-way ANOVA was performed for each binder and soak time to determine the effect of cleaning on the *POTS*. The *p*-value is provided in column 3 of Table 14. Further, each cleaning method's mean was compared to the other cleaning method's mean by using a Student's *t*-test to compare pairs of means. Chemical cleaning is not significantly different than the baseline results. However, heat cleaning was found to be significantly different than baseline results in two sets of results. Subsequently, two more binders, SBS-lg (B6295) and PG70-22 (B6298), were tested in the dry condition to determine if there is a difference between the *POTS* values before and after chemical cleaning. There is no statistical difference between the *POTS* values for binders SBS-lg (B6295) and PG70-22 (B6298) before and after chemical cleaning. Based on these results, specimens were chemically cleaned specimens rather than oven cleaned.

Table 14. Statistical Analysis Data to Determine Stone Substrate Cleaning Method

Binder ID	Soak Time (hours)	ANOVA Prob > F	Cleaning Method Pairs					
			baseline-chemical		baseline-heat		chemical-heat	
			p-value	Significantly Different?	p-value	Significantly Different?	p-value	Significantly Different?
AAD	0	0.0287	0.2972	NO	0.04331	YES	0.0087	YES
	24	0.1899			0.1899	NO		
AAM	0	0.3275	0.7252	NO	0.17082	NO	0.2659	NO
	24	0.0361			0.0361	YES		
SBS-lg 6295	0	0.2237	0.2237	NO				
PG70-22 6298	0	0.5725	0.5725	NO				

The following surface cleaning process was used for stone substrates used in the pull-off test method:

1. Freeze stone plates for approximately thirty minutes. In the case of sticky asphalt, longer freezing times up to two hours may be required.
2. Remove specimens from freezer and using a thin, plastic knife (not metal so as not to scratch the surface) scrape excess asphalt from surface.
3. Using a pipette, rinse the area of the asphalt layer with trichloroethylene until the solution runs clear.
4. Finally, rinse each specimen with a small amount of acetone to facilitate the drying process.
5. Place specimens in an 110^{o} C (230^{o} F) oven to dry for at least twenty-four hours.

4.3.1.2 Aggregate Characterization

In order to gain insight into the surface characteristics of each aggregate, the Aggregate IMaging System (AIMS) device, Figure 23, was used to take images of the surface of each type of aggregate plate: diabase, limestone, and sandstone. Rectangular diabase plates were used that have been saw cut using 13" (33 cm) diameter diamond-tipped saw and cleaned. Circular limestone and sandstone plates were used that have been cut using the 10" (25.4 cm) diameter tile saw.

The AIMS device consists of a grid of dots on a backlit table. An aggregate is placed on each dot and a camera moves across the grid and takes images of the aggregate on top of each dot. After the images are taken, they are analyzed to determine surface texture.

In the first case, a diabase plate was set on each dot on the AIMS table. However, due to the size of the plates, some images contained a crack which is the space between two plates. The analysis was re-run and as the machine moves, a new plate was placed and centered over the dot before the image is taken. This procedure was followed for the sandstone and limestone plates, as well. This method provided images of the center of the stone plates where asphalt is applied during the pull-off test. In Figure 24 the result of surface texture analysis of each aggregate substrate is given. The results show that diabase has a rough texture that varies from low to high roughness. Limestone and sandstone have a polished texture. The AIMS analysis indicates that limestone and sandstone have similar textures which are in agreement with *POTS* results for each substrate type. However, AIMS indicates that limestone and sandstone have a more polished surface texture than diabase. The results from the pull-off test for diabase are

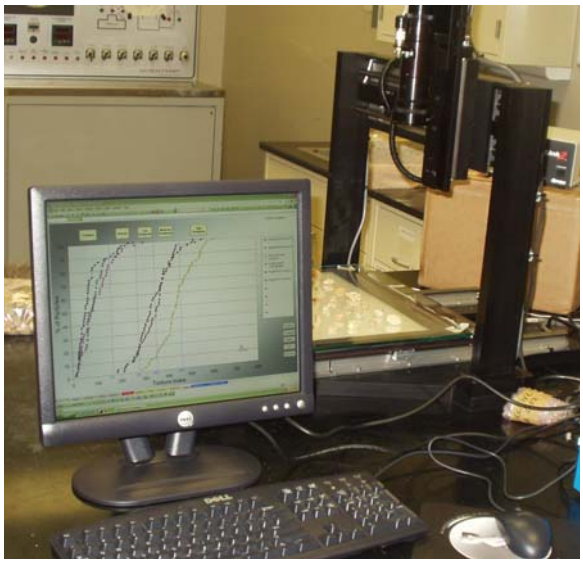

Figure 23. Aggregate IMaging System

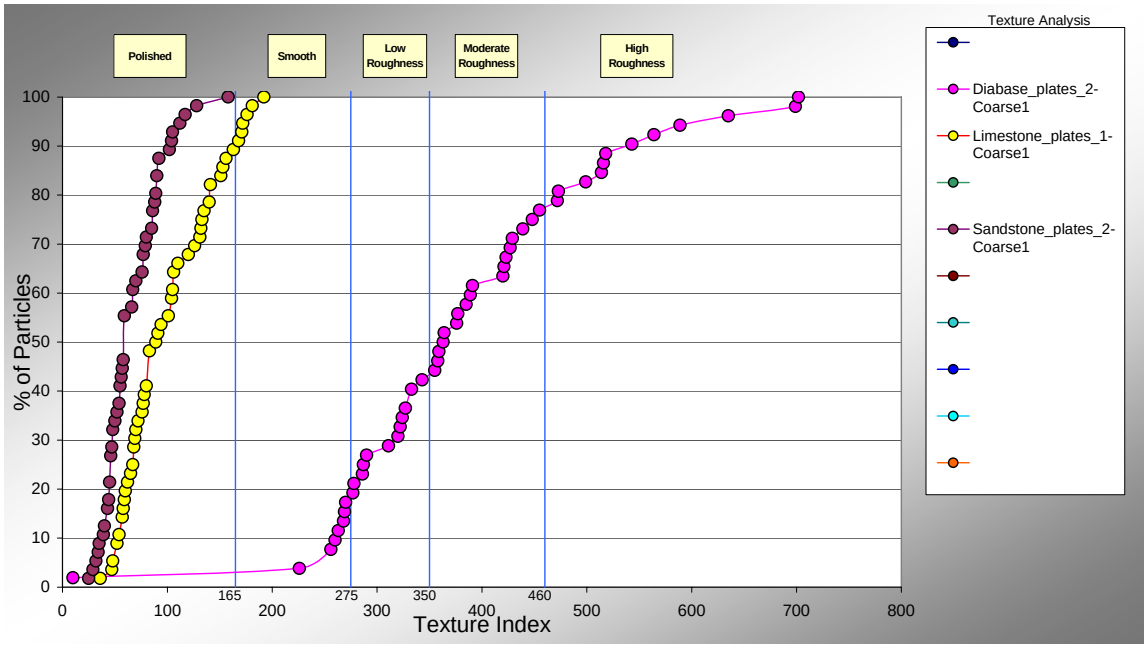

Figure 24. Texture Analysis on Aggregate Substrates

more in agreement with the results from glass plates indicating that diabase may have a polished surface similar to glass. Visual observation and touch also indicates that diabase's surface is more polished and smooth than limestone or sandstone. The use of saw cut aggregate plates to analyze surface texture using AIMS highlights possible limitations of using imaging to determine surface texture of aggregates.

Each aggregate type was analyzed using a Scanning Electron Microscope (SEM) equipped with an Energy Dispersive X-ray fluorescence spectrometer (EDX). The SEM is an Amray instrument, Model 1810T, variable voltage capability (0-30 kV), and capable of magnifications of 50,000x with resolutions of the order of 200 Å. SEM/kEDX samples were fracture surfaces which were mounted on carbon stubs and vacuum dried at 55^{o} C (131^{o} F). The EDX is a model DX4 manufactured by EDAX, Inc. in Mahwah, New Jersey. It has a resolution of approximately 140 keV. EDX spectra were taken using an accelerated voltage of 20 kV, sample tilt of 30 degrees, and a working distance of sixteen millimeters. Raw data were analyzed using a ZAF –standardless computing method. Results of the analyses are provided in Appendix B in Table B 3. Diabase is predominately silicon (33.58 wt percent) and oxygen (20.30 wt percent) and for purposes of this investigation is classified as siliceous aggregate. Limestone, on the other hand, because of its high calcium content, is a calcerous aggregate (even though it has significant amounts of silicon). Sandstone is considered to be a siliceous aggregate, even though the chemical analysis gives significant amounts of calcium (part of this can be attributed to the strong fluorescence of elemental calcium).

Using surface energy measurements of asphalt and aggregate, Cheng, Little et al (2002a) showed that the adhesive bond between granite (i.e. siliceous aggregate) and

asphalt is higher than limestone and asphalt when measured in energy per unit of surface area. However, when they considered energy per unit of aggregate mass, the calcareous (limestone) aggregate had higher adhesive strength than the siliceous aggregate.

4.3.2 Sample Preparation and Test Procedure

4.3.2.1 Improving Operator Variability

Previously in the pull-off test method, the test operator pressed the pull stub with asphalt applied to the ceramic onto the substrate. This process can result in an uneven film thickness which will cause error in the results not to mention adds uncertainty to results due to operator dependency. A device manufactured by Perkins-Elmer called a Potassium Bromide (KBr) press that is used to manufacture Fourier Transform Infrared Spectroscopy cells was modified to press the pull-stub onto the substrate. A metal cylinder approximately 3.5 cm (1.38 in) high with an outer diameter of 2 cm (1/2 in) and an inner diameter of 0.5 cm (1/5 in) on one end and 1 cm (2/5 in) on the other end was attached to the hammer of the device. The inner diameter's size was chosen to accommodate the size of the pull-stub. The device allows the pull-stub to be applied to the substrate in a uniform manner. However, the device does not control the pressure with which the specimen is applied. The device is shown in Figure 25.

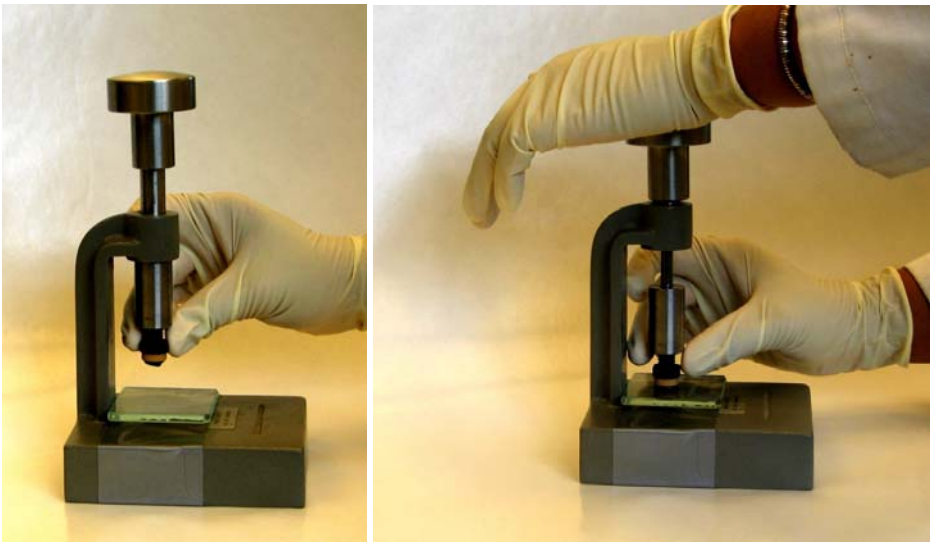

Figure 25. Pull-off Test Press

Aggregate substrates were cleaned and place in an 110^{o} C (230^{o} F) overnight. A schematic of the specimens is shown in Figure 26 and a photograph is shown in Figure 27. The specimens were made following the procedure used by Youtcheff and Aurilio (1997); and the press was used to adhere the loading fixture with asphalt to the aggregate plate.

After curing at ambient conditions for twenty-four hours, dry specimens were tested. Moisture conditioned specimens were immersed in a bath of distilled water maintained at 25^{o} C (77^{o} F). The loading fixture was pulled apart from the stone substrate using a Pneumatic Tensile Testing Instrument (PATTI) at a speed of 65.7 kPa/sec and ambient conditions, about 22 ± 2^{o} C (71.6^{o} F). Using the PATTI device and a chart recorder, the burst pressure (*BP*) necessary to debond the specimen is measured and *POTS* in psi is determined using the equation 2-13. Upon failure the burst pressure and location of failure was recorded. If failure occurred within a given material such as the asphalt binder, the failure location was denoted the letter for the material given in

Figure 26 (i.e. “b” for binder). If failure occurs between two materials, the failure location was denoted by specifying both materials (i.e. “a/b” for failure at the interface of the asphalt binder and aggregate). Bond strength is then given as the mean tensile stress at failure or break.

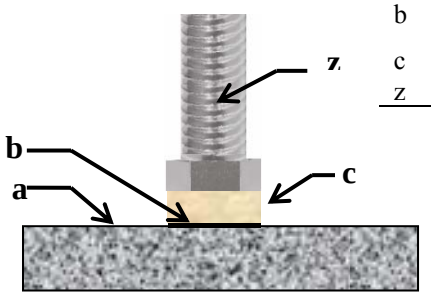

Component	Description	Thickness
a	Rock substrate	Varies
b	Mastic with glass beads	200 μm
c	Ceramic	6.35 mm
z	Pull-stub	N/A

Figure 26. Pull-off Test Specimen with Aggregate Substrate

Figure 27. Photograph of Pull-off Test Method Specimens: Limestone and Diabase Substrates

4.4 Results and Analysis of Pull-off Tensile Strength Data

Each specimen was tested at ambient conditions and the test temperature was recorded. Upon failure the burst pressure was recorded and the location of failure was noted. Failure occurs along the weakest plane within the system comprised of the loading fixture, adhesive, porous disc, asphalt specimen, and substrate and is evident by a fractured surface. Failure typically occurs within the asphalt specimen in the dry condition and in some cases, wet conditions. Failure is hypothesized to occur at the interface of the asphalt specimen and the substrate after soaking in water for certain periods of time. If failure occurred anywhere except cohesively within the binder (location b) or adhesively between the binder and aggregate (location a/b), the specimen was discarded from calculations to determine *POTS*.

The stress rate is linear until failure at a well-defined maximum force. After the maximum force is reached, there is a rapid decrease in the load. In addition, in specimens that failed cohesively various sizes of cavitations were observed and recorded. Since the bond strength of binder is directly related to its thickness, an understanding of the behavior of asphalt film at the given test thickness is required. According to Majidzadeh and Herrin (1965) asphalt films of this thickness (~ 200 μm) fail predominately by tensile rupture. This implies that the load-deformation curve is linear and there is a rapid decrease in load after the maximum load is reached. Majidzadeh and Herrin (1965) also characterize this failure mode by observation of the presence of cavitations that occur as a result of localized stresses as characteristic of this failure mode. In both phenomena, rapid decrease in load upon failure and occurrence of cavitations were observed during pull-off testing. Although, at this time the pull-off test

does not provide information on the amount of deformation (Δh) that the asphalt binder experiences during loading, the pull-off test does provide a constant load rate as evident by the linear relationship between *POTS* and time to failure (t_f) shown in Figure 28.

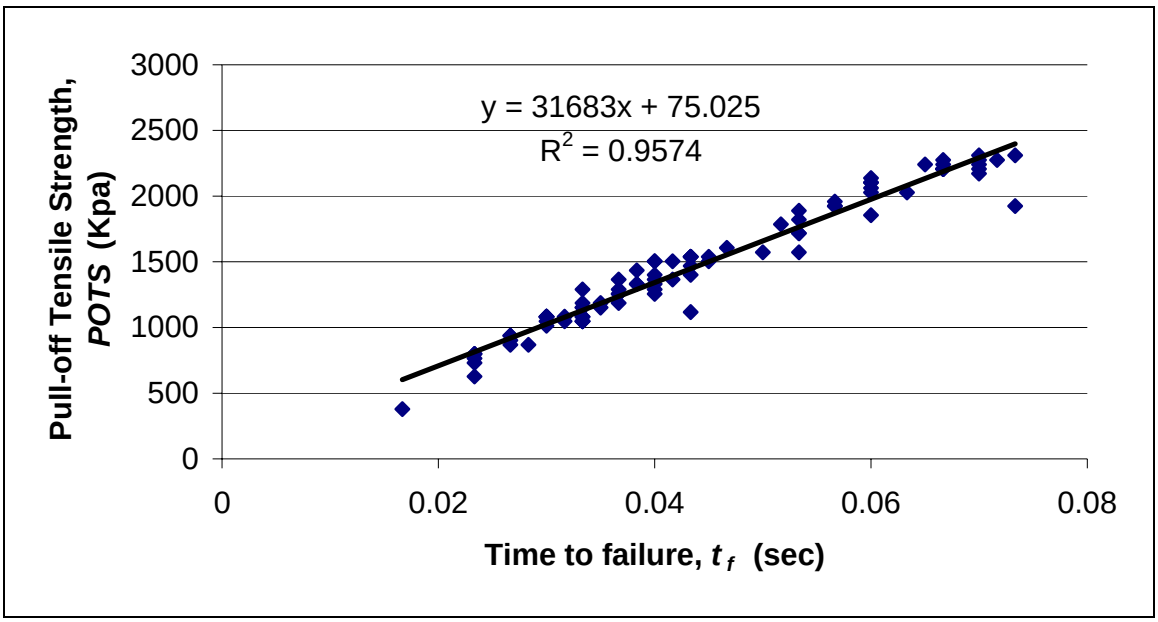

Figure 28. Linear Relationship between *POTS* and Failure Time Indicating Constant Load Rate is Applied During Pull-off Test

4.4.1 Bond Strength in Dry Condition

Specimens were first tested after curing but before any conditioning procedure (zero hours). It is assumed that the *POTS* value at zero hours is the bond strength in the undamaged state between asphalt binder and aggregate. The mean *POTS* and standard deviation for each binder on glass, diabase, limestone and sandstone substrate is provided

in Figure 29. The mean POTS values are plotted in Figure 29. The y-error bars represent the standard deviation from the mean value.

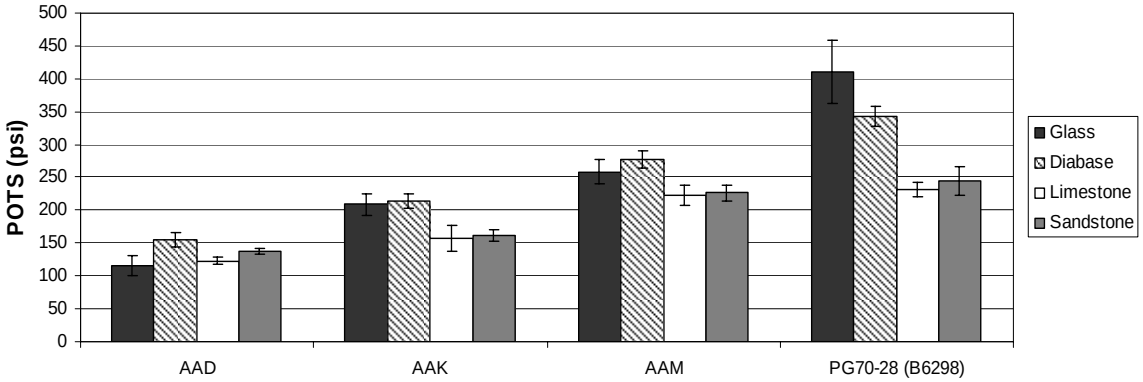

Figure 29. Pull-off Tensile Strength of Binders on Various Substrates

4.4.1.1 Influence of Substrate on Cohesive Bond Strength

Observing Figure 29, AAD had the lowest *POTS* for each substrate and PG70-22 had the highest. Binder AAD is ranked lower than AAK and AAM in regards to water sensitivity. Also, considering each binder's PG grade which indicates the stiffness of the material, the binders are ranked from lowest PG grade (AAD) to highest PG grade (PG70-22). As shown in Chapter III, binder type influences pull-off strength.

A statistical analysis was performed to determine if the pull-off test distinguishes between different substrates for each binder. First a one-way ANOVA was performed to determine if *POTS* values for each factor are statistically equivalent. The results of the ANOVA analysis are provided in Table B 5. The Prob > F values are provided in the last column in Table 15 and since they are each less than 0.05 the *POTS* for each substrate type is statistically different. Thus, substrate type significantly influences *POTS*. A paired Student's *t*-test was performed to determine if the results for each pair

of substrates is statistically different. Comparing each substrate for each binder type, it was determined if the mean *POTS* values are significantly different. In most cases, the substrates differ from one another. However the results for sandstone and limestone were not significantly different.

Table 15. Results of Paired *t*-test and ANOVA Analysis to Determine Influence of Substrate on Cohesive Bond Strength

Binder	glass/ diabase	glass/ limestone	glass/ sandstone	diabase/ limestone	diabase/ sandstone	limestone/ sandstone	Prob > F from ANOVA
AAD	yes	no	yes	yes	yes	no	0.0009
AAK	no	yes	yes	yes	yes	no	0.0001
AAM	yes	yes	no	yes	yes	no	0.0021
PG70-22 (B6298)	yes	yes	yes	yes	yes	no	<.0001

4.4.1.2 Influence of Cure Time on Cohesive Bond Strength

The bond strength at zero hours represents the undamaged bond strength between asphalt and aggregate. Bond strength is believed to increase over time. Binders AAD and AAM were chosen to determine effect of curing on bond strength. Each binder was applied to diabase substrate, cured at ambient conditions overnight and then put in a 25^{o} C oven and tested after certain times (i.e. 8, 24, 48 hours). The mean *POTS* values and standard deviations are provided in Table B 6. The results are plotted in Figure 30.

A linear regression analysis was performed to determine the predicted $POTS_{dry}$ values for binders AAD and AAM on diabase substrate and the predicted values are also plotted in Figure 30. Considering the slope of a linear trend line fitted to the predicted

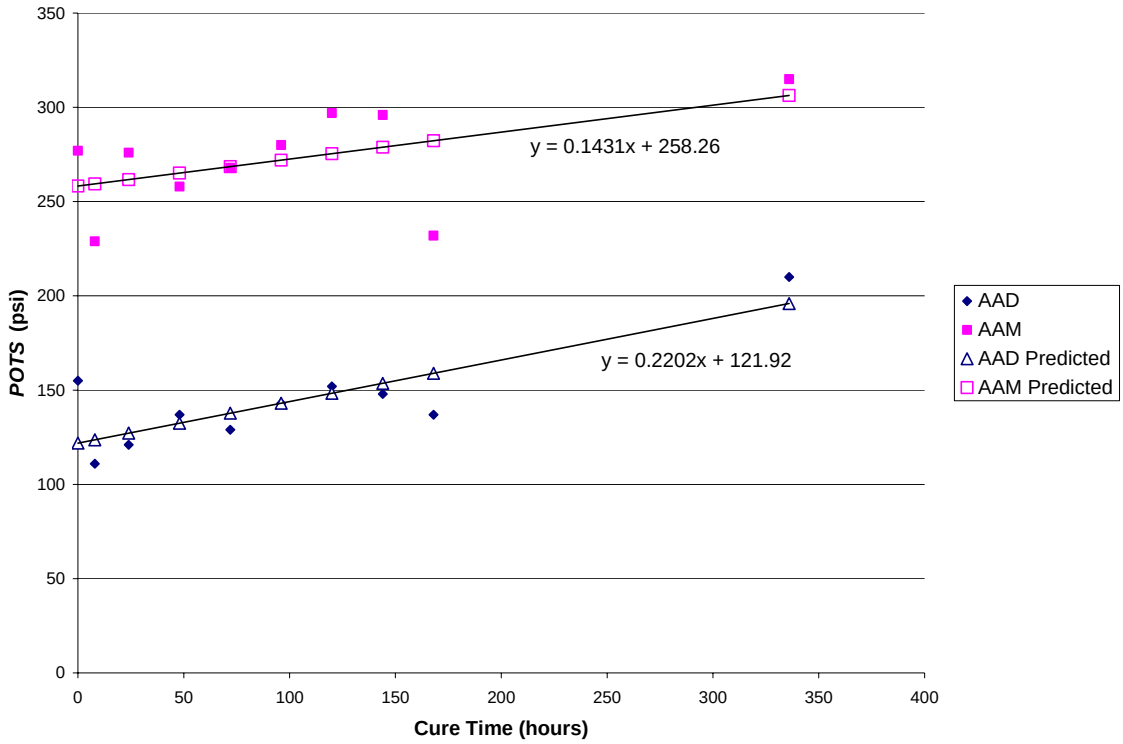

Figure 30. Predicted $POTS_{dry}$ Values versus Actual $POTS_{dry}$ Values for Binders on Diabase Susbstrate

regression values, the slope is positive for both AAD and AAM. A positive slope indicates that bond strength increases as a function of cure time.

The $POTS_{dry}$ of AAD at zero hours is 155 psi and the $POTS_{dry}$ of AAM at zero hours is 277 psi designated by "control" in Table 16. If all *POTS* values for each cure time are averaged, AAM has *POTS* of 143 psi and AAD has *POTS* of 272 psi, designated "all times combined" in Table 16. A statistical analysis was performed to determine if each cure time is significantly different. For binder AAD the following cure times were significantly different than zero hours: 8, 24, 72 and 336 hours. Those time periods for which *POTS* values were not statistically different than at zero hours were combined and the average *POTS* for this subset is equal to 145 psi, designated "statistically equivalent" in Table 16. The percent difference between control at zero hours and the statistically

equivalent binders is 6.45 percent decrease. For binder AAM the following cure times were significantly different than zero hours: 8, 168, and 336 hours. Those times that were not statistically different than zero hours were combined and their average *POTS* is 279 psi. The percent difference between control at zero hours and the statistically equivalent binders is 0.72 percent increase. The percent difference between the control *POTS* at zero hours and the average *POTS* for all cure times for AAD is 7.74 percent decrease and for AAM is 1.81 percent decrease. According to these results (percent differences less than ten percent), a conservative estimate of bond strength in the undamaged (i.e. dry) state can be determined by testing specimens at zero hours (i.e. after curing at twenty-four hours in ambient conditions) and no additional curing time is required. In addition, Figure 30 indicates that $POTS_{dry}$ is a conservative estimate of the undamaged bond strength.

Table 16. Summary Statistics for Cohesive Bond Strength

	AAD Binder			AAM Binder		
	Control	All times combined	Statistically equivalent	Control	All times combined	Statistically Equivalent
Average POTS (psi)	155	143	**145**	277	272	**279**
Std. dev. (psi)	11.9	27.7	**7.61**	13.23	32.90	**14.08**
CV (%)	7.68	19.37	**5.23**	4.78	12.10	**5.05**

4.4.2 Influence of Moisture on Bond Strength Between Asphalt Binder and Diabase Aggregate

Binders AAD and AAM on Diabase substrate were submerged in water at 25^{o} C for different amounts of time. The results are given in Table B 8 and plotted in Figure 31. The *y*-error bars represent the standard deviation from the mean. Moisture

conditioning decreases bond strength between AAD and diabase and AAM and diabase. However, for each soak time cohesive failure occurred within the binder (b), between the binder and the ceramic frit (b/c) or between the frit and loading fixture (c/z). Failure did not occur at the interface between binder and aggregate (a/b).

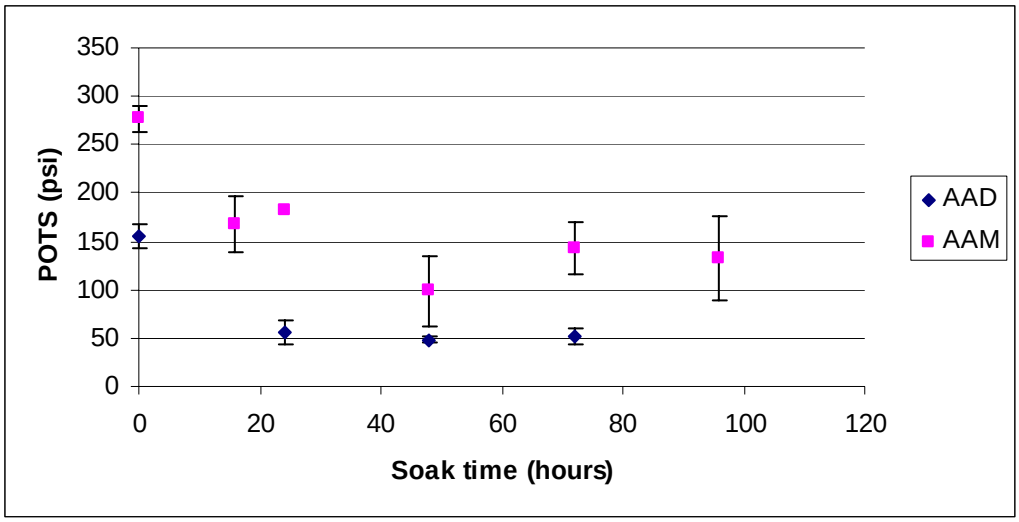

Figure 31. The Effect of Moisture Conditioning on Bond Strength of Asphalt Binders on Diabase Substrate

The weakest link in the dry condition and after moisture conditioning is the binder since failure occurs within the binder in all cases in the dry condition and the majority of cases after moisture conditioning. The size of the cavitations changed depending on conditions. An in-depth analysis of cavitations size and its relationship to failure mode was out of the scope of this study.

For adhesive rather than cohesive failure to occur, moisture should be isolated to the interface between asphalt and aggregate. The experiment set-up was modified so water only enters the aggregate substrate, Figure 32. The water level in the water bath

was kept at or below the top of the aggregate substrate. This ensures that liquid water does not have an effect on the binder. Water is hypothesized to migrate through the aggregate substrate and eventually reach the interface resulting in weakening of the bond between asphalt and aggregate.

Binders AAD, AAK, AAM and PG70-22 were tested after 8, 24, 48 and 168 hours in the water bath. The results are plotted in Figure 33. *POTS* decreased after eight and twenty-four hours of moisture conditioning; however *POTS* increased after forty-eight hours of moisture conditioning and in the case of AAK and AAM is higher than the control *POTS* value (i.e. $POTS_{dry}$, zero hours). At 168 hours, the *POTS* decreased again. In each case, the specimens failed cohesively within the asphalt binder. The binders ranked the same in terms of *POTS* as in the dry condition. However after 168 hours of

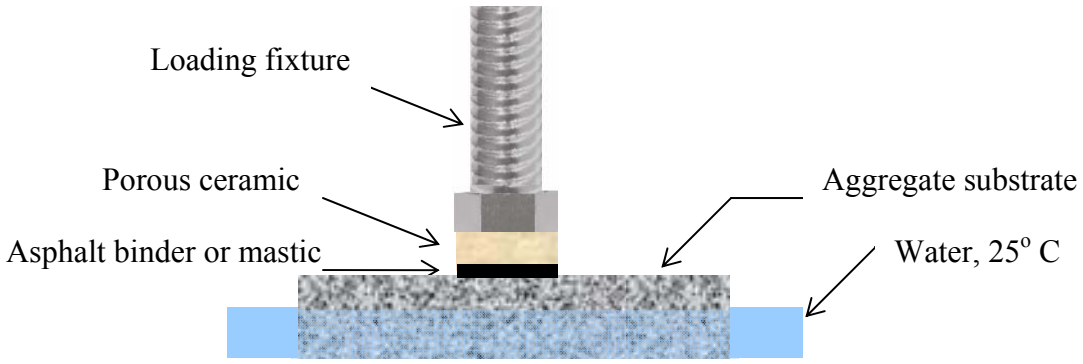

Figure 32. Experimental Set-up for Aggregate Plate Moisture Conditioning

soak time, the trend is not the same. This implies that simply because a binder has a high strength in the dry condition does not mean that it is less moisture sensitive. The shape of the data in Figure 33 is interesting to note as compared to the specimens that were

entirely submerged given in Figure 31. In Figure 33 the tensile strength decreases until between eight and twenty-four hours and then increases between twenty-four and forty-eight hours and then appears to decrease again after forty-eight hours. This behavior may be due to stresses developed in the binder after exposure to a high humidity condition in the water bath. According to Perera (1996, 2004) there may be an initial increase in compressive stress due to moisture, which will result in a decrease in tensile stress within asphalt binder shown in phase one of Figure 34. Then there is a decrease in compressive stress which results in an increase in tensile stress within the asphalt binder, phase two. Finally in phase three, loss of adhesion between adhesive and adherend occurs.

To further characterize the relationship between bond strength and soak time, additional specimens of binders AAD and AAM on diabase were tested after 16, 72, 96, 120, 144, and 336 hours of soak time. The results are plotted in Figure 35. Binder AAM's *POTS* increases after 168 hours of soak time. Binder AAD's *POTS* decreases after 168 hours of soak time. The location of all failures was in the binder, failure mode "b", except AAM-1 which experienced a mixture of failure modes, "b" and "a/b" at 144 hours and 336 hours. This indicates that the bond at the asphalt-aggregate interface is stronger than the binder even after moisture conditioning the aggregate substrate. However, moisture may not be reaching the interface due to the porosity of the aggregate substrate.

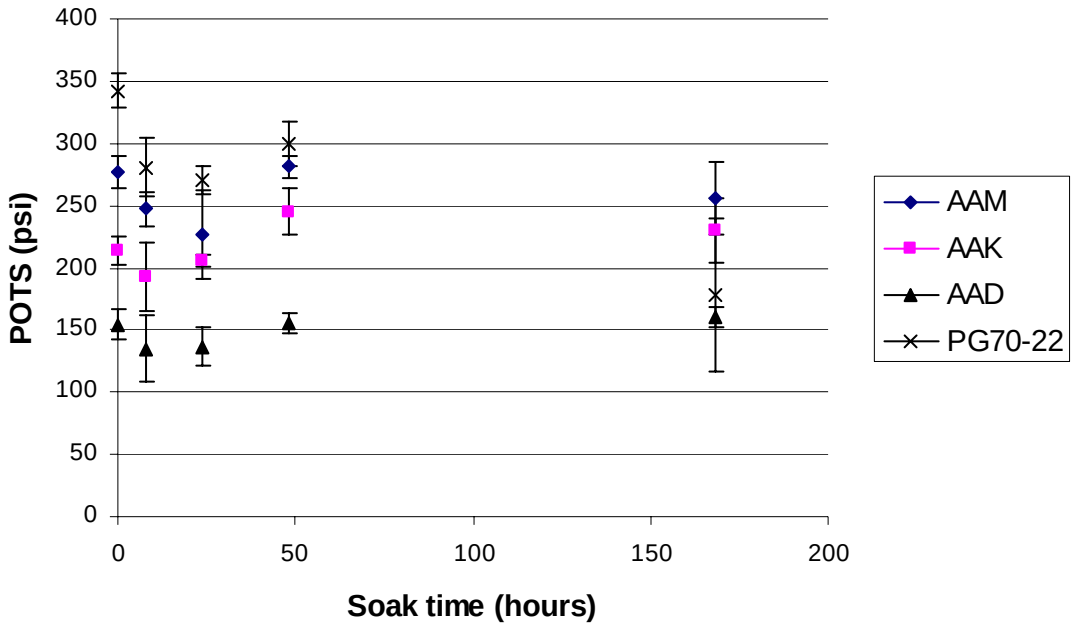

Figure 33. Influence of Soak Time on Bond Strength of Asphalt Binders on Diabase Substrate

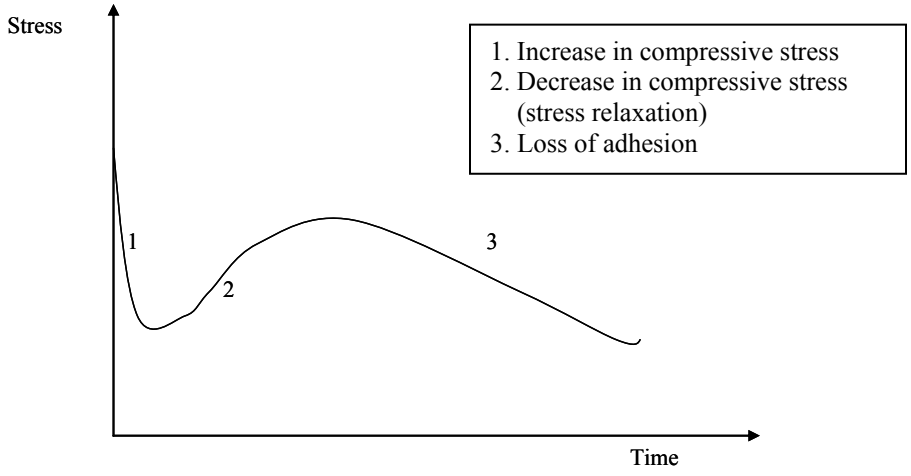

Figure 34. Schematic Representation of Stress Dependence on Soak Time (Perera 2004)

The development of bond strength for dry specimens versus moisture conditioned specimens is plotted in Figure 36 which is a combination of data from Figure 30 and Figure 35. The graphs display similar characteristics for each binder. At 8 hours of soak time, the wet condition has higher *POTS*. However at 48 hours of soak time, the wet condition also has higher *POTS* values. After 72 hours of time, the graphs switch and the dry condition has higher *POTS* values until around 150 hours when the plots switch again. In both cases the dry condition provides higher *POTS* values at 336 hours of time.

Figure 34 indicates that moisture conditioning at 25° C (77° F) influences pull-off tensile strength differently than curing at 25° C (77° F). Moisture conditioning does not always result in lower *POTS* than curing. The influence of moisture may result in cohesive (i.e. within the binder), adhesive (i.e. at the asphalt-aggregate interface) or mixed mode failures. The failure mode that controls may be determined based on a time scale and/or the moisture content in the component materials or at the asphalt-aggregate interface. However, the pull-off test method alone cannot determine which failure mode is dominant.

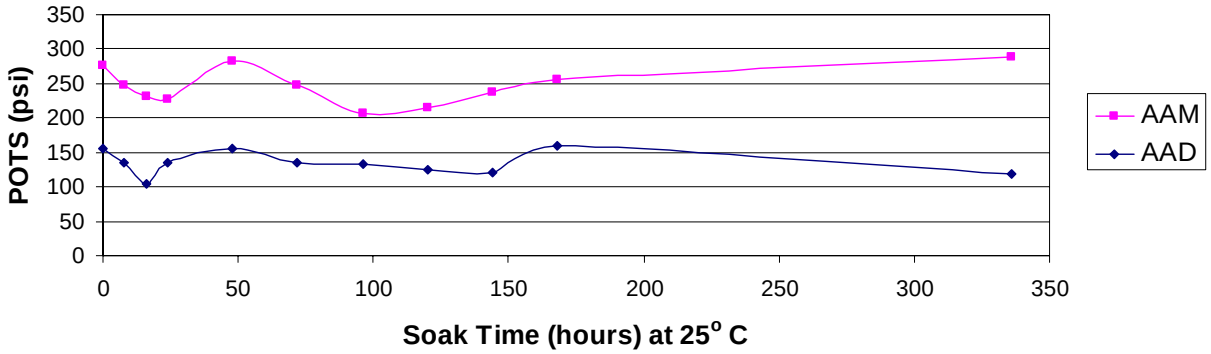

Figure 35. Development of Adhesive Bond Strength on Diabase Substrate

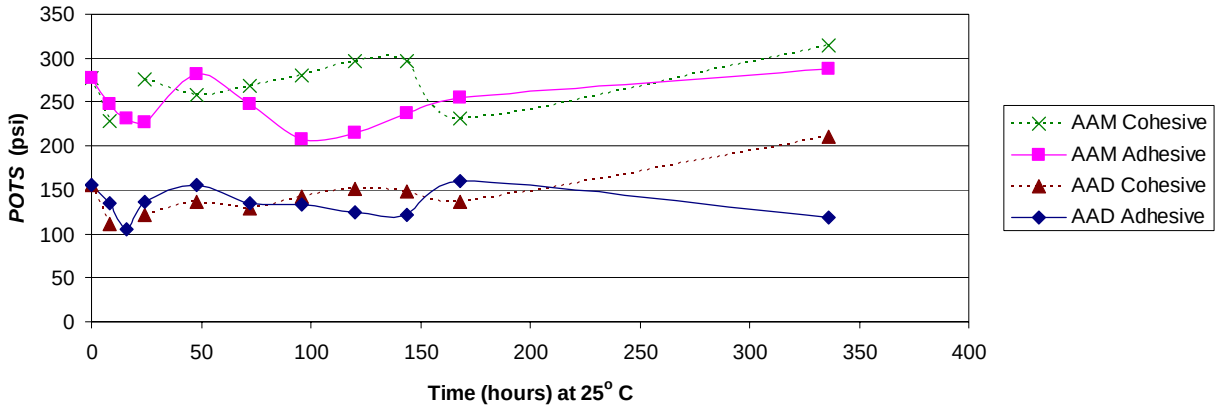

Figure 36. Development of Bond Strength on Diabase Substrate

4.5 Conclusion

The modified pull-off test method has been applied to quantify pull-off strength between asphalt binders and aggregate substrates. Aggregate plates were obtained from hand boulders using water-cooled saws and a chemical cleaning procedure was developed to remove asphalt binder from aggregate surface after testing so that aggregate plates may be reused for testing. After modifying the pull-off test so that aggregate substrates may be used rather than glass substrates, an experiment was performed to determine undamaged (i.e. dry condition) pull-off strength between asphalt and aggregate and the influence of moisture conditioning on bond strength between asphalt binders and aggregate substrates.

The pull-off test successfully distinguishes between the *POTS* of asphalt binders on aggregate substrates and appears to rank them according to how they may perform. Binder type and substrate type both affect $POTS_{dry}$. Limestone, a calcareous aggregate, and sandstone, considered a siliceous aggregate, had lower $POTS_{dry}$ values in the dry condition than diabase, a siliceous aggregate; however the difference in *POTS* is more

dependent on surface properties and texture than on substrate type. For example, the sandstone aggregates lower $POTS_{dry}$ strength is most likely due to a thin, fine grain film on the surface. $POTS_{dry}$, which is tested after an initial curing period of twenty-four hours, is a reasonable estimate of the dry bond strength between aggregate and asphalt and represents the undamaged state of asphalt-aggregate adhesion.

Moisture conditioning decreases the bond strength of asphalt binder on aggregate substrate; however cohesive rather than adhesive failure at the asphalt-aggregate interface was observed. In an effort to isolate failure to the asphalt-aggregate interface, only the aggregate substrate was submerged in the water bath. A porous aggregate allows water to pass through; however the aggregate plate may not have interconnected voids which would allow the water to reach the interface in a reasonable time. Evaluating the porosity of aggregate substrates was out of the scope of this project. A recommendation is that in the future that the porosity and interconnected voids of aggregate substrates be determined. The inherent variability in each aggregate substrate's ability to absorb water is not captured in this test method, but is an important component with regards to the loss of bond strength at the asphalt-aggregate interface.

Again moisture conditioning was shown to influence bond strength as determined by the pull-off test method; however it does not always degrade the bond. After moisture conditioning, cohesive failure was the most common failure mode. While adhesive failure or mixed-mode failure between the asphalt and aggregate were observed in some cases, obtaining consistent adhesives failure between asphalt and aggregate was difficult while soaking only the aggregate. Thus, the pull-off test method used alone cannot

determine which failure mode (i.e cohesive or adhesive) controls between asphalt and aggregate.

CHAPTER V

DETERMINATION OF BOND STRENGTH AS A FUNCTION OF MOISTURE CONTENT AT THE MASTIC-AGGREGATE INTERFACE

5.1 Introduction

A primary failure mode as a result of moisture is loss of bond strength between asphalt and aggregate. Measuring bond strength between asphalt and aggregate alone, however, cannot predict the occurrence of moisture damage in an asphalt mixture. The mode in which moisture reaches the interface and the amount of moisture required to cause failure is critical. Moisture may reach the interface between the asphalt and aggregate as a result of diffusion through the components. To gain insight into the timescale on which moisture damage may occur and accurately model and predict the failure process, a relationship must be established between the amount of moisture present at or near the interface (i.e. where failure occurs) and the loss of bond strength.

In this chapter a methodology is presented that establishes a relationship between moisture content and the reduction of strength of the asphalt-aggregate bond, by measuring the *POTS* of various moisture-conditioned mastic-aggregate specimens and relating them to finite element simulation of moisture diffusion.

The modified pull-off test is used to determine the bond strength of asphalt mastic applied to a substrate. The modified pull-off test has been used to study the effects of moisture on asphalt binder and mastic (Chapter IV), and asphalt binder-aggregate bond strength (Chapter V). In this chapter, based on a combination of experimental measurements and computational analyses, bond strength degradation as a function of the

amount of moisture at the mastic-aggregate interface is established. For the moisture diffusion analyses of the tested samples, the finite element analysis tool RoAM (Kringos and Scarpas 2004, 2005b) developed at Delft University of Technology is utilized.

5.2 Methodology

The pull-off test, as described in Chapter IV, provides a relationship between the binder-aggregate bond strength and conditioning time in the water-bath, Figure 37(a). When the purpose of the test is to compare particular asphalt-aggregate combinations, results of the pull-off test may directly provide useful information (Chapter V), provided that similar geometries and moisture conditioning are used. However, to determine the fundamental relationship of the influence of moisture on bond strength, the amount of moisture at the interface is of paramount importance. Since this type of information cannot be determined from the test, an additional procedure was developed (Copeland, et al. 2006) to relate bond strength to the quantity of moisture in the bond. By simulating the test specimens with the finite element tool RoAM (Kringos and Scarpas 2005a), modeling the same geometries and moisture boundary conditions as applied in the experiment, the relationship between the quantity of moisture at the mastic-aggregate interface and soaking time is found, Figure Figure 37(b). Since the degradation of bond strength and movement of water through aggregate are a function of time, the results of finite element simulations and the pull-off test can be combined and a relationship between bond strength and moisture content is determined, Figure 37(c).

Experimental evidence indicates that the presence of moisture in the asphalt binder-aggregate interface results in degradation of its mechanical properties. In order to

define a relationship for the physical moisture-induced damage development, a moisture-induced damage parameter due to diffusion, d_θ, is defined here as the scalar measure of moisture-induced damage at the interface:

$$d_\theta = f(\theta). \tag{5-1}$$

The reduction in strength due to damage can be postulated to be of the form:

$$S^\theta = (1 - d_\theta)^\alpha S_o \tag{5-2}$$

where S_o is the undamaged strength of the material (Kringos and Scarpas 2005b).

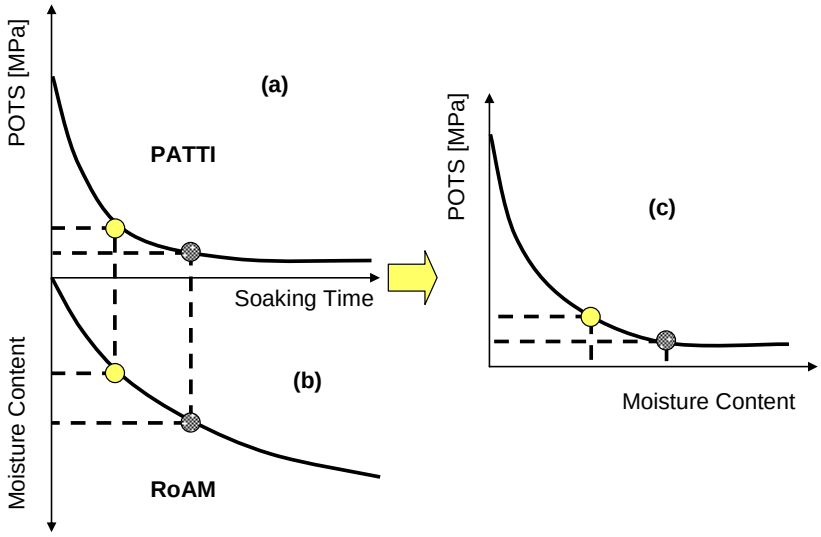

Figure 37. Computational-Experimental Procedure for *POTS* versus Moisture Content Determination (Copeland, et al. 2006)

5.3 Quantification of Bond Strength at Mastic-Aggregate Interface

5.3.1 Materials and Specimen Preparation

In an effort to more accurately quantify bond strength between asphalt and aggregate, mastic was used instead of asphalt binder. Mastic is more representative of the material adhered to aggregate in an asphalt mixture. Strategic Highway Research Program (SHRP) core asphalt AAD (PG58-28) was used to make mastic. Diabase material, passing the #200 sieve (75 μm), was used as mineral filler to combine with the asphalt binder to make mastic. Filler in the amount of thirty percent by volume was chosen, based on the fact that the fine aggregate passing the #200 sieve is approximately twenty-seven to twenty-eight percent by volume of the binder in most fully graded aggregate systems (Shenoy 2001). The mastic is prepared by heating measured quantities of binder and filler to 165^{o} C (329^{o} F) for approximately two hours. The binder was removed from the oven and stirred for one minute at 600 rpm with a mechanical stirrer. The filler is added and the mixture is stirred at 600 rpm for an additional two minutes (adapted from Shenoy 2001). The mastic is stored at ambient conditions, approximately 22^{o} C (71.6^{o} F), until the pull-off specimens are made.

Diabase stone was used as the substrates in the pull-off test. Cobble-sized samples of diabase rock were obtained from a quarry in Sterling, VA. The rocks were cut into plates using a 33 cm (13 in) diamond-tip, water-cooled saw. The geometry of the rock plates vary due to the varying sizes of rocks obtained from the quarry, limitations of the cutting process and requirements for substrate size given in the pull-off test

specifications[ii]. However, the geometry of each stone plate was approximately square or rectangular in shape and its geometry was measured. The top surface of the rock plates were polished using a 600-grit resin bonded diamond grinding disc. All stone plates were oxidized to a temperature of 482° C (900° F). The oxidized plates were rinsed with distilled water, allowed to dry overnight, and then stored in an oven at 60° C (140° F) until they were used to make the pull-off specimens.

5.3.2 Test Procedure

The experimental unit for the pull-off test is provided in Figure 38. First a porous, ceramic stub, C, was applied to the pull-stub (i.e. loading fixture) using two-part epoxy glue. The surface of the ceramic stubs used in the pull-off test was coated with a silane solution to enhance the adhesion of asphalt mastic to the ceramic. A sample of approximately 5.0 g of mastic was mixed with one percent (by weight) glass beads. The beads ensure a uniform film thickness of 200 μm is attained. Youtcheff and Aurilio (1997) and Nguyen et al (1996) found that this method for controlling film thickness is convenient and reduces the time to prepare the test specimens. The mastic, B, was heated to approximately 100° C (212° F) and applied to the ceramic. The test operator presses the loading fixture, D, onto the substrate, A. The excess mastic that surrounds the edge of the pull-stub was not trimmed. The specimens were allowed to cure at 20 ± 1° C (68 ± 1.8° F) for at least twenty-four hours.

[ii] This experiment was performed before the tile saw was obtained for the improved cutting procedure introduced in Chapter V.

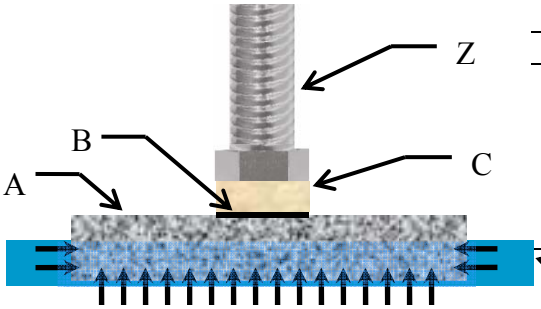

Component	Description	Thickness
A	Rock substrate	Varies (see Table 1)
B	Mastic with glass beads	200 µm
C	Ceramic	6.35 mm
Z	Pull-stub	N/A
E	Water	Varies (see Table 1)

Figure 38. Pull-off Test Set-up (not to scale)

After curing, dry specimens were tested. The other specimens were immersed in a bath of distilled water maintained at 24 ± 1° C (75 ± 1.8° F). The depth of the water bath was kept below the mastic-aggregate interface to ensure moisture diffusion through the aggregate substrate to the mastic-aggregate interface. Two different water depths (8 and 16 mm) were chosen based on average specimens' thicknesses. The specimens were withdrawn from the water bath after fourteen, twenty-four, and thirty-seven hours and immediately tested.

Using the PATTI device and a chart recorder, the burst pressure (*BP*) necessary to debond the specimen at a temperature of 21 ± 1° C (70 ± 1.8° F) is measured. The *POTS* in psi is determined using equation 2-13.

5.3.3 Results of Pull-Off Tensile Experiment

The average tensile bond strength of four specimens, tested at dry conditions, was 1.3 MPa (189 psi). Each specimen that was tested dry exhibited cohesive failure within the mastic (component B in Figure 38). Visual observation of the fractured mastic surface on the rock substrate showed small, pinpoint-size cavitations.

Table 17 shows the *POTS* results of the specimens exposed to moisture including their soak times, the height of the water bath measured from the bottom, and specimen geometries. After moisture conditioning, almost all tested specimens experienced a clear adhesive failure; i.e. they left very little or no mastic on the stone substrate and the surface of the mastic layer on the ceramic stub was observed to be smooth (i.e. no cavitations). Only one specimen, C24, showed a mixed failure mode (i.e. partially cohesive and partially adhesive) after moisture conditioning. Specimens A24 and B24 left behind a small amount of mastic (5-10%) on the rock substrate in the center of the test area. However, their failure mode is classified as adhesive since more than fifty percent of the mastic was removed from the substrate.

Table 17. Adhesive Pull-off Tensile Strength Results

Spec ID	Moisture Conditioning		Specimen Geometry		POTS [MPa]
	Soak Time [hrs]	Water Height [mm]	Surface [mm x mm]	Thickness [mm]	
A14	14	8	48.06 x 46.92	16.84	0.767
B14	14	8	55.89 x 53.44	13.39	1.01
C14	14	8	52.29 x 43.07	14.10	1.01
A24	24	16	45.10 x 38.27	23.19	1.12
B24	24	16	63.17 x 56.15	18.92	1.15
C24	24	16	55.33 x 45.63	26.75	1.22
A37	37	8	47.27 x 46.66	15.68	0.56
B37	37	8	51.79 x 46.47	16.79	0.59
C37	37	8	47.54 x 50.17	16.93	0.767

5.4 Simulation of Moisture Diffusion via RoAM

In order to gain fundamental insight into the predominant processes that control moisture induced damage in asphalt mixes, a finite element tool RoAM has been developed (Kringos and Scarpas 2004) at Delft University of Technology as a subsystem

of the finite element system CAPA-3D (Scarpas 2000). From previously performed computational identification of the controlling parameters (Kringos and Scarpas 2005a), moisture diffusion was identified as one of the important processes. In the same publication, the calibration of RoAM for diffusivity studies has been shown.

For the simulation of the moisture diffusion flux $\mathbf{J}_d$ RoAM assumes a Fick's Law type diffusion:

$$\mathbf{J}_d = -\mathbf{D}\nabla\left(C_m\right) \tag{5-3}$$

where C_m is the moisture concentration and $\mathbf{D}$ is the molecular diffusion tensor. The ratio of moisture concentration, present in the material, with respect to the maximum moisture concentration uptake is defined as moisture content θ

$$\theta = \frac{C_m}{C_m^{\max}} \tag{5-4}$$

A moisture content of $\theta = 1.0$ therefore indicates that the material has reached its maximum uptake of moisture concentration $C_m^{\max}$.

5.4.1 Diffusion Analysis Results

For the moisture diffusion analyses an effective diffusivity of 0.6 mm^2/hr was used for diabase aggregate (Bradbury, et al. 1982). Since all specimens had different geometries and water tables (as shown in Table 17), a new finite element mesh was made for each specimen that simulates the specific geometry and moisture conditions given for that specimen. Figure 39 shows the geometry and the moisture diffusion for specimen A37 at zero and thirty-seven hours.

Figure 40 shows an analysis of the moisture profiles, over time, on the surface of the middle cross-section of specimen A37. From observing the profiles, the region of the stone to which the mastic film is adhered is exposed to a fairly uniform moisture front. Simulations of the moisture diffusion into each specimen can be seen in Figure 41 where the moisture content depicted in the graphs is measured at the center of the top surface of the diabase specimen.

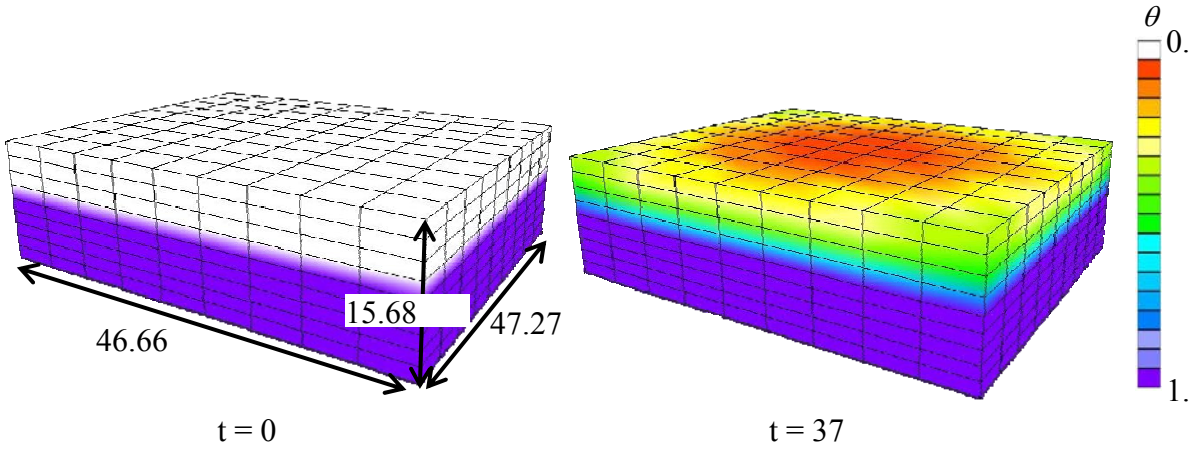

Figure 39. Moisture Diffusion Simulation in Specimen A37 (Copeland, et al. 2006)

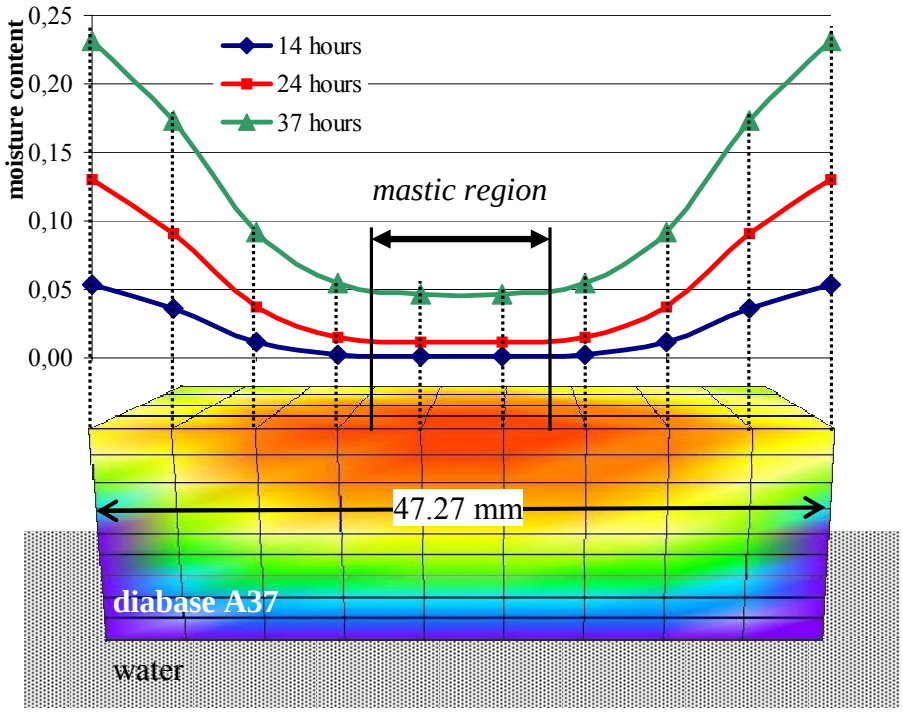

Figure 40. Moisture Content Profiles for Specimen A37 at Substrate Surface Cross-section (Copeland, et al. 2006).

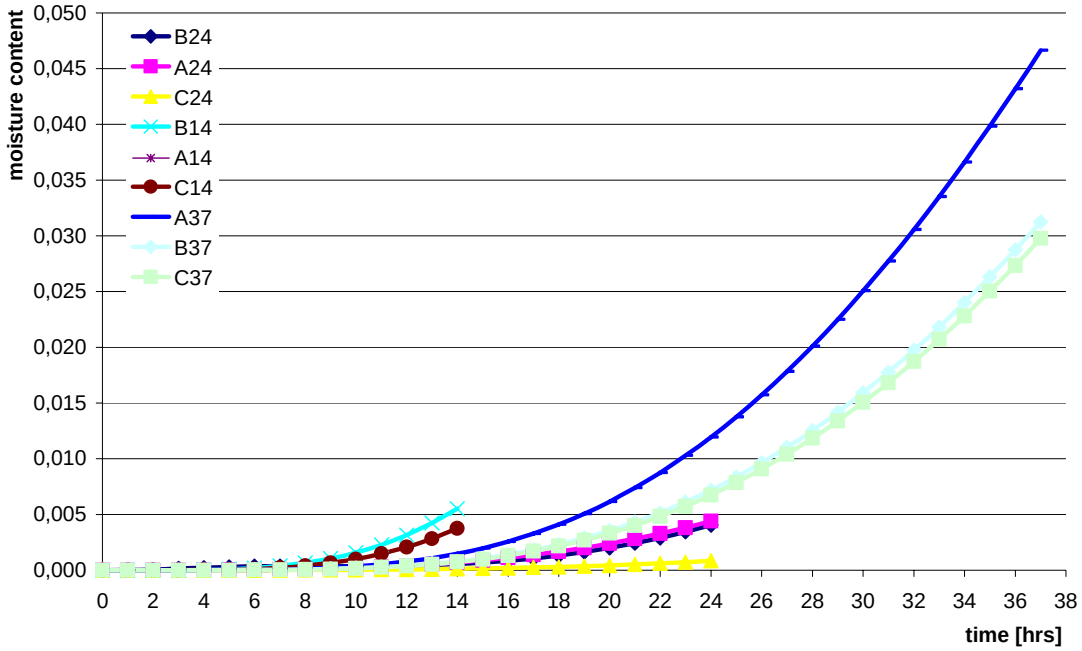

Figure 41. Moisture Diffusion Simulations for the Test Specimen (Copeland, et al. 2006)

5.5 Results

The methodology illustrated in Figure 37 was applied to all specimens and the results are plotted in Figure 42. As can be seen, the overall results confirm the hypothesis that moisture at the interface reduces *POTS* (i.e. bond strength). The results of specimen A14 were excluded due to an unexpectedly low tensile strength value that was a result of poor specimen preparation.

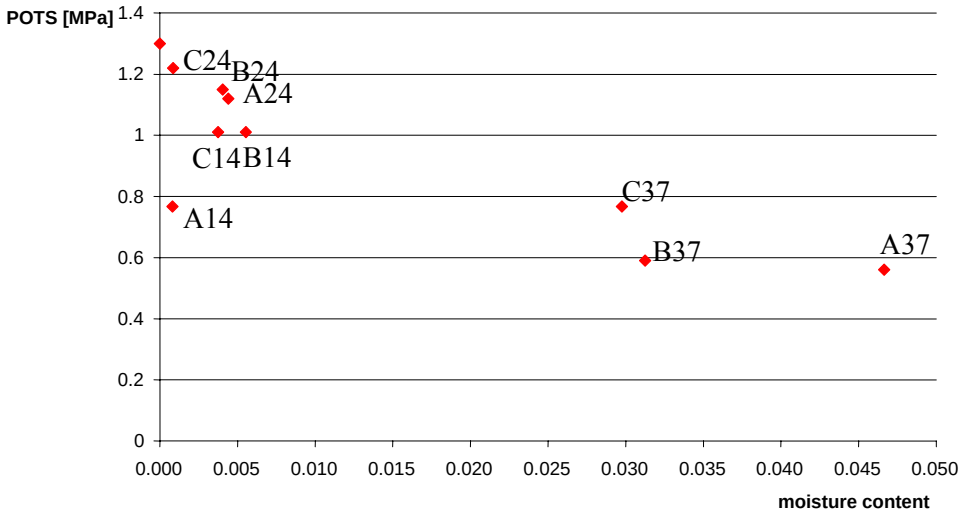

Figure 42. Measured *POTS* versus Computed Moisture Content for All Specimens (Copeland, et al. 2006)

As shown in Figure 43, the relationship between interface strength, *POTS*, and moisture content, θ, was determined using regression analysis as

$$POTS = e^{(0.30-3.76\sqrt{\theta})}. \tag{5-5}$$

Assuming that no damage due to moisture has occurred when specimens are tested in the dry condition, there is no loss of bond strength at zero moisture content. The relationship

between interface tensile strength percentage reduction and moisture content, Figure 44, was then determined as

$$\%Strength = 100e^{-3.76\sqrt{\theta}}. \tag{5-6}$$

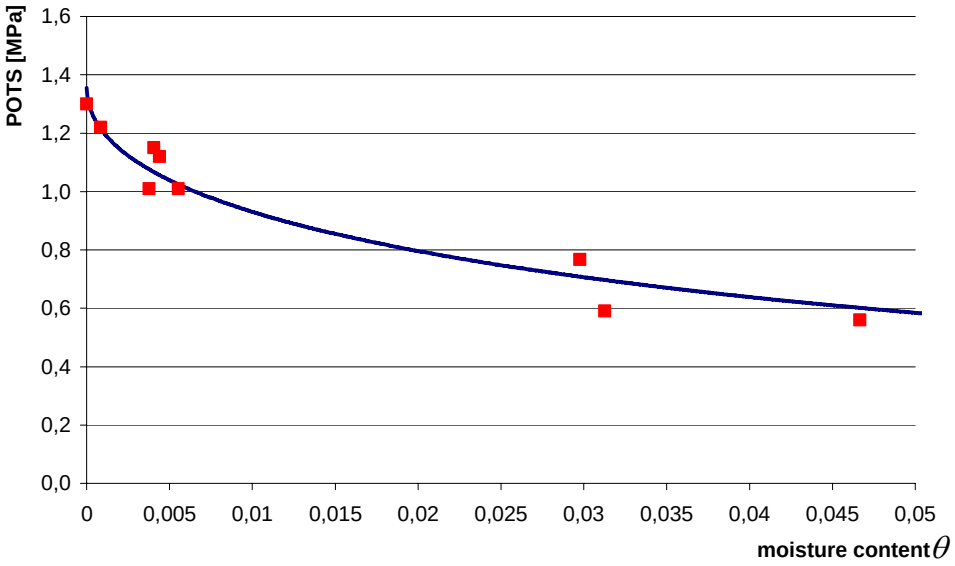

Figure 43. Relationship between Interface Strength and Moisture Content (Copeland, et al. 2006)

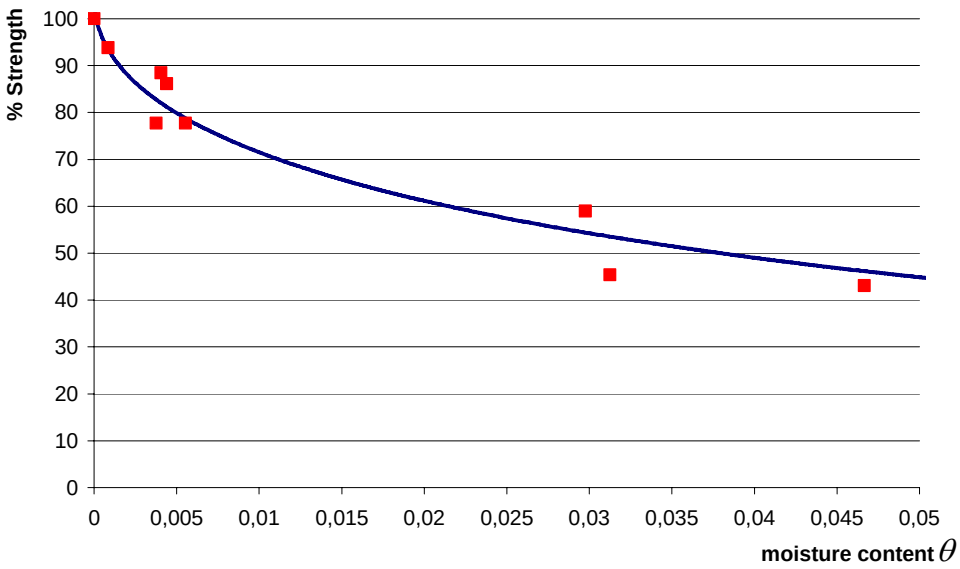

Figure 44. Relationship between Reduction of Strength and Moisture Content (Copeland, et al. 2006)

On the basis of equations 6-5 and 6-6 the evolution of moisture damage as a function of moisture content, Figure 45, can be determined as

$$1 - d_\theta = 1 - e^{-3.76\sqrt{\theta}}. \qquad (5\text{-}7)$$

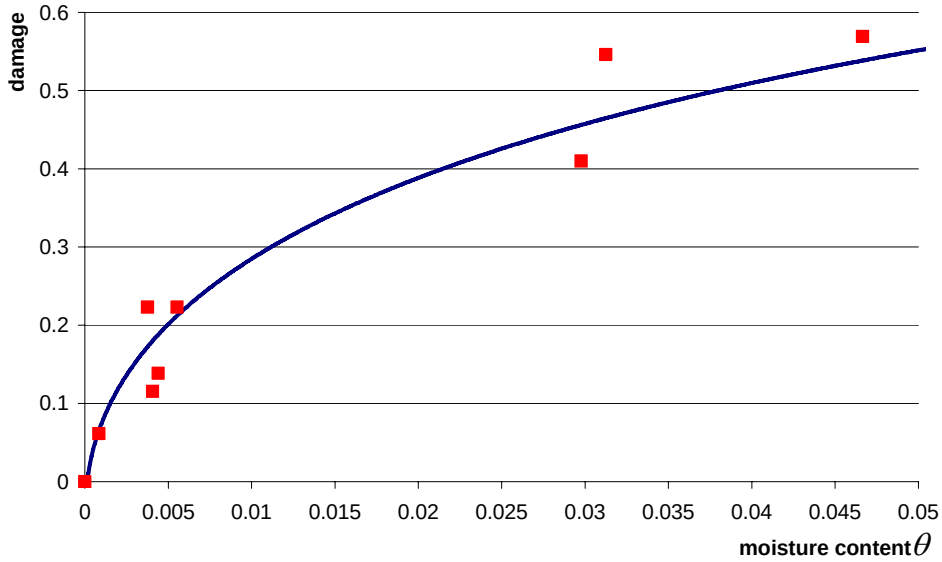

Figure 45. Relationship between Interface Bond Damage and Moisture Content (Copeland, et al. 2006)

5.6 Methodology Verification

5.6.1 Substrates with Different Histories

The above described procedure was demonstrated for nine test specimens, hereafter classified as Type I diabase. Encouraged by the results of the first set of tests, additional tests were performed to verify the proposed methodology, again using a diabase material as the substrate in the pull-off test. The new results using diabase samples are referred to as Type II diabase. Table 18 shows the test results of the pull-off experiments of these samples. Again, the average tensile bond strength of four specimens, tested at dry conditions, was measured and the mean $POTS_{dry}$ value was 1.5 MPa (218 psi).

Combining pull-off results with finite element analyses, whereby using the same parameters as before, the results were plotted in the same bond strength- moisture content space as the Type I samples as shown in Figure 46. As can be seen from the graph, the Type II samples seem to veer off substantially from the Type I results. Diabase substrates were utilized which had been used previously in other experiments and were subjected to one or more cleaning cycles before preparing them for the pull-off experiments. The cleaning cycle's purpose is to remove the residual asphalt mastic from the surface of the stone substrate. All reusable stone plates were oxidized in an oven to a temperature of 482^{o} C (900^{o} F). The specimens were then rinsed with distilled water, dried, and stored in a 60^{o} C (140^{o} F) oven. In order to achieve a better understanding of the causes of these scattered results, moisture sorption experiments were performed on the Type II diabase to better understand absorption behavior.

Table 18. Pull-off Test Results for Type II Diabase Samples

Diabase Type	Specimen ID	Soak Time (hours)	Water Level (mm)	Surface (mm x mm)	Thickness (mm)	*POTS* (MPa)
Type II	A6	6	6	63.17 x 56.15	18.92	0.77
Type II	D14	14	8	48.29 x 49.10	12.89	0.697
Type II	A19	19	7	43.36 x 51.68	16.97	0.943
Type II	B19	19	7	44.87 x 32.82	18.77	1.083
Type II	C19	19	7	46.13 x 47.01	11.71	1.048
Type II	D37	37	8	56.59 x 55.12	21.53	0.591
Type II	A408	408	8	50.72 x 40.74	19.31	<0.345

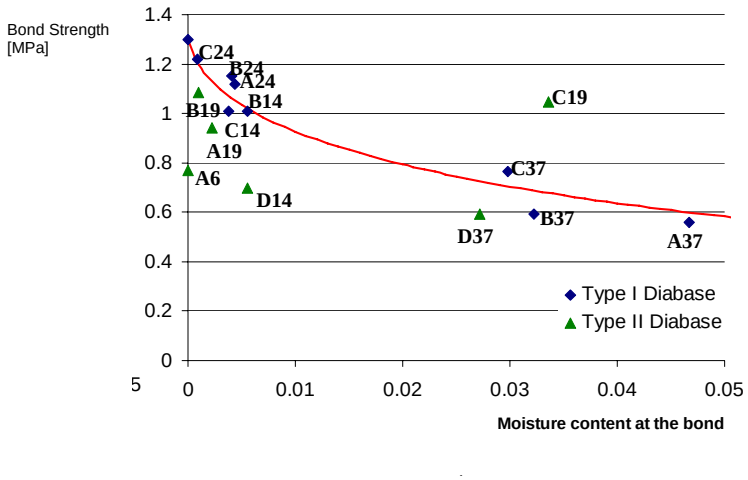

Figure 46. Results of the Experimental-Numerical Procedure using a Diffusivity of 0.6 mm^2/hr for Type I & II diabase (Copeland, et al. 2007).

5.6.2 Moisture Sorption Characteristics of Type II Diabase

5.6.2.1 Specimen Preparation

The moisture sorption behavior of the Type II diabase was determined using the gravimetric method. Three samples were chosen with different dimensions. The samples

were obtained using the same process that was used to cut the plates used in the pull-off test method.

After the cutting process, each specimen's geometry was measured using a method known as dimensional analysis. The length, width and height were each measured in four different places for a total of twelve measurements per plate. Therefore the value for a specimen's length, width or height used for subsequent analyses (i.e. volume calculations) is the average of the four measurements. The geometries of each sample are provided in Table 19. After cutting, the specimens were rinsed with distilled water and dried to a constant mass. Two samples (A and B) were placed in the oxidizing oven to simulate the cleaning process. The third sample (C) was not placed in the oxidizing oven.

Table 19. Geometry and Moisture Uptake of Sorption Samples

Diabase Type	Sample ID	Surface (mm x mm)	Thickness (mm)	Water level (mm)	Dry mass (g)	Moisture uptake (g)	Maximum Moisture uptake (%, g/g_{dry})	Moisture Concentration x 1E-06 (g/mm^3)
Type II	A	61.99 x 50.53	13.66	16	127.67	0.21	0.16	4.9
Type II	B	62.27 x 50.27	14.77	16	137.54	0.22	0.16	4.8
Type II	C	54.48 x 53.05	8.33	6	68.25	0.12	0.18	4.9

5.6.2.2 Absorption of Aggregate Substrate

The samples were placed in a water bath at 25° C (77° F) and weighed periodically. Two samples were completely submerged (sample A and B) and a third sample (Sample C) was submerged in water at a constant depth of 6 mm (0.23") to create a different boundary condition. Each specimen's surface was patted with a paper towel

until it reached saturated surface-dry condition before weighing. Table 19 shows the dry mass, water level and moisture uptake for each sample. The fully saturated samples A and B absorbed a maximum of about 0.22 g moisture and specimen C reached equilibrium at around 0.12 g. Equilibrium was defined to be reached when change in weight over a seven day period is smaller than 0.03%. All three specimens seem to converge to a maximum moisture concentration $C_m^{\max}$ of about 4.9e-06 g/mm^3.

5.7 Combined Sorption Analyses

Reflecting upon these observations, and in order to visualize the difference between the apparent moisture sorption behavior of the Type II stones versus the molecular diffusion behavior exhibited by the Type I stones, finite element simulations were performed using RoAM on the sorption samples, Figure 47, whereby assuming a molecular diffusion process as used in Section 5.4. From these comparisons, even though the process of diffusion seems to capture the moisture infiltration in the stone at a later stage (after about 50 hours), the initial absorption was clearly not diffusion driven.

Based on these comparisons, Type II diabase samples are postulated to exhibit an initial sorption behavior caused by the action of hydraulic suction, rather than a molecular diffusion flux. A plausible reason for Type II diabase to have exhibited this initial sorption behavior may be found in temperature induced micro-scale fissures and cracks in the matrix of the stone, due to the cutting process and heating of the samples to clean them for re-use. After an initial increase in moisture mass, the Type II samples seem to follow again the diffusion dominated sorption as indicated by literature. The hydraulic suction was therefore induced by the filling up of the micro-pores or micro-cracks in the

stone matrix, which became saturated after a short time. Therefore, after the initial hydraulic suction, the remaining moisture uptake of the samples is caused by a molecular diffusion process of the moisture from the cracks into the bulk material, Figure 48.

Table 20(a). Detailed Moisture Sorption Measurements for Diabase Plates

Sample A				
Time [hours]	Moisture Uptake [g]	Absorption [g/g]	Moisture Concentration [E-06 g/mm^3]	Moisture Uptake [%]
0	0.0000	0.0000	0.0	0
0.27	0.1260	0.0010	2.9	60
0.83	0.1640	0.0013	3.8	78
3.33	0.1850	0.0014	4.3	88
5.33	0.1870	0.0015	4.4	89
8.43	0.1917	0.0015	4.5	91
22.33	0.1922	0.0015	4.5	91
25.17	0.1955	0.0015	4.6	93
28.37	0.1921	0.0015	4.5	91
32.33	0.1931	0.0015	4.5	92
46.33	0.1951	0.0015	4.6	93
48.83	0.1962	0.0015	4.6	93
52.50	0.2039	0.0016	4.8	97
56.17	0.2019	0.0016	4.7	96
76.33	0.2036	0.0016	4.8	97
149.33	0.2052	0.0016	4.8	98
214.66	0.2103	0.0016	4.9	100

Table 20(b). Detailed Moisture Sorption Measurements for Diabase Plates

Sample B				
Time [hours]	Moisture Uptake [g]	Absorption [g/g]	Moisture Concentration [E-06 g/mm^3]	Moisture Uptake [%]
0	0.0000	0.0000	0.0	0
0.27	0.1160	0.0008	2.5	53
0.83	0.1660	0.0012	3.6	75
3.33	0.1900	0.0014	4.1	86
5.33	0.1970	0.0014	4.3	90
8.43	0.1947	0.0014	4.2	89
22.33	0.2014	0.0015	4.4	92
25.17	0.2034	0.0015	4.4	92
28.37	0.2009	0.0015	4.3	91
32.33	0.2013	0.0015	4.4	92
46.33	0.2046	0.0015	4.4	93
48.83	0.2064	0.0015	4.5	94
52.50	0.2053	0.0015	4.4	93
56.17	0.2031	0.0015	4.4	92
76.33	0.2127	0.0015	4.6	97
149.33	0.2199	0.0016	4.8	100
214.66	0.2175	0.0016	4.8	100

Table 20(c). Detailed Moisture Sorption Measurements for Diabase Plates

Sample C				
Time [hours]	Moisture Uptake [g]	Absorption [g/g]	Moisture Concentration [E-06 g/mm^3]	Moisture Uptake [%]
0.00	0.0000	0.0000	0.0	0
0.50	0.0292	0.0004	1.2	25
1.50	0.0483	0.0007	2.0	41
3.62	0.0682	0.0010	2.8	58
5.53	0.0751	0.0011	3.1	63
7.70	0.0768	0.0011	3.2	65
24.37	0.0964	0.0014	4.0	81
33.65	0.0950	0.0014	3.9	80
48.53	0.0969	0.0014	4.0	82
77.87	0.1064	0.0016	4.4	90
152.20	0.1094	0.0016	4.5	92
175.37	0.1115	0.0016	4.6	94
199.37	0.1115	0.0016	4.6	94
246.37	0.1114	0.0016	4.6	94
483.87	0.1109	0.0016	4.6	94
557.37	0.1130	0.0017	4.7	96
749.70	0.1172	0.0017	4.9	99
918.20	0.1183	0.0017	4.9	100

In order to verify this postulate, new simulations of the sorption analysis were made with RoAM, whereby this time both hydraulic suction and effective diffusion were included in the simulations. Several analyses were made utilizing several diffusion coefficients. Comparing results of the finite element analyses with experimental data, a diffusion coefficient of 0.6 mm^2/hr (0.0009 in^2/hr) resulted. Observing Figure 49, the simulation of the combined hydraulic suction and diffusion action seem to capture the sorption behavior quite well, showing an initial dominant hydraulic suction action, followed by a more dominant diffusion process.

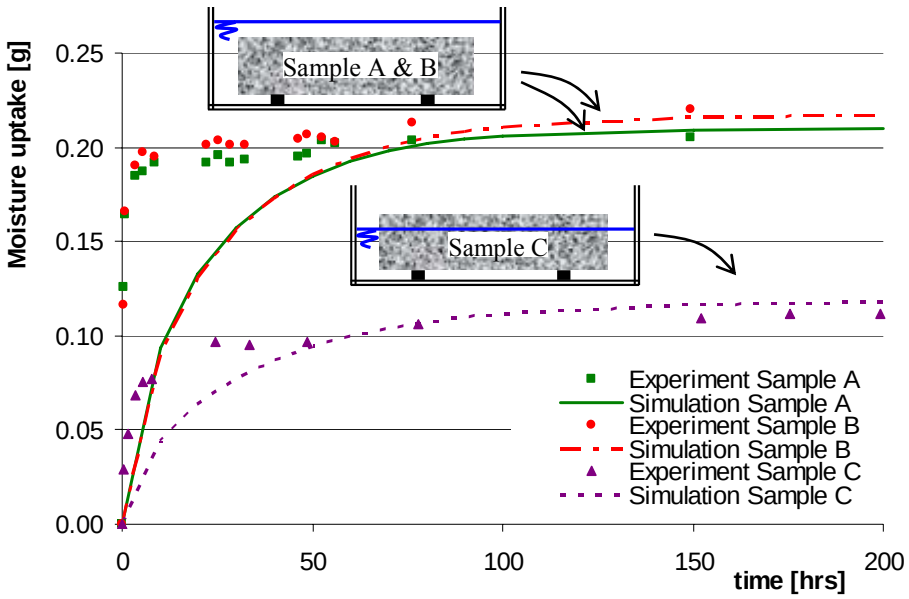

Figure 47. Comparison between Sorption Data and Finite Element Diffusion Analyses, Using D= 0.6 mm^2/hr (Copeland, et al. 2007)

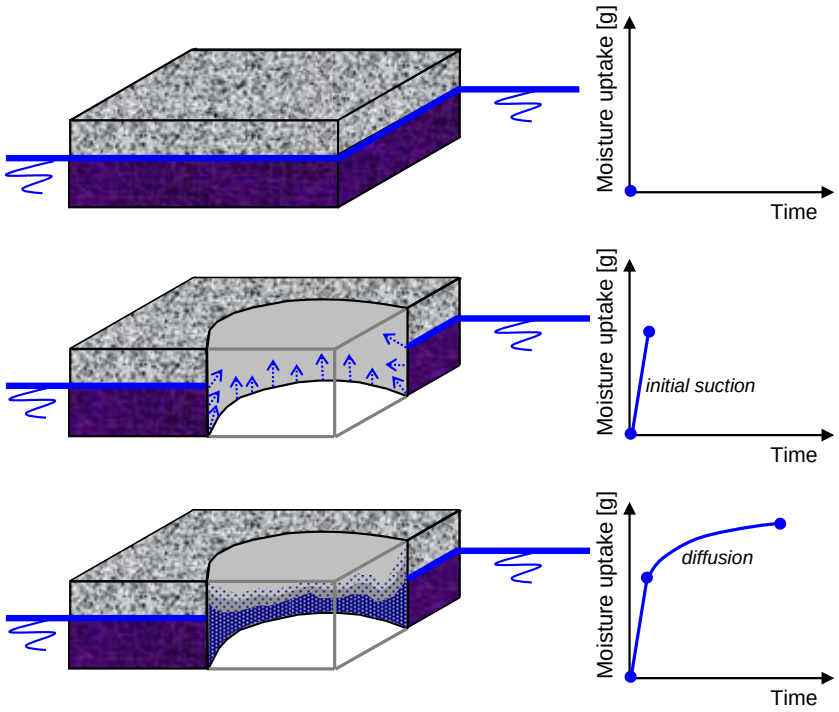

Figure 48. Postulate of Moisture Sorption Behavior in Type II Diabase (Copeland, et al. 2007)

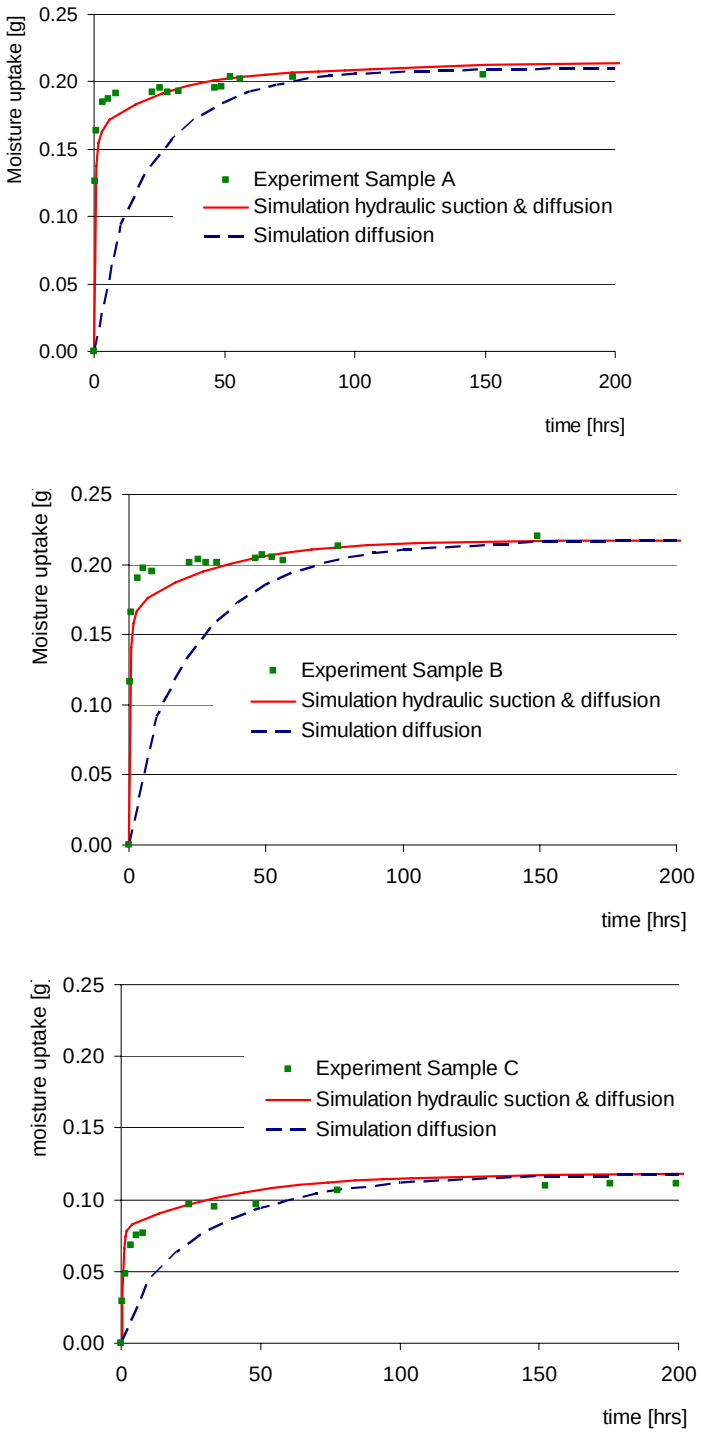

Figure 49. Simulated Moisture Sorption via a Combined Hydraulic Suction and Diffusion Action (Copeland, et al. 2007)

5.8 Updated Aggregate-Mastic Bond Strength Calculation

After examining the absorption behavior, the simulations of the Type II diabase specimens that were used in the pull-off test were repeated, but this time allowing for both hydraulic suction and diffusion. The results of these analyses are shown in Figure 50(a). Via regression analyses, the bond strength, measured by *POTS*, as a function of moisture content θ for Type II diabase was determined as

$$POTS(\theta) = 2.15 - 0.65e^{\theta}. \tag{5-8}$$

The reason that the bond strength reduction curve of equation 6-8 is different from equation 6-5 is because the moisture content variable is dependent on the maximum moisture concentration $C_m^{\max}$ of each material, equation 5-4. Since this is clearly a different value for the two types of diabase, the test results of the two types can not be plotted in the same bond strength-moisture content space. Instead, the test results can only be plotted together in strength-moisture concentration space. Unfortunately, insufficient data is available for Type I diabase. To illustrate the methodology, however, a maximum sorption concentration $C_m^{\max}$ of 2e-04 g/mm^3 was assumed for Type I diabase. In Figure 50(b) the results of both Type I and Type II diabase samples are plotted as bond strength versus moisture concentration. Performing a regression analysis on this data leads to the following representation of the aggregate-mastic bond strength as a function of moisture concentration C_m

$$POTS(C_m) = e^{(0.35 - 300\sqrt{C_m})}. \tag{5-9}$$

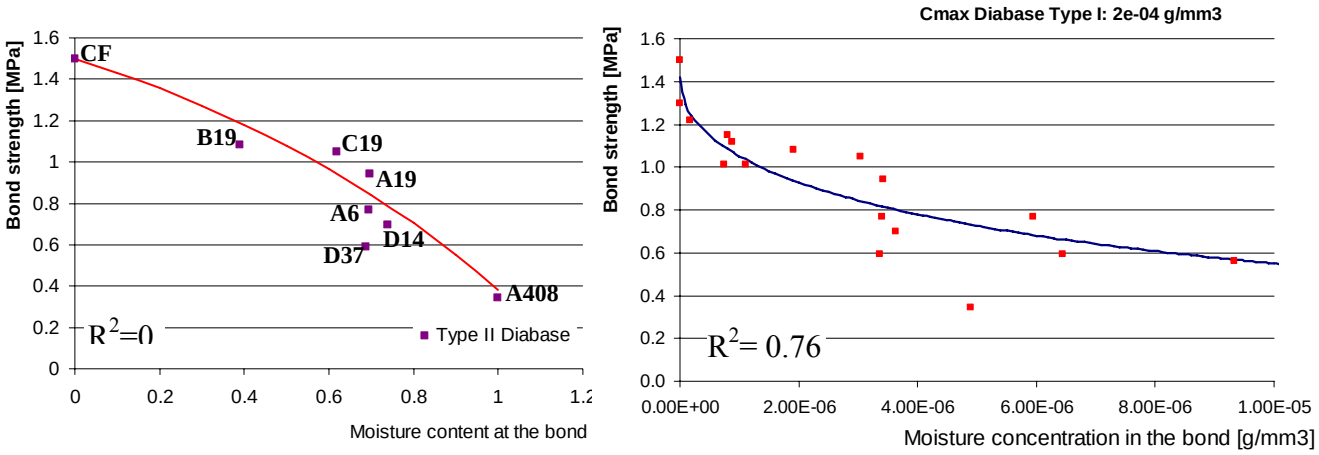

(a) (b)

Figure 50. (a) Bond strength as a Function of Moisture Content for Type II Diabase; (b) Bond Strength as a Function of Moisture Concentration for Both Type I & II diabase, with $C_m^{max} = 2e^{-04}$ g/mm^3 for Type I Diabase (Copeland, et al. 2007)

5.9 Conclusion

A computational-experimental procedure was presented for determining the relationship between bond strength degradation and moisture content at the mastic-aggregate substrate interface of asphalt mixtures. The methodology was applied to experimental tensile pull-off data, using a PATTI device, and finite element results of the diffusion of moisture into aggregate substrates obtained via the finite element tool RoAM. Combined results show that bond strength between mastic and aggregate decreases as moisture content increases. Considering that bond strength measured in the dry condition represents an undamaged state, a moisture-induced damage parameter, d_θ, was developed that relates bond strength to moisture concentration at the mastic-aggregate interface.

Upon verification of the methodology, however, the absorption of moisture by aggregate substrates is not a pure diffusive process, but follows a hydraulic suction process followed by diffusion. Further, moisture absorption process of aggregate specimens may significantly vary depending on the characteristics of the surface and the internal matrix due to temperature-induced cracking. In order to accurately capture the moisture concentration at the aggregate-mastic interface, numerical simulations should include both hydraulic suction and molecular diffusion processes that occur in the aggregate. The developed procedure has excellent potential for capturing bond strength reduction as a function of moisture infiltration at the mastic-aggregate interface. In addition, the moisture-induced damage parameter developed in this chapter may be used in a reliability analysis to quantify reliability of the bond at the mastic-aggregate interface as described in the next chapter.

CHAPTER VI

RELIABILTY ANALYSIS OF MOISTURE-INDUCED DAMAGE FAILURE

6.1 Introduction

An asphalt mixture experiences loading demand as a result of moisture as well as cyclic loading due to traffic during its service life. Moisture-induced damage is a complex process due to the complex, highly variable stress state imposed and the condition of the components of the asphalt mixture. In Chapter II, the loss of bond strength within the asphalt mastic (cohesive failure) and at the asphalt-aggregate interface (adhesive failure) was identified as the primary damage mechanisms that may eventually lead to pavement cracking and deformation. The strength of the bond between asphalt and aggregate is an important index for mixture durability. The durability of the mixture is compromised when the stresses imparted due to moisture combined with traffic loading exceed the strength of the bond between asphalt and aggregate.

This chapter begins by introducing the concept of a risk assessment framework for determining the moisture susceptibility of asphalt mixtures. The purpose is not to assess the actual risk but explore how a risk assessment framework may be undertaken. By understanding the causes of damage at each level (component, subsystem, and system), a designer can iterate the design process to eliminate or mitigate the effect of deterioration. Understandings of the mechanisms (i.e. failure modes) that contribute to moisture-induced damage, and the effects of the individual materials on these failure modes are valuable steps in the risk assessment process.

Statistical variations exist in the moisture and loading history and the material properties that affect the life of an asphalt mixture. Additional uncertainties exist due to approximations in the modeling process and availability of limited data. Thus, this chapter also considers a probabilistic approach to address uncertainties in moisture-induced damage prediction analysis. Three moisture-induced failure modes are considered and a reliability analysis is performed for one failure mode to estimate probability of failure due to damage at the mastic-aggregate interface as a function of moisture content. System reliability analysis concepts are introduced to illustrate how the probability of failure due to multiple failure modes is estimated.

6.2 Conceptual Risk Assessment Framework

A flow chart of the moisture damage process in asphalt mixtures is provided in Figure 51 where the root cause of moisture damage has been identified as the loss of bond strength within mastic and/or at the asphalt-aggregate interface. In effect, cohesive or adhesive failure occurs which leads to fracture at the asphalt-aggregate interface and within the asphalt binder and a loss of stiffness of the asphalt mastic. Subsequently, primary distress modes such as cracking and permanent deformation will occur, which propagate over time resulting in pavement deterioration and can lead to an overall failure of the pavement system which results in costs due to repair or replacement of the pavement layers.

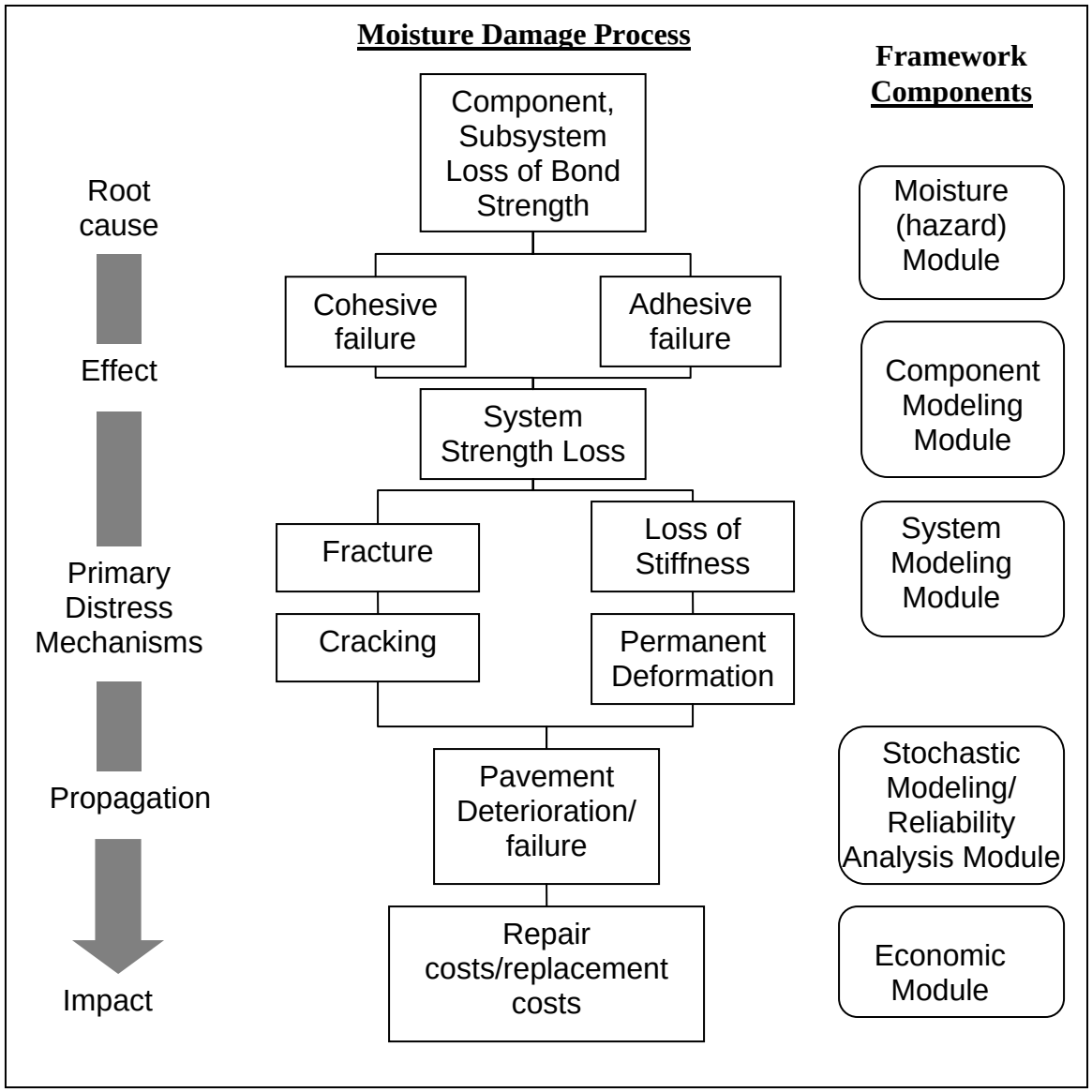

Figure 51. General Risk Assessment Framework for Moisture-Induced Damage of Asphalt Mixtures used in Highway Pavement Applications

Moisture damage risk is defined by the distribution of the loss of strength resulting from variation in possible damage outcomes, their likelihood (i.e. probability) and subjective values. Risk, in this context, is a function of:

- The likelihood and magnitude of moisture-induced damage,
- Susceptibility of the asphalt mixture as a result of damage,
- The impact of damage to the function of the compacted asphalt mixture and pavement structure,

summed over the full spectrum of possible moisture-related incidences and magnitudes capable of impacting the asphalt mixture. This concept is illustrated in Figure 52.

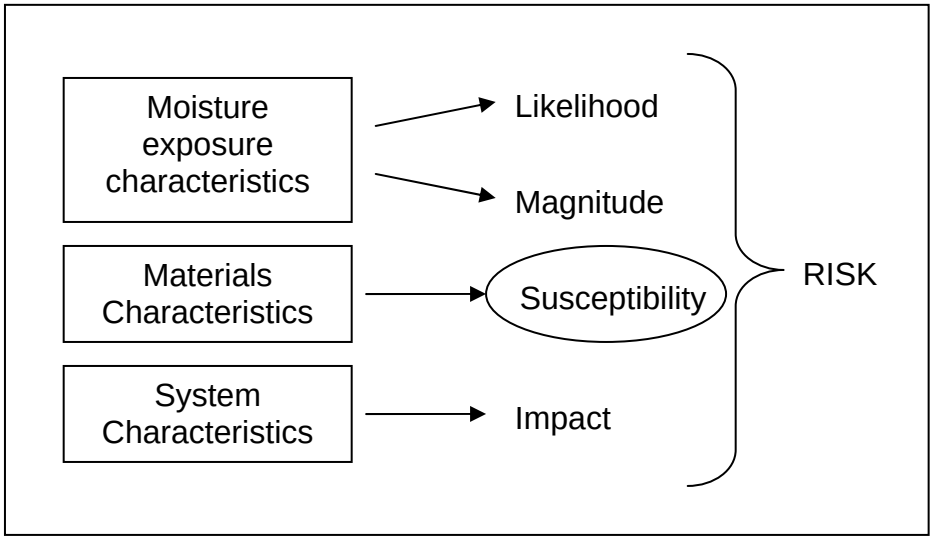

Figure 52. Major characteristics considered in estimating risk to asphalt mixture performance (adapted from Seville and Metcalfe (2005))

There is very little information available on the likelihood and magnitude of damage as result of moisture in an asphalt pavement. Distress as a result of moisture is similar to distress caused by other factors such as poor materials, design, or construction. Once damage has occurred, many State DOTs have various methods of damage classification that may be qualitative assessments rather than quantitative or are unable to distinguish moisture damage from other deterioration processes. In addition, current pavement forensic techniques may not accurately classify moisture-related failures. Thus, there is a lack of field-performance data or consistent data on the risks associated with the presence of moisture in bituminous mixtures and pavement failures may be correctly or incorrectly attributed to moisture damage. As part of a comprehensive risk assessment framework, the availability of data to indicate the probability of a hazard due to moisture conditions should be assessed. This includes analyzing historical data such as climatic information and groundwater levels (exposure), measurements of moisture levels (severity) in the asphalt mixture layer of pavements, and observations of moisture-induced damage (impact). A systematic methodology for classifying damage related to moisture is required. The goal of the methodology would be to identify consequences that have the most negative impact on pavement properties. The result of this effort would be defined hazard scenarios based on conditions experienced in the area the pavement is constructed and as indicated in Figure 51, would be part of the moisture (hazard) module in the overall risk assessment framework.

Based on the conditions the asphalt mixture will experience and hazard scenario information, the individual materials are evaluated within a component modeling module and material combinations are evaluated as part of the system module for susceptibility to

moisture. The compacted asphalt mixture (i.e. system) is then evaluated to determine the impact of the combination of the exposure to moisture and probability of the materials to experience distress due to moisture on the system in the stochastic model/reliability analysis module.

In this chapter, focus is placed on the susceptibility of the individual materials and asphalt mixture (circled in Figure 52) to moisture-induced damage by assessing the probability of failure due to moisture content at the asphalt-aggregate interface in the mixture.

6.3 Moisture-induced Damage Model

In Chapter II, a combined physical and mechanical moisture-induced damage constitutive model developed by Kringos (2007) was introduced. Equation 2-14 provides a multi-factor interaction model for a progressively damaging material based on two moisture-induced damage parameters (i.e. physical and mechanical) and the original properties of the material, $\mathbf{S}_0$. The physical moisture-induced damage parameter is estimated by ξ_m which is a function of damage due to moisture diffusion, d_θ, and advective transport, $d_{\hat{\rho}}$. The mechanical damage parameter is estimated by ξ_d. Damage (i.e. loss of strength) as a result of moisture is expressed by a multifactor equation:

$$S_d = (1-\xi_m)^a (1-\xi_d)^b S_0 . \tag{6-1}$$

where S_d is a strength related performance index that quantifies material properties after degradation due to moisture and mechanical damage. The physical moisture-related damage terms are combined through the equation:

$$(1-\xi_m)^a = (1-d_\theta)^{a_1} (1-d_{\hat{\rho}})^{a_2} . \tag{6-2}$$

In Chapter V, a moisture-induced damage parameter (1 - d_θ) given in equation 5-7, was developed to quantify loss of bond strength due to moisture diffusion through the aggregate component and is a function of moisture content, θ, and the moisture damage susceptibility parameter, α. The controlling parameters for the moisture diffusion process leading to an estimate of the moisture content, θ, are the moisture diffusion coefficient D_m and the maximum moisture capacity $C_m^{\max}$.

Kringos (2007) performed a numerical parametric study varying the mastic moisture diffusion coefficient, D_m, mastic film thickness, and the mastic-aggregate moisture-induced damage susceptibility parameter, α. The purpose of the parametric analysis was to determine the time in which the reduction in bond strength at the mastic-aggregate interface may become relevant in practice. Simulations were performed for 10%, 25%, 50%, 75%, and 100% reduction in bond strength. The analysis highlights the need to determine moisture diffusion coefficients of asphalt mixture components and choose materials that minimize the moisture damage susceptibility parameter, α (Kringos 2007). However, this analysis does not consider uncertainties associated with the model parameters. Thus, a probabilistic (rather than deterministic) approach to predicting moisture-induced damage is presented in the following sections.

6.4 Proposed Moisture-induced Damage Failure Function

The loading history and amount of moisture present in the asphalt mixture affects the serviceability life of asphalt materials. In practical applications, there is uncertainty associated with the amount of moisture that the mastic-aggregate interface is exposed. In addition, the thickness of the mastic film coating the aggregate is a random variable and

there is also uncertainty associated with the moisture diffusion coefficient especially in the case of mastic where the amount of mineral filler varies thereby influencing the porosity and diffusivity properties of the mastic film. The mastic-aggregate moisture-induced damage susceptibility parameter, α, also has inherent randomness due to model uncertainty. In this chapter, a new moisture-induced damage failure model is proposed with a continuous non-linear function. The criterion is a function of two random parameters that model the uncertainty due to limited test data.

First, moisture-induced damage due to diffusion processes is considered and may be expressed as (Kringos 2007):

$$S_d^{\theta} = f(S_0, d_\theta, a_1) = (1 - d_\theta)^{a_1} S_0 \tag{6-3}$$

where a_1 determines the non-linearity of the relationship and for simplicity is assumed to equal 1. Equation 6-3 is a special case of equation 6-2 where there is no damage due to advective transport and no mechanical damage. The damage relationship at failure may be written as:

$$(1 - d_\theta) = D_\theta^{cr} \tag{6-4}$$

where d_θ is the moisture-induced damage parameter due to diffusion and is a function of moisture content, θ, and the moisture susceptibility parameter, α. Failure occurs when $(1 - d_\theta) > D_\theta^{cr}$, where D_θ^{cr} is the critical damage level, discussed in detail in Section 6.6.

6.5 Reliability Analysis Concepts

A performance function $g(X)$ where X is a vector of random variables may be defined corresponding to a performance criterion. Failure occurs when $g(X) < 0$ while

$g(X) > 0$ denotes the safe region and $g(X) = 0$ is the limit state or failure surface. This limit state represents the boundary between the safe and unsafe (i.e. failure) regions of the design space. Assuming there are two random variables, X_1 and X_2, the general concept of a limit state and the safe and unsafe regions are shown in Figure 53.

The probability of failure, p_f, for this performance function, $g(X)$, is computed as:

$$p_f = P\{g(X) < 0\} = \int \ldots \int_{g(X)<0} f_x(x_1, x_2, \ldots x_n) dx_1 dx_2 \ldots dx_n \tag{6-5}$$

where $f_x(x_1, x_2, \ldots x_n)$ is the joint probability function (PDF) for the basic random variables $X_1, X_2, \ldots X_n$ and n is the number of random variables. The integration is performed over the failure region, $g(X) < 0$. The computation of the above multiple integral is difficult and joint probability functions for random variables are typically not available. Approximate computational methods have been developed to estimate reliability in the form of analytical and sampling-based procedures (Haldar and Mahadevan 2000). Analytical methods construct first- or second-order approximations to the limit state and probability of failure. Sampling-based methods generate a multitude of samples of the random variables and evaluate the performance criterion for each simulation.

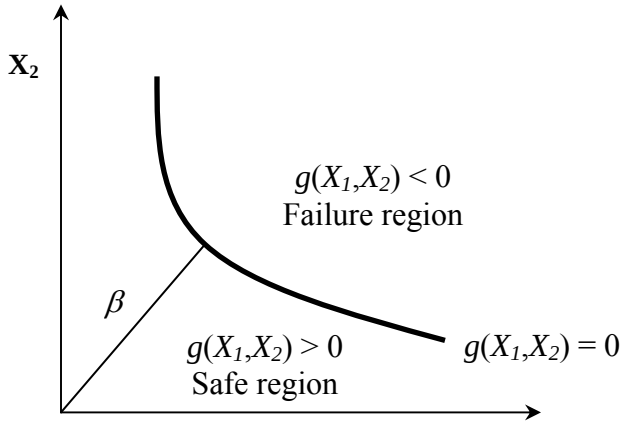

Figure 53. Limit State Concept (Haldar and Mahadevan 2000)

6.4.1 First-Order Reliability Method (FORM)

FORM computes a first-order approximation of the failure probability, p_f. FORM is exact for linear limit state functions with uncorrelated normal variables. FORM may also be applied for a non-linear limit sate with correlated non-normals if the limit state can be approximated by a linear function with equivalent normal variables. In the FORM method, all random variables, X, are converted to equivalent uncorrelated standard normal variables, X', and a linear approximation of the limit state is constructed at the point of minimum distance on the limit state from the origin to estimate the probability of failure. The point on the limit state closest to the origin is referred to as the Most Probable Point (MPP) and represents the most probable limit state combination of the random variables. The distance from the origin to the MPP is referred to as the reliability index, β. The probably of failure is then estimated as:

$$p_f = \Phi(-\beta) = 1 - \Phi(\beta) \tag{6-6}$$

where Φ is the cumulative distribution function (CDF) of a standard normal variable. A Newton-Raphson type algorithm suggested by Rackwitz and Fiessler (1978) is used to

find the minimum distance point (Haldar and Mahadevan 2000), through the following recursive formula:

$$\mathbf{x}'^{*}_{k+1} = \frac{1}{\left|\nabla g(\mathbf{x}'^{*}_{k})\right|}\left[\nabla g(\mathbf{x}'^{*}_{k})^{t}\,\mathbf{x}'^{*}_{k} - g(\mathbf{x}'^{*}_{k})\right]\nabla g(\mathbf{x}'^{*}_{k}) \tag{6-7}$$

where $\nabla g(\mathbf{x}'^{*}_{k})$ is the gradient vector of the performance function at $\mathbf{x}'^{*}_{k}$, the k-th iteration point. The vector, $\mathbf{x}'^{*}_{k}$, has components $\left\{x'^{*}_{1k}, x'^{*}_{2k}, ..., x'^{*}_{nk}\right\}^{t}$. As the name indicates, the probability of failure calculated by FORM is only a first-order approximation. As the amount of random variables increases and for highly nonlinear limit states, second-order and multi-point approximation methods are available (Breitung 1984, DerKiureghian, et al. 1987, Fiessler, et al. 1979, Mahadevan and Shi 2001, Tvedt 1990).

6.4.2 Simulation Techniques

Monte Carlo (MC) analysis is a simple simulation technique which can be used to determine the probability of failure for a component or system. MC analysis is particularly useful in system reliability analysis because it is difficult to determine the joint probabilities of multiple failure events in closed form. During MC analysis samples are drawn from distributions of each random variable and then the functional relationships between the variables are evaluated for each draw. Failure probabilities may be estimated by simply dividing the number of failures by the number of samples. Using the MC approach, statistical data on the results such as PDF, CDF and draw histograms (Haldar and Mahadevan 2000) may be obtained. The appeal of the MC technique is that MC analysis is simple to implement even for complicated engineering systems to provide accurate results. However, this accuracy comes at the expense of conducting numerous simulations for small probabilities of failure. For large systems if

the computational model is expensive, using pure MC analysis becomes infeasible. Therefore, several efficient sampling techniques, such as importance sampling, have been developed in the literature (Harbitz 1986, Karamchandani, et al. 1989, Melchers 1989, Wu 1992).

6.6 Numerical Example for Moisture-induced Damage Due to Moisture Diffusion

A primary failure mode in the onset of moisture-induced damage is the loss of bond strength at the mastic-aggregate interface. In this example, we consider the probability of failure due to damage at the mastic-aggregate interface as a result of moisture diffusion processes. The corresponding limit state function, assumed to represent moisture-induced damage of all mastic-aggregate interfaces, is based on equation 5-7 and 6-4 and given as:

$$g(\alpha,\theta) = D_{\theta}^{cr} - (1 - e^{-\alpha\sqrt{\theta}}) \tag{6-8}$$

where θ is moisture content and α is the mastic-aggregate moisture-induced damage susceptibility parameter. According to equation 5-7, the loss in bond strength due to moisture content at a given time (second term in right hand side of equation 6-8) is described by an exponential model where damage, d_{θ}, is cumulative and α represents a rate of damage. This indicates that for each mastic-aggregate combination, there is a constant failure rate. An exponential model is suitable since it captures the portion of the curve (long, flat portion) where damage is most likely to occur due to increased θ, assuming early failure or wear out is not an issue.

The variable D_θ^{cr} represents a critical damage (i.e. loss of strength) level due to moisture diffusion. The impact may be quantified by determining if a given distress level exceeds a critical distress level. The value for D_θ^{cr} is assumed to be deterministic and may be chosen based on an acceptable amount (i.e. percentage) of damage related to conditions of the materials and environment based on experimental results. The critical distress levels may be determined by discretizing the critical damage index, D_θ^{cr}, as shown in Table 21, and correlating each value to a physical condition of the system. For example, failure at the mastic-aggregate interface may be assumed to occur when there is damage is greater than fifty percent. The value of D_θ^{cr} would then be 0.50.

Table 21. Illustration of Critical Damage Index (D_θ^{cr}) Levels

D_θ^{cr} Target	Physical Condition
~0	No damage under greater than expected demand
0.1	No damage
0.2	Functional
0.3	
0.4	
0.5	Damage threshold
0.6	
0.7	
0.8	
0.9	Total loss of bond strength – mixture failure

The variable α is uncertain due to the limited amount of data available (data is available for only one mastic-aggregate combination) and possible model error. Therefore α is modeled as a continuous random variable and assumed to have a normal distribution. The moisture content, θ, is also treated as a continuous random variable. The distribution

and values of the distribution parameters for θ may be obtained through results of experiments to determine moisture diffusivity coefficients, *D*, and the maximum moisture capacity, $C_m^{\max}$. Moisture diffusion coefficient data are available for SHRP Material Reference Library binders (Cheng, et al. 2002b, Little and Jones 2003, Nguyen, et al. 1992) and experiments for determining moisture diffusion coefficients of asphalt mix components and subsystems such as mastic are suggested in Kringos (Kringos 2007), section 6.3. However, due to significant variations in reported moisture diffusion coefficient data for asphalt binders and the limited amount of data, the expected values for θ at fourteen, twenty-four and thirty-seven hours of soak time are determined based on simulation results from Chapter V. The uncertainty of θ is modeled using a Beta distribution since θ does not take on negative values and the maximum value that θ can take on is 1, $0 < \theta \leq 1$. The assumed values of the distribution parameters are shown in Table 22.

Table 22. Statistics of random variables

Parameter	Mean Values	CV	Distribution
$\theta(14)$, $\theta(24)$,$\theta(37)$	0.005, 0.15, 0.045	0.15	Beta
α	3.76	0.10	Normal
D_θ^{cr}	0.1, 0.25, 0.5, 0.75, 0.95	0	Deterministic

The mastic-aggregate interface failure probability is

$$p_f = P(\textit{failure}) = P(g(\alpha,\theta) < 0) \tag{6-9}$$

The limit state that was defined in equation 6-6 is nonlinear. Since FORM method is only a first order approximation and the limit state is not computationally demanding,

Monte Carlo simulation was chosen to evaluate the reliability of the tensile strength of the mastic-aggregate interface by estimating the p_f at a given soak time. Over 10,000 simulations were performed and the number of failures (i.e. number of times that g is less than zero) were summed, N_f, and divided by the number of simulations (10,716 simulations), N. The probability of failure can then be calculated as:

$$p_f = \frac{N_f}{N} \tag{6-10}$$

The results are provided in Table 23, for different levels of D_θ^{cr}.

Table 23. Summary of Simulation Results (Case 1)

Soak Time	D_θ^{cr} 10%		25%		50%		75%		90%	
t	p_f	COV	p_f	COV	p_f	COV	p_f	COV	p_f	COV
14	0.9999	0.000	0.2381	0.018	0*	n/a	0*	n/a	0*	n/a
24	0.9999	0.000	0.9995	0.000	9.83E-5	1.000	0*	n/a	0*	n/a
37	0.9999	0.000	0.9999	0.000	0.8473	0.004	0*	n/a	0*	n/a

*N_f is zero for these cases, and N = 10,716.

In the case where D_θ^{cr} equals ten percent which indicates that failure occurs after a ten percent loss in bond strength (i.e. no damage is desired according to Table 21), this particular asphalt-aggregate pair will fail (p_f = 0.9999) at each soak time. If D_θ^{cr} is set to fifty percent, there is a low probability that this asphalt-aggregate pair will fail after fourteen hours (p_f = 0) and twenty-four hours (p_f = 9.83E-5), however there is an eighty-five percent chance (p_f = 0.8473 in Column 6 of Table 23) of failure at thirty-seven hours of soak time. If the damage tolerance level is set to seventy-five or ninety percent which

indicates that a seventy-five or ninety percent loss in bond strength is acceptable, then there is no (p_f = 0) chance of failure. No matter what critical damage level is chosen, according to the parameters of the example, failure will occur at approximately fifty hours of soak time. In reality, complete failure at the mastic-aggregate interface does not occur after fifty hours. Thus, a more realistic representation of the moisture content for this specific example is preferred.

Recall that in Chapter V, a gravimetric analysis was performed on diabase aggregate plates similar to those used in the pull-off test methodology used to develop equation 5-7. Considering the conditioning procedure used in the pull-off test method, the following logarithmic equation is a quantitative approximation of the absorption of a partially submerged diabase aggregate:

$$\mu(\text{absorption}) = 2.0E-4 * \ln(t) + 7.0E-4 . \qquad (6\text{-}11)$$

Using the mean absorption value corresponding to each soak time, *t*, to generate values for θ in equation 6-6, the results of the Monte Carlo simulation in this case (referred to as case 2) are given in Table 24.

If the critical damage level is ten percent loss in bond strength, there is a greater than ninety-five percent change of failure at the mastic-aggregate interface after fourteen hours of soak time. However, if failure is assumed to occur when damage is equal to or greater than twenty-five percent, after one year (8,760 hours), there is approximately no chance of failure and after 100 years (876,000 hours); the probability of failure is still less than one percent. In situations where a fifty, seventy-five or ninety percent loss in bond strength is acceptable, there is no chance of failure according to the parameters of case 2.

Table 24. Summary of Simulation Results (Case 2)

Soak Time	D_θ^{cr} 10%		25%		50%		75%		90%	
t	p_f	COV	p_f	COV	p_f	COV	p_f	COV	p_f	COV
0.5	0.0669	0.037	0*	n/a	0*	n/a	0*	n/a	0*	n/a
4	0.7869	0.005	0*	n/a	0*	n/a	0*	n/a	0*	n/a
8	0.9004	0.003	0*	n/a	0*	n/a	0*	n/a	0*	n/a
12	0.9356	0.003	0*	n/a	0*	n/a	0*	n/a	0*	n/a
14	0.9476	0.002	0*	n/a	0*	n/a	0*	n/a	0*	n/a
24	0.9723	0.002	0*	n/a	0*	n/a	0*	n/a	0*	n/a
37	0.9830	0.001	0*	n/a	0*	n/a	0*	n/a	0*	n/a
48	0.9874	0.001	0*	n/a	0*	n/a	0*	n/a	0*	n/a
8760	0.9999	0.000	9.83E-05	1.0	0*	n/a	0*	n/a	0*	n/a
87600	0.9999	0.000	0.0014	0.267	0*	n/a	0*	n/a	0*	n/a
876000	0.9999	0.000	0.0093	0.102	0*	n/a	0*	n/a	0*	n/a

*N_f is zero for these cases, and N = 10,716.

The true nature of the moisture content and absorption characteristics of asphalt binder and aggregate are most likely between case 1 and case 2. This highlights the importance of determining individual material parameters such as the moisture diffusion coefficients of asphalt binders and aggregates and the ability of the materials to absorb and retain water. It is not feasible to determine this information for each and every material, however ranges may be specified for material types and a probabilistic analysis as shown above can be applied to simulate the randomness inherent in the parameters.

6.7 System Reliability Analysis

In the previous section, reliability was estimated for a single performance criterion or limit state, equation 6-6 (damage at the mastic-aggregate interface due to moisture diffusion). However, an asphalt mixture may fail due to moisture-induced

damage in more than one failure mode as indicated by the multiple factors (i.e. damage due to the physical process of moisture damage or due to mechanical damage) included in equation 6-1. Consider an asphalt mixture where three damage mechanisms are considered: physical damage due to moisture diffusion, physical damage due to advective transport, and mechanical damage due to traffic and moisture-induced loading. For example, failure may occur due to diffusion followed by advective transport (i.e. washing away of the mastic) or a combination of the two failure modes. In addition, failure may occur due to mechanical damage and combined physical moisture-induced and mechanical damage. The three possible failure modes and combinations for moisture-induced damage are shown in Figure 54. Implementation of the scheme in Figure 54 requires definition of various critical damage levels for D_{θ}^{cr}, $D_{\hat{\rho}}^{cr}$, D_{m}^{cr}, D_{d}^{cr}, and D^{cr}. An alternative approach to the last box (combined failure) in Figure 54 is to use system reliability techniques**.**

System reliability evaluation is a complex process that depends on multiple factors including (1) the contribution of the individual failure modes to the overall system's failure, (2) redundancy in the system, (3) the behavior of each component and the system after individual failure mode occurences and combinations, (4) the correlation between failure modes, and (5) the progression of failure modes (Haldar and Mahadevan 2000). In the case of an asphalt mixture, failure due to one or more damage mechanisms may result in failure of the system. Since there are multiple failure modes, the simplest

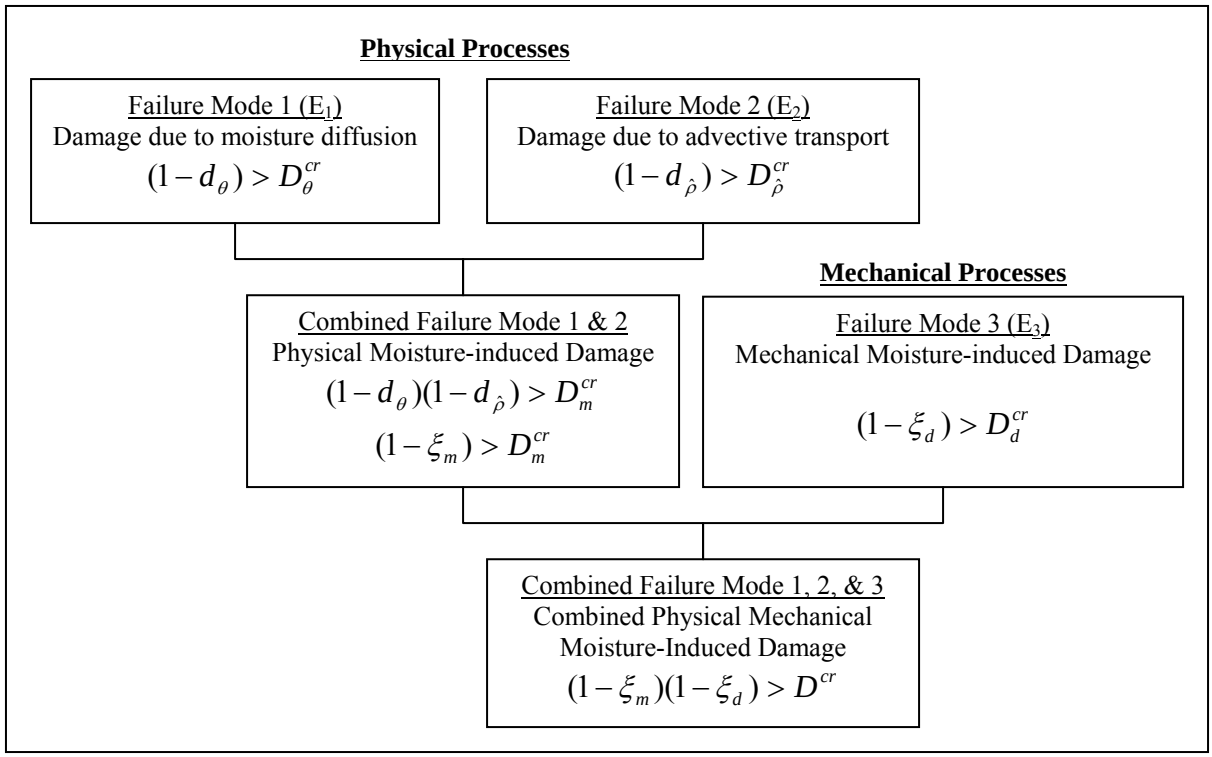

Figure 54. Failure Modes and Combinations for Moisture-Induced Damage in Asphalt Mixtures

case is to define system failure as occurring when any performance critierion or failure mode is violated which is referred to as a series or "weakest link" system. The system failure probability is computed as the probability of union of individual failure events (Haldar and Mahadevan 2000):

$$P(E_1 \cup E_2 \cup E_3) = P(E_1) + P(E_2) + P(E_3) - P(E_1E_2) - P(E_2E_3) - P(E_3E_1) + P(E_1E_2E_3) \quad (6\text{-}12)$$

where $P(E_1E_2)$ is the joint probability of E_1 and E_2, and so on.

Consider the physical moisture-induced damage parameter, ξ_m. The asphalt mixture in this case is subjected to two loads, damage due to moisture content and due to advective transport (i.e. mastic erosion). Failure may occur due to diffusion (failure mode 1 in Figure 54 designated E_1) followed by advective transport (failure mode 2

designated E_2) or vice versa or failure may occur due to a combination of failure modes (i.e. failure modes 1 & 2).

The limit states corresponding to these mechanisms are shown in Figure 55. The system failure domain is illustrated by the region shaded in gray, which is the union of the failure domains for each individual limit state. System failure probability is then defined as the integral of the joint PDF of the random variables, d_θ and $d_{\hat{\rho}}$, over the system failure domain (Haldar and Mahadevan 2000), which is the union of the individual failure domains.

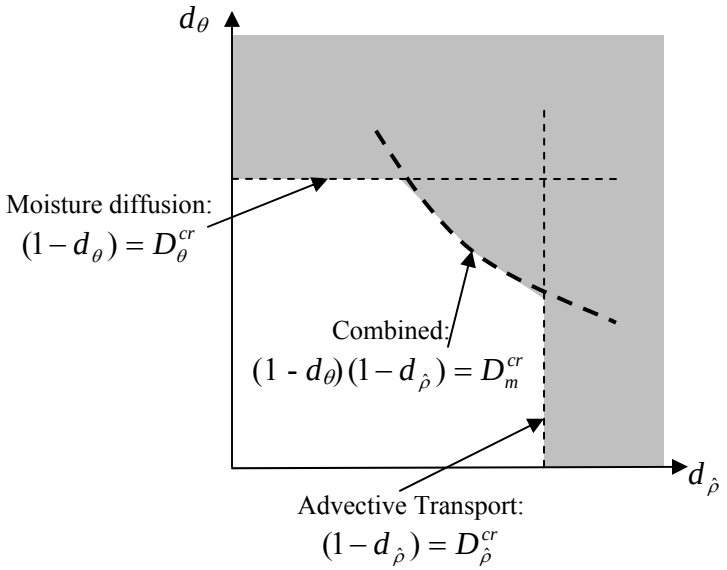

Figure 55. Physical Moisture-induced Damage – Three Damage Limit States (adapted from Haldar and Mahadevan 2000)

Failure may occur due to any one of two damage events: diffusion of moisture or washing away of the mastic. If E_i represents the failure event of the *i*th limit state, the event of failure of a system in series is defined by the union of all the individual failure

events. It is difficult to determine the joint probabilities of more than two failure events except by using simulation or numerical integration, so first-order bounds (Ang and Amin 1967, Cornell 1967) have been proposed for the probability of failure of the system, p_{fs}:

$$\max[P(E_i)] \le p_{fs} \le \min\left[\sum_{i=1}^{n} P(E_i), 1\right] \tag{6-1}$$

where $P(E_i)$ is the probability of failure of the ith limit state and n is the number of limit states. First-order bounds can be quite wide, therefore second order bounds have also been developed (Ditlevsen 1979).

Although d_θ was quantified in Chapter V, there is only scarce data available for the variables d_θ depends on in order to determine d_θ's probabilistic distribution and estimate the p_f due to moisture content as discussed in section 6.5. In addition, $d_{\hat{\rho}}$, has not been determined yet; therefore, so at this time even the first order bounds for system reliability cannot be determined.

It is also possible that the failures are not simultaneous, but sequential. In that case, multiple failure sequences are possible as shown in Figure 56. Conditional probabilities need to be calculated, and system failure is the union of all the failure sequences. When there are a large number of individual failure modes, the number of sequences can be very large; therefore, efficient methods for identifying the dominant failure sequences have been developed (Haldar and Mahadevan 2000).

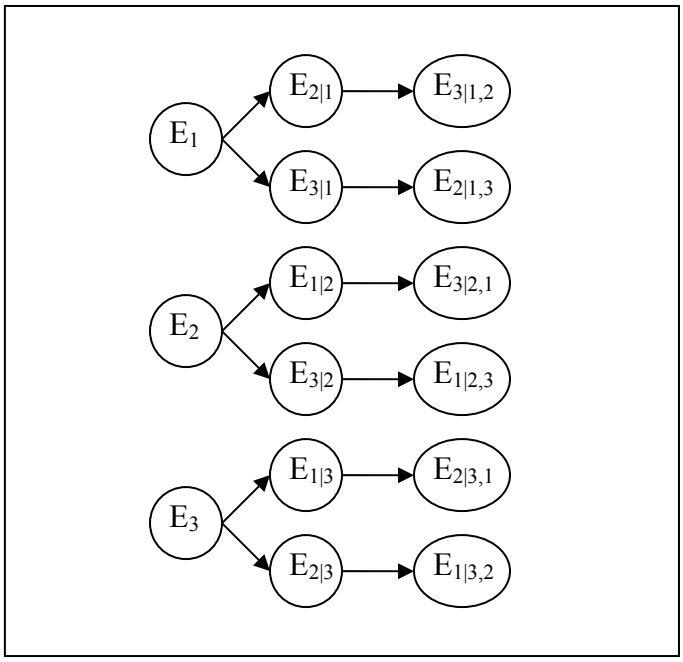

Figure 56. Possible Failure Sequences Among Three Failure Modes

6.8 Conclusion

This chapter discussed the conceptual issues for assessing the risk of asphalt mixtures to moisture-induced damage. Moisture damage-related research in asphalt pavements has been on-going for many years; however the need for a framework rather than a specific test to address moisture-induced damage has been recognized and developed. The author's intent in this chapter was to highlight the need to base this framework on risk and reliability principles. A conceptual risk assessment framework was introduced to illustrate how the onset of moisture damage results in loss of bond strength and propagates from primary moisture-induced failure modes such as adhesive and cohesive failure to primary pavement distress mechanisms, pavement deterioration and eventual pavement failure. The full benefits of this framework cannot be realized without performing a full-scale risk assessment. This is a significant task but will result

in key benefits such as providing information for optimal design and use of resources to maximize safety. In addition, including probabilistic design concepts provides more information about the asphalt mixture system, the influence of different uncertain variables on system performance, and relationships between system components which is crucial information regarding the development and degradation of bond strength between asphalt binder and aggregate.

The primary goal of moisture damage-related research is to improve serviceability of flexible pavements. One way to determine pavement serviceability is to measure the pavement structure's strength. However, it is difficult to precisely quantify the strength of a structure and even more difficult to quantify the effects of moisture on the strength of an asphalt mixture. Therefore a framework is proposed that identifies four major areas of research effort:

1. Determination of the primary (i.e. most influential) mechanisms that contribute to moisture damage;
2. Knowledge of the component materials and their behavior in dry and moisture conditions;
3. Development, validation, and verification of response predictions; and
4. Adequacy of the design procedure to address moisture-induced damage in asphalt mixtures.

In an asphalt mixture, the primary cause of moisture damage is determined to be loss of bond strength within the asphalt binder, mastic and/or at the asphalt-aggregate interface. Mechanical bond strength measurements were used to develop a moisture-

induced damage parameter that may be used as part of the risk assessment framework to predict the occurrence of failure of the bond between asphalt and aggregate.

This chapter proposed a probabilistic approach for moisture-induced damage reliability analysis by considering uncertainties in the demand on the system in terms of moisture (i.e. moisture diffusion and advective transport) and in the material properties by considering the uncertainty of moisture content, θ, at the mastic-aggregate interface and of the moisture susceptibility parameter, α. The proposed model for moisture-induced damage at the mastic-aggregate interface as a function of moisture content is the first of its kind in quantifying damage due to moisture. The model parameters in the proposed failure function address uncertainty due to unavailability of test data. In addition to illustrating the application of reliability analysis concepts for a single performance criterion, the evaluation of multiple failure modes or system reliability is discussed.

Finally, the results and discussion of this chapter highlight the need for future research which addresses the collection of essential data for modeling the uncertainty in variables in an asphalt mixture and the mixture's components for successful implementation of a reliability analysis. In order to quantify the uncertainty in the moisture content, diffusion coefficients for binders, mastics and aggregates are required as well as moisture capacity of the individual component materials. The damage parameter due to loss of bond strength as a function of moisture content has been modeled; however the damage parameter due to advective transport is still required. The moisture susceptibility parameter, α, requires additional pull-off tensile testing to estimate the loss in bond strength. This parameter may be quantified for other damage

mechanisms such as erosion of the mastic and shear strength between mastic and aggregate. Also, critical values of damage indices need to be decided for risk assessment.

CHAPTER VII

CONCLUSIONS, RECOMMENDATIONS, AND FUTURE RESEARCH

7.1 Summary

The research reported in this study is part of an overall effort at the Federal Highway Administration (FHWA) to develop a systematic risk assessment framework that may be used during the design process to make choices based on material characteristics that mitigate moisture damage in asphalt mixtures. This dissertation has focused on the development of test methods to assess moisture effects on asphalt mixture strength, which is an essential step is the risk assessment process.

Moisture is the major climatic condition that adversely affects hot mix asphalt (HMA) quality. Moisture damage occurs when there is a loss of bond either between asphalt and aggregate or within the asphalt mastic. Experimental methods were developed in this study to measure bond strength of asphalt binders, mastics and asphalt-aggregate pairs. In parallel, researchers at TU Delft have developed a finite-element tool known as RoAM (Raveling of Asphalt Mixtures) that simulates the critical moisture damage-inducing processes. These include diffusion of water through mastic to the mastic-aggregate interface, advective transport of mastic, and mechanical damage. A critical parameter to these processes is bond strength failure (i.e. damage) between asphalt and aggregate in the presence of water. Bond strength is determined via a modified version of the pull-off test (ASTM D 4541) method typically used in the paint coating and adhesives industry. Experimental results for bond strength are linked to

moisture diffusion simulations from RoAM and, for the first time, bond strength degradation as a function of the amount of moisture at the asphalt-aggregate interface is established. Based on this relationship, the amount of damage that occurs over time in regards to the amount of moisture is quantified.

7.2 Major Outcomes

The major outcomes of this research are arranged according to the objectives and the three major components of this dissertation research discussed in Chapter I.

Modified Pull-off Test to Measure Bond Strength and Influence of Moisture on Bond Strength

The modified pull-off test quickly measures bond strength (i.e. maximum strength at failure) of binders and mastics. The pull-off test is repeatable method for measuring bond strength of asphalt binders adhered to glass and aggregate substrates and can accurately assess effects of variables such as modification, moisture, aging, and mineral filler on bond strength. The pull-off test can distinguish among different binders and is able to rank binders according to how they may perform when compared when mixture moisture sensitivity tests such as the HWTD. Comparisons of pull-off tensile strength to binder permanent deformation results highlight the need for a test method that can properly evaluate binder adhesive characteristics when subjected to moisture conditions.

Operator variability was addressed by using a press that uniformly applied the loading fixture to the substrate. A procedure was developed to uniformly cut stones into aggregate plates to facilitate testing bond strength between asphalt and aggregate. Moisture decreases adhesive properties of binders and is an influential factor on bond strength. However, cohesive failure within the binder was common even after moisture

conditioning. The variability in the porous nature of the aggregate substrates presents difficulty in consistently obtaining adhesive failure at the asphalt-aggregate interface. This variation is due to surface texture and the internal aggregate matrix.

The modified pull-off test method is recommended for use as a simple test method to determine the contribution of factors and system components before and after moisture conditioning. The test method is useful because it can evaluate components such as binder and binder on aggregate and subsystems such as mastics under varying conditions. A suggested pull-off test method is given in Appendix C.

Combined Experimental-Numerical Model to Quantify Damage at Mastic-Aggregate Interface

A computational–experimental procedure was developed to quantify moisture damage at the mastic-aggregate interface based on loss of bond strength as determined by the pull-off test method and amount of moisture at the interface. For a more realistic estimation of damage at the asphalt-aggregate interface, mastics (rather than binder) were applied to aggregate plates to measure bond strength before and after moisture conditioning. Bond strength at the mastic-aggregate interface decreased as moisture content, simulated by RoAM, increased. The moisture absorption process in aggregate plates was shown to be a two-part process consisting of rapid absorption due to hydraulic suction (i.e. capillary action) and then slower absorption due to diffusion. Eventually the specimens reach equilibrium moisture content. Moisture-induced damage at the mastic-aggregate interface was quantified as a function of moisture content.

Risk Assessment Framework and Reliability Analysis

There is a need for a risk-based framework to address moisture-induced damage in asphalt pavements. The framework should be developed with principles of risk and

reliability in mind. The proposed framework identifies four areas: (i) determining the primary mechanisms that contribute to moisture damage and quantifying their likelihood and severity, (ii) knowledge concerning the component materials and their response under moisture conditions, (iii) development of models that simulate the response of the system under moisture scenarios, and (iv) adequacy of the design procedure.

A probabilistic approach for moisture-induced damage analysis was proposed by considering uncertainties in the moisture content and moisture susceptibility parameter. The developed limit state facilitates implementation of analytical reliability analysis methods; however extensive additional data is required for a complete reliability analysis.

7.3 Future Work

This section offers ideas to improve procedures to measure bond strength of asphalt materials and ideas for future research.

Improvements to pull-off test method

The pull-off test method has been established as a quick, repeatable method for measuring bond strength of asphalt binders and mastics. However, for the pull-off method to become a standardized method, a precision and reproducibility study should be performed. A variety of asphalt materials were used in this study, however additional materials that are chosen to correspond to monitored field pavements should be considered. With the use of aggregate substrates, the pull-off test method could prove to be a powerful tool for determining the influence of antistripping additives added to binder or applied to the surface of the aggregate substrate on the cohesive and adhesive behavior of the asphalt binder.

The pull-off test has been shown to be an effective test method for measuring the effect of moisture on binders and mastics and the effect of other factors such as aging, polymer modification and mineral fillers. The tensile strength is easy to measure and is reproducible, making the pull-off test method practical for specification purposes. Currently, the pull-off test method measures the maximum tensile strength of asphalt materials, for example binder, under uniaxial loading conditions. However, this value is of little *fundamental* significance with regard to the strength of the binder. In order for results from the modified pull-off test method to be used for providing input to materials models and to provide information to predict the risk to moisture-induced damage, the elongation of the material should be measured. As part of this effort, control of the film thickness should be exercised or a device manufactured to permit reliable control of the film thickness. Measuring the amount of elongation during loading will provide information to develop stress-strain curves providing insight concerning deformation such as elastic and plastic behavior. In addition information regarding the mechanical energy can be calculated be determining the area under the stress-strain curve. Mechanical energy can then be compared to results from surface energy analyses of the asphalt materials to determine fracture energy. The pull-off tensile force exceeds thermodynamic energy by several orders of magnitude and a small change in measured surface energy is hypothesized to correspond to a large change in pull-off tensile strength. Pull-off values should be compared to and combined with measured surface-energy values in order to determine the effective fracture energy at that asphalt-aggregate interface.

Significant effort should be focused on two areas in further development of the modified pull-off test method: evaluation of different load rates and controlling temperature and determining influence of temperature on bond strength of asphalt materials. In this study, only one (i.e. static) load rate was used to assess bond strength of asphalt materials. Thus, the effect of load rate on bond strength of asphalt materials was not determined. It should be noted that *POTS* results will change when using different load rates. In reality an asphalt mixture is subjected to dynamic loading as a result of external effects such as traffic. By considering multiple load rates, the effect of dynamic loading may be determined. In addition, when combined with moisture conditioning, the effects of absorbed moisture on the bond strength of binder and mastic may be determined at high and low load rates. As shown in this dissertation, in some instances, moisture increases the tensile strength of asphalt binder adhered to aggregate substrate indicating moisture is beneficial to fracture sensitivity. The effect of load rate may provide insight developing criteria for when moisture may be beneficial versus detrimental.

Proper control of the conditions in which the pull-off test method is conducted is crucial. Effort should be made to control the curing temperature of specimens. In addition, the effects of different conditioning and testing temperatures on the pull-off tensile strength should be evaluated. The use of different temperatures may correlate to temperatures that an actual asphalt mixture experiences during mixing, construction, and over the life of a pavement. The use of a range of conditioning temperatures may provide further indication in distinguishing adhesive and cohesive failure.

Reliability Analysis

In Chapter V, a damage parameter was developed due to moisture at the mastic-aggregate interface. Subsequently, this parameter was used in Chapter VI as a performance criterion in the development of a limit-state equation and to perform a reliability analysis. The development of additional limit-state equations, $g(X)$, for each failure mode based on moisture and mechanical damage parameters developed as part of RoAM is suggested. The distribution of the random variables should be determined. Limit states may then be combined for a system-level reliability analysis. The probability of damage due to multiple failure modes may then be quantified.

APPENDIX A

MODIFIED BINDER AND MASTIC STUDY DATA

Table A 1. Means and Coefficients of Variation for Neat Modified Binders

Binder Type	Soak Time (hours)	No. of Specimens	Mean *POTS*	CV (%)
Airblown	0	4	336.25	0.7435
	4	4	114.75	8.2482
	8	4	107.25	5.8662
	24	4	76.25	6.2782
PG64-28	0	9	267.89	5.582
	4	4	140.25	5.7448
	8	4	126	8.5724
	24	4	96	7.3657
EVA	0	4	169.5	2.9499
	4	6	117.67	8.3557
	8	4	108.5	2.6606
	24	3	85.67	6.4291
EVA-g	0	4	165.75	5.7103
	4	6	111.83	4.3958
	8	4	89.75	2.7855
	24	4	86	0
Elvaloy	0	5	206	2.7674
	4	6	111.83	3.3656
	8	6	101	7.0011
	24	6	95.17	6.9833
ESI	0	13	209.54	3.1392
	4	3	104.33	7.3204
	8	3	76.67	3.7653
	24	5	67	8.5088
PG54-28	0	6	115.17	3.2682
	4	5	46.94	5.951
	8	6	50	0
	24	6	49.15	4.2361
PG70-28	0	4	351.5	2.5286
	4	4	97.25	2.5707
	8	4	99.75	10.334
	24	4	85.75	5.2478
SBS-l	0	5	228	2.193
	4	5	72	3.8036
	8	4	63.75	7.5092
	24	4	51.25	4.878
SBS	0	4	243.25	4.6313
	4	4	109.75	2.2779
	8	4	89.75	2.7855
	24	6	60	5.2705
SBS-rg	0	4	251.25	2.7262
	4	4	114.75	8.2482
	8	5	85.6	6.4305
	24	4	66.25	18.868

Table A 2. Means and Coefficients of Variation for Modified Bitumen- Aggregate Filler Combinations

Binder Type	Soak Time (hours)	6 % RA			31 % RA		
		Number of Specimens Tested	Mean *POTS* (psi)	CV (%)	Number of Specimens Tested	Mean *POTS* (psi)	CV (%)
Airblown	0	4	240.75	2.85	4	236.75	1.06
	4	4	61.25	18.1	4	102.25	29.67
	8	4	71.5	36.98	4	72.75	23.42
	24	4	65.25	37.76	4	69	23.7
PG64-28	0	6	211.33	2.44	6	198	1.6
	4	6	84.67	15.28	6	87.33	9.04
	8	6	89.17	6.16	6	82.17	10.54
	24	6	68.33	10	6	75	4.22
EVA-g	0	4	155.75	4.04	6	125.17	3.01
	4	4	122.25	12.66	6	106	2.98
	8	5	110	3.8	6	98.5	9.5
	24	4	92	11.61	6	73.33	8.26
Elvaloy	0	4	221.75	3.85	4	195.5	1.48
	4	4	117.25	8.07	4	133.75	5.12
	8	4	103.5	2.79	4	127.25	1.96
	24	4	103.5	2.79	4	121	3.37
PG54-28	0	6	99.33	5.2	6	98.5	4.25
	4	6	42.81	5.36	6	50	0
	8	6	42.97	8.93	6	50.83	4.02
	24	6	37.7	8.75	6	43.5	4.97
PG70-28	0	4	312.5	1.6	4	270.25	1.77
	4	4	101	7	4	98.5	2.93
	8	4	103.5	12.78	4	112.25	9.18
	24	4	81.75	6.5	4	107.25	4.46

Table A 2. Means and Coefficients of Variation for Modified Bitumen- Aggregate Filler Combinations (continued)

Binder Type	Soak Time (hours)	6 % RD			31 % RD		
		Number of Specimens Tested	Mean *POTS* (psi)	CV (%)	Number of Specimens Tested	Mean *POTS* (psi)	CV (%)
Airblown	0	4	251.3	5.44	6	239.33	6.7
	4		no data		8	93.88	26.56
	8	4	80.5	7.89	8	86.75	30.31
	24	4	69	16.78	8	81.13	27.28
PG64-28	0	6	215.5	3.2	6	198	1.6
	4	6	84	3.69	6	78.67	10.95
	8	6	83	10.42	6	76.83	7.15
	24	6	86.5	6.24	6	72.5	10.46
EVA-g	0	7	148.9	9.59	6	128.5	3.26
	4	12	85.17	8.54	5	97	6.72
	8	10	86.8	6.93	5	94	6.06
	24	10	75.7	11.42	5	82.2	5.98
Elvaloy	0	5	226	3.36	6	206.33	2.93
	4	5	108	10.66	4	157	2.6
	8	4	103.5	11.5	4	122.25	6.13
	24	5	89	3.08	5	111	10.07
PG54-28	0	6	104.3	4.95	6	79.5	6.79
	4	6	44.2	3.87	6	46.6	5.65
	8	6	44.9	0	6	50	0
	24	6	40.41	8.08	6	44.35	7.77
PG70-28	0	4	313.75	1.53	4	238.5	5.36
	4	4	122.25	3.92	4	106	3.85
	8	4	97.25	11.4	4	107.25	5.87
	24		no data		4	89.75	2.79

Table A 2. Means and Coefficients of Variation for Modified Bitumen- Aggregate Filler Combinations (continued)

Binder Type	Soak Time (hours)	6 % Diabase			31 % Diabase		
		Number of Specimens Tested	Mean *POTS* (psi)	CV (%)	Number of Specimens Tested	Mean *POTS* (psi)	CV (%)
Airblown	0	5	247.6	2.84	4	203	3.48
	4	5	95.8	14.58	4	126.25	8.92
	8	4	97.25	2.57	4	121	10.67
	24	4	68.75	18.18	4	88.25	10.15
PG64-28	0	5	261	3.21	5	198	3.09
	4	6	146	4.22	6	105.17	3.58
	8	5	139.6	4.43	5	93.8	12.69
	24	6	83.83	5.46	5	85.8	4.54
EVA-g	0	4	183.75	6.7	4	119.75	2.09
	4	6	120.33	9.93	4	107.25	4.46
	8	4	118.5	5.45	4	93.5	6.9
	24	6	107.67	3.79	4	72.5	3.98
Elvaloy	0	8	161.5	12.37	8	147.25	8.46
	4						
	8		no data			no data	
	24						
PG54-28	0	6	111	0	6	101.83	5.74
	4	6	48.3	5.45	6	51.67	5
	8	6	46.89	12.27	6	50	0
	24	6	35.69	6.89	6	47.45	5.89
PG70-28	0	4	315	0	4	307.5	0.94
	4	4	83	4.17	4	111	14.24
	8	4	81.5	3.68	4	119.75	8.61
	24	4	88.25	7.76	4	97.25	7.71

Table A 3. Coefficients of Variation (CV) and Average CVs for Modified Bitumen- Aggregate Filler Combinations

Binder	Filler Type	Filler Amount	Soak Time (hours) 0	4	8	24	Average CV (%)	Average CV (%) - 6%	Average CV (%) - 31%
PG54-28 (B6224)	RA	6%	5.20	5.36	8.93	8.75	7.06	5.81	4.17
		31%	4.25	0.00	4.02	4.97	3.31		
	RD	6%	4.95	3.87	0.00	8.08	4.23		
		31%	6.79	5.65	0.00	7.77	5.05		
	Diabase	6%	0.00	5.45	12.27	6.89	6.15		
		31%	5.74	5.00	0.00	5.89	4.16		
	Average CV (%)		4.49	4.22	4.20	7.06			
PG64-28 (B6225)	RA	6%	2.44	15.28	6.16	10.00	8.47	6.23	6.62
		31%	1.60	9.04	10.54	4.22	6.35		
	RD	6%	3.20	3.69	10.42	6.24	5.89		
		31%	1.60	10.95	7.15	10.46	7.54		
	Diabase	6%	3.21	4.22	4.43	5.46	4.33		
		31%	3.09	3.58	12.69	4.54	5.98		
	Average CV (%)		2.52	7.79	8.57	6.82			
PG70-28 (B6226)	RA	6%	1.60	7.00	12.78	6.50	6.97	5.50	5.64
		31%	1.77	2.93	9.18	4.46	4.59		
	RD	6%	1.53	3.92	11.40	n/a*	5.62		
		31%	5.36	3.85	5.87	2.79	4.47		
	Diabase	6%	0.00	4.17	3.68	7.76	3.90		
		31%	0.94	14.24	8.61	7.71	7.88		
	Average CV (%)		1.87	6.02	8.59	5.84			
Airblown (B6227)	RA	6%	2.85	18.10	36.98	37.76	23.92	14.50	16.83
		31%	1.06	29.67	23.42	23.70	19.46		
	RD	6%	5.44	n/a	7.89	16.78	10.04		
		31%	6.70	26.56	30.31	27.28	22.71		
	Diabase	6%	2.84	14.58	2.57	18.18	9.54		
		31%	3.48	8.92	10.67	10.15	8.31		
	Average CV (%)		3.73	19.57	18.64	22.31			
Elvaloy (B6228)	RA	6%	3.85	8.07	2.79	2.79	4.38	7.97	5.63
		31%	1.48	5.12	1.96	3.37	2.98		
	RD	6%	3.36	10.66	11.50	3.08	7.15		
		31%	2.93	2.60	6.13	10.07	5.43		
	Diabase	6%	12.37	n/a	n/a	n/a	12.37		
		31%	8.46	n/a	n/a	n/a	8.46		
	Average CV (%)		5.41	6.61	5.60	4.83			
EVA-g (B6233)	RA	6%	4.04	12.66	3.80	11.61	8.03	7.87	5.27
		31%	3.01	2.98	9.50	8.26	5.94		
	RD	6%	9.59	8.54	6.93	11.42	9.12		
		31%	3.26	6.72	6.06	5.98	5.51		
	Diabase	6%	6.70	9.93	5.45	3.79	6.47		
		31%	2.09	4.46	6.90	3.98	4.36		
	Average CV (%)		4.78	7.55	6.44	7.51			
Overall Average CV (%)			**3.80**	**8.42**	**8.85**	**9.41**		**7.79**	**7.31**

*n/a - indicates that no data is available

Table A 4. Results for Addition of RD Filler for Each Soak Time

Aggregate RD - 4 hours							
	p- values						ANOVA
Binder Type	Neat - 6 %	Significantly Different?	Neat - 31 %	Significantly Different?	6 % - 31 %	Significantly Different?	Prob > F
PG54-28 6224	0.0803	no	0.8183	no	0.1052	no	0.1446
PG64-28 6225	0	yes	0	yes	0.2019	no	<0.0001
PG70-28 6226	0	yes	0.0114	yes	0.0002	yes	<0.0001
Airblown 6227			0.1438	no			0.1438
Elvaloy 6228	0.4069	no	0	yes	0	yes	<0.0001
EVA-g 6233	0	yes	0.0014	yes	0.0031	yes	<0.0001
All Binders Combined	**0.0214**	**yes**	**0.1501**	**no**	**0.3601**	**no**	**0.0679**

Aggregate RD - 8 hours							
	p -values						ANOVA
Binder Type	Neat - 6 %	Significantly Different?	Neat - 31 %	Significantly Different?	6 % - 31 %	Significantly Different?	Prob > F
PG54-28 6224	0	yes	1	no	0	yes	<0.0001
PG64-28 6225	0	yes	0	yes	0.2155	no	<0.0001
PG70-28 6226	0.7174	no	0.2915	no	0.1693	no	0.3426
Airblown 6227	0.0779	no	0.1142	no	0.6143	no	0.1631
Elvaloy 6228	0.6669	no	0.0032	yes	0.0115	yes	0.008
EVA-g 6233	0.3734	no	0.2617	no	0.0281	yes	0.0823
All Binders Combined	**0.0595**	**no**	**0.2823**	**no**	**0.3946**	**no**	**0.1676**

Table A 4. Results for Addition of RD Filler for Each Soak Time (continued)

Aggregate RD - 24 hours							
	p -values						ANOVA
Binder Type	Neat - 6 %	Significantly Different?	Neat - 31 %	Significantly Different?	6 % - 31 %	Significantly Different?	Prob > F
PG54-28 6224	0.0001	yes	0.0141	yes	0.0372	yes	0.0006
PG64-28 6225	0.0467	yes	0.0001	yes	0.0031	yes	0.0003
PG70-28 6226			0.1712	no			0.1712
Airblown 6227	0.564	no	0.6534	no	0.2736	no	0.5348
Elvaloy 6228	0.2032	no	0.0044	yes	0.0005	yes	0.0015
EVA-g 6233	0.0231	yes	0.4258	no	0.1062	no	0.0498
All Binders Combined	**0.1403**	**no**	**0.7882**	**no**	**0.202**	**no**	**0.2766**

Table A 5. Results for Addition of RA Filler for Each Soak Time

Aggregate RA - 4 hours							
	p-values						ANOVA
Binder Type	Neat - 6 %	Significantly Different?	Neat - 31 %	Significantly Different?	6 % - 31 %	Significantly Different?	Prob > F
PG54-28 6224	0.0046	yes	0.0258	yes	0	yes	0.0001
PG64-28 6225	0	yes	0	yes	0.6571	no	<0.0001
PG70-28 6226	0.2825	no	0.4656	no	0.712	no	0.532
Airblown 6227	0.0037	yes	0.3867	no	0.0154	yes	0.0091
Elvaloy 6228	0.2303	no	0.0003	yes	0.0047	yes	0.0011
EVA-g 6233	0.073	no	0.2436	no	0.0094	yes	0.0301
All Binders Combined	**0.0213**	**yes**	**0.2083**	**no**	**0.2702**	**no**	**0.069**

Table A 5. Results for Addition of RA Filler for Each Soak Time (continued)

Aggregate RA - 8 hours							
	p -values						ANOVA
Binder Type	Neat - 6 %	Significantly Different?	Neat - 31 %	Significantly Different?	6 % - 31 %	Significantly Different?	Prob > F
PG54-28 6224	0.0002	yes	0.5736	no	0	yes	0.0001
PG64-28 6225	0	yes	0	yes	0.1634	no	<0.0001
PG70-28 6226	0.6519	no	0.1543	no	0.3045	no	0.3526
Airblown 6227	0.0232	yes	0.0272	yes	0.926	no	0.0381
Elvaloy 6228	0.4693	no	0	yes	0	yes	<0.0001
EVA-g 6233	0.0007	yes	0.0632	no	0.0141	yes	0.0022
All Binders Combined	**0.255**	**no**	**0.4904**	**no**	**0.6417**	**no**	**0.5173**

Aggregate RA - 24 hours							
	p -values						ANOVA
Binder Type	Neat - 6 %	Significantly Different?	Neat - 31 %	Significantly Different?	6 % - 31 %	Significantly Different?	Prob > F
PG54-28 6224	0	yes	0.0017	yes	0.0014	yes	<0.0001
PG64-28 6225	0	yes	0	yes	0.0668	no	<0.0001
PG70-28 6226	0.2761	no	0.0001	yes	0	yes	<0.0001
Airblown 6227	0.3918	yes	0.5678	yes	0.7661	yes	0.6704
Elvaloy 6228	0.0301	yes	0	yes	0.0006	yes	<0.0001
EVA-g 6233	0.2451	no	0.0161	yes	0.0015	yes	0.0039
All Binders Combined	**0.1771**	**no**	**0.7347**	**no**	**0.2993**	**no**	**0.3686**

Table A 6. Results for Addition of Diabase Filler for Each Soak Time

Aggregate Diabase - 4 hours							
	p-values						ANOVA
Binder Type	Neat - 6 %	Significantly Different?	Neat - 31 %	Significantly Different?	6 % - 31 %	Significantly Different?	Prob > F
PG54-28 6224	0.4131	no	0.0109	yes	0.0459	yes	0.0274
PG64-28 6225	0.1563	no	0	yes	0	yes	<0.0001
PG70-28	0.0619	no	0.0699	no	0.0023	yes	0.0077
Airblown 6227	0.0398	yes	0.2037	no	0.0035	yes	0.0103
Elvaloy 6228							
EVA-g 6233	0.1008	no	0.4096	no	0.0302	yes	0.0719
All Binders Combined	**0.7229**	**no**	**0.4688**	**no**	**0.7074**	**no**	**0.7678**

Aggregate Diabase - 8 hours							
	p-values						ANOVA
Binder Type	Neat - 6 %	Significantly Different?	Neat - 31 %	Significantly Different?	6 % - 31 %	Significantly Different?	Prob > F
PG54-28 6224	0.1253	yes	1	yes	0.1253	yes	0.2062
PG64-28 6225	0.0644	no	0.0005	yes	0	yes	<0.0001
PG70-28	0.0149	yes	0.0094	yes	0.0001	yes	0.0005
Airblown 6227	0.1272	no	0.0462	yes	0.0032	yes	0.01
Elvaloy 6228							
EVA-g 6233	0	yes	0.3572	no	0.0001	yes	<0.0001
All Binders Combined	**0.857**	**no**	**0.8887**	**no**	**0.76**	**no**	**0.9538**

Aggregate Diabase - 24 hours							
	p-values						ANOVA
Binder Type	Neat - 6 %	Significantly Different?	Neat - 31 %	Significantly Different?	6 % - 31 %	Significantly Different?	Prob > F
PG54-28 6224	0	yes	0.2502	no	0	yes	<0.0001
PG64-28 6225	0.0032	yes	0.0118	yes	0.5384	no	0.0085
PG70-28 6226	0.5949	no	0.0319	yes	0.0785	no	0.0727
Airblown 6227	0.2835	no	0.1013	no	0.0158	yes	0.0447
Elvaloy 6228							
EVA-g 6233	0	yes	0	yes	0	yes	<0.0001
All Binders Combined	**0.5586**	**no**	**0.4986**	**no**	**0.913**	**no**	**0.758**

Table A 7. Results for Four Hours Soak Time for Each Aggregate Pair

4 hours in water bath							
6% Filler							
	***p* -values**						**ANOVA**
Binder Type	RA - RD	Significantly Different?	RA - Diabase	Significantly Different?	RD - Diabase	Significantly Different?	Prob > F
PG54-28 6224	0.2984	no	0.0007	yes	0.0065	yes	0.002
PG64-28 6225	0.8933	no	0	yes	0	yes	<0.0001
PG70-28 6226	0.0003	yes	0.001	yes	0	yes	<0.0001
Airblown 6227			0.0051	yes			0.0051
Elvaloy 6228	0.2377	no					0.2377
EVA-g 6233	0	yes	0.7761	no	0	yes	<0.0001
All Binders Combined	**0.924**	**no**	**0.0683**	**no**	**0.0716**	**no**	**0.1167**
31% Filler							
	***p* -values**						**ANOVA**
Binder Type	RA - RD	Significantly Different?	RA - Diabase	Significantly Different?	RD - Diabase	Significantly Different?	Prob > F
PG54-28 6224	0.0144	yes	0.1953	no	0.0009	yes	0.0029
PG64-28 6225	0.0513	no	0.0006	yes	0	yes	<0.0001
PG70-28 6226	0.2967	no	0.0979	no	0.479	no	0.2318
Airblown 6227	0.5786	no	0.1809	no	0.0463	yes	0.126
Elvaloy 6228	0.0011	yes					0.0011
EVA-g 6233	0.0105	yes	0.6999	no	0.0089	yes	0.0133
All Binders Combined	**0.8804**	**no**	**0.6877**	**no**	**0.5813**	**no**	**0.8531**

Table A 8. Results for Eight Hours Soak Time for Each Aggregate Pair

8 hours in water bath							
6% Filler							
	***p* -values**						**ANOVA**
Binder Type	RA - RD	Significantly Different?	RA - Diabase	Significantly Different?	RD - Diabase	Significantly Different?	Prob > F
PG54-28 6224	0.4124	no	0.1088	no	0.4023	no	0.2648
PG64-28 6225	0.1471	no	0	yes	0	yes	<0.0001
PG70-28 6226	0.4049	no	0.0132	yes	0.0551	no	0.0342
Airblown 6227	0.4403	no	0.0462	yes	0.1672	no	0.117
Elvaloy 6228	1	no					1
EVA-g 6233	0	yes	0.0411	yes	0	yes	<0.0001
All Binders Combined	**0.6063**	**no**	**0.2079**	**no**	**0.076**	**no**	**0.1973**
31% Filler							
	***p* -values**						**ANOVA**
Binder Type	RA - RD	Significantly Different?	RA - Diabase	Significantly Different?	RD - Diabase	Significantly Different?	Prob > F
PG54-28 6224	0.2396	no	0.2396	no	1	no	0.3911
PG64-28 6225	0.3134	no	0.0473	yes	0.0068	yes	0.0208
PG70-28 6226	0.4602	no	0.277	no	0.0859	no	0.2072
Airblown 6227	0.3146	no	0.0081	yes	0.0238	yes	0.0207
Elvaloy 6228	0.2528	no					0.2528
EVA-g 6233	0.3473	no	0.328	no	0.9235	no	0.5156
All Binders Combined	**0.7939**	**no**	**0.628**	**no**	**0.4616**	**no**	**0.7594**

Table A 9. Results for Twenty-Four Hours Soak Time for Each Aggregate Pair

24 hours in water bath							
6% Filler							
	***p*-values**						**ANOVA**
Binder Type	RA - RD	Significantly Different?	RA - Diabase	Significantly Different?	RD - Diabase	Significantly Different?	Prob > F
PG54-28 6224	0.143	no	0.2695	no	0.0167	yes	0.0511
PG64-28 6225	0	yes	0.0003	yes	0.4287	no	0.0001
PG70-28 6226			0.1844	no			0.1844
Airblown 6227	0.7661	no	0.7812	no	0.9841	no	0.9433
Elvaloy 6228	0.0001	yes					0.0001
EVA-g 6233	0.0032	yes	0.0077	yes	0	yes	<0.0001
All Binders Combined	**0.9222**	**no**	**0.4353**	**no**	**0.4816**	**no**	**0.6945**
31% Filler							
	***p*-values**						**ANOVA**
Binder Type	RA - RD	Significantly Different?	RA - Diabase	Significantly Different?	RD - Diabase	Significantly Different?	Prob > F
PG54-28 6224	0.6129	no	0.0299	yes	0.0793	no	0.0701
PG64-28 6225	0.4305	no	0.0048	yes	0.001	yes	0.0027
PG70-28 6226	0.0012	yes	0.0265	yes	0.0781	no	0.004
Airblown 6227	0.3051	no	0.1659	no	0.5413	no	0.3578
Elvaloy 6228	0.1365	no					0.1365
EVA-g 6233	0.0132	yes	0.8023	no	0.0142	yes	0.0193
All Binders Combined	**0.9075**	**no**	**0.7455**	**no**	**0.6594**	**no**	**0.9037**

Table A 10. Results for All Soak Times Combined for Each Aggregate Pair

All Times Combined							
6% Filler							
	***p*-values**						**ANOVA**
Binder Type	RA - RD	Significantly Different?	RA - Diabase	Significantly Different?	RD - Diabase	Significantly Different?	Prob > F
PG54-28 6224	0.2189	no	0.1328	no	0.7785	no	0.2758
PG64-28 6225	0.547	no	0	yes	0	yes	<0.0001
PG70-28 6226	0.0111	yes	0.025	yes	0	yes	0.0002
Airblown 6227	0.2688	no	0.0031	yes	0.0952	no	0.0111
Elvaloy 6228	0.0661	no					0.0661
EVA-g 6233	0	yes	0.0926	no	0	yes	<0.0001
All Binders Combined	**0.8819**	**no**	**0.0259**	**yes**	**0.0146**	**yes**	**0.0287**
31% Filler							
	***p*-values**						**ANOVA**
Binder Type	RA - RD	Significantly Different?	RA - Diabase	Significantly Different?	RD - Diabase	Significantly Different?	Prob > F
PG54-28 6224	0.3099	no	0.1534	no	0.0167	yes	0.054
PG64-28 6225	0.0694	no	0	yes	0	yes	<0.0001
PG70-28 6226	0.275	no	0.4645	no	0.0733	no	0.1922
Airblown 6227	0.4803	no	0.0027	yes	0.0049	yes	0.0049
Elvaloy 6228	0.8469	no					0.8469
EVA-g 6233	0.7484	no	0.7659	no	0.9975	no	0.9342
All Binders Combined	**0.8374**	**no**	**0.6904**	**no**	**0.5496**	**no**	**0.8339**

Table A 11. Means and Coefficients of Variation for Aged Modified Binders – Dry Condition

Binder Type	PAV 30 hours N	PAV 30 hours Mean *POTS* (psi)	PAV 30 hours CV (%)	PAV 40 hours N	PAV 40 hours Mean *POTS* (psi)	PAV 40 hours CV (%)
Airblown	4	406.3	1.1	4	370.8	10.0
PG64-28	4	433.3	1.1	4	402.5	4.7
EVA	4	280.3	1.7	3	340.3	10.0
EVA-g	4	280.3	4.7	3	295.7	1.0
Elvaloy	5	306.8	4.4	3	326.7	6.2
ESI	4	309.5	9.4	4	270.0	9.4
PG54-28	4	335.0	1.2	3	306.3	2.1
PG70-28	4	417.8	9.5	3	418.7	1.8
SBS-l	5	358.4	2.9	4	287.0	8.3
SBS	4	320.0	3.8	4	340.0	2.1
SBS-rg	4	373.5	2.8	4	320.0	3.8

Table A 12. Means and Coefficients of Variation for PAV 40 Aged Modified Binders – Moisture Conditioned

Binder Type	Soak Time (hours)	N	PAV 40 hours Mean *POTS* (psi)	CV (%)
PG64-28	4	1	70	n/a
	8	1	55	n/a
	24	2	57.5	18.0
Elvaloy	4	4	145.5	19.0
	8	4	104.75	25.0
	24	3	152	5.7
PG54-28	4	3	73.67	15.0
	8	4	58.75	15.0
	24	4	58.75	8.1
PG70-28	4	3	70	7.1
	8	1	86	n/a
	24	1	86	n/a
SBS-l	4	4	55	31.0
	8	3	55	9.1
	24	3	61.67	23.0
SBS-lg	4	1	75	n/a
	8	3	60	17.0
	24	2	60	24.0

Table A 13. Dynamic Shear Rheometer Data for Binders

Binder Name	Binder Code	19°C			25°C		
		|G*| (Pa)	|G*|/sinδ (Pa)	|G*|sinδ (Pa)	|G*| (Pa)	|G*|/sinδ (Pa)	|G*|sinδ (Pa)
PG54-28	6224	378043	393435	363254	133550	137148	130045
PG64-28	6225	2201767	2467359	1964763	723427	775623	674743
PG70-28	6226	3935733	4656898	3326248	1311300	1445966	1189175
Airblown	6227	1822900	2236475	1485804	678683	784555	587098
Elvaloy	6228	1087733	1232468	959995	398230	440705	359848
SBS-lg	6229	1269533	1470641	1095927	453657	507533	405499
SBS-l	6230	1522900	1767266	1312323	543547	607596	486249
SBS-rg	6231	1731033	1997037	1500461	580493	644549	522804
EVA	6232	510460	597378	436189	208550	245352	177268
EVA-g	6233	1299033	1580616	1067614	516957	612807	436099
ESI	6243	527603	637010	436987	215797	267691	173963
SBS-lg	6295	1156800	1323572	1011041	375497	418015	337303
Control	6298	3925067	4803391	3207348	1286767	1445886	1145158

Table A 14. Results of Dynamic Shear Rheometer Tests on Aged Binders (measured at grade temperature)

Binder Name	Binder Code	PAV 30 $\|G^*\|/\sin\delta$ (Pa)	PAV 40 $\|G^*\|/\sin\delta$ (Pa)
PG54-28	6224	21811	23811
PG64-28	6225	14823	21788
PG70-28	6226	14746	18962
Airblown	6227	13950	23432
Elvaloy	6228	11374	12758
SBS-lg	6229	11051	12172
SBS-l	6230	11214	14231
SBS-rg	6231	10598	13382
EVA	6232	5421	7493
EVA-g	6233	5161	8473
ESI	6243	5175	8054

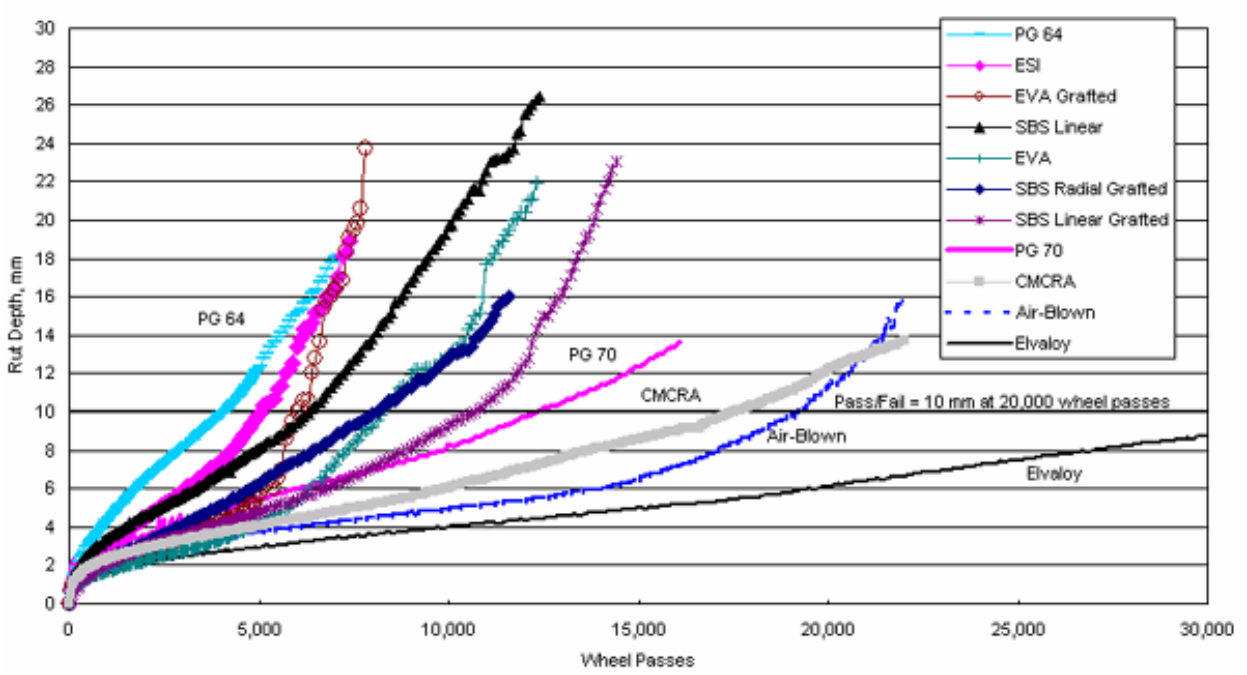

Figure A 1. Rut Depth versus Wheel Passes from the Hamburg Wheel Tracking Device at 58° C (Stuart, et al. 2002)

Table A 15. Results of Dynamic Shear Rheometer Tests for Mastics

Mastic	Binder Code	19°C			25°C		
		|G*|	**|G*|/sinδ**	**|G*|sinδ**	**|G*|**	**|G*|/sinδ**	**|G*|sinδ**
PG52-28	6224	3088100	3370794	2829114	1040067	1101144	982377
PG64-28	6225	11493667	14105873	9365203	3916467	4460882	3438493
PG70-28	6226	18478667	22889165	14918024	6317300	7169788	5566173
Airblown	6227	9847300	12357785	7846820	3627567	4253419	3093803
Elvaloy	6228	5218167	6092421	4469367	1860500	2086630	1658876
SBS-l	6230	5823567	6920035	4900832	2058833	2334211	1815943
EVA	6232	7174033	8825225	5831778	2672667	3133506	2279603
EVA-g	6233	5826067	7094557	4784380	2196033	2567502	1878309

APPENDIX B

THE USE OF THE PNEUMATIC ADHESION TEST TO EVALUATE BOND STRENGTH BETWEEN ASPHALT AND AGGREGATE

Table B 1. Diabase Plate Dimensions

Sample ID	Length (mm)	Average Length (mm)	Width (mm)	Average Width (mm)	Height (mm)	Avgerage Height (mm)	Average Volume (cm^3)	M_{dry} (g)
1-1	57.17	57.16	56.54	56.38	10.37	10.32	33.24	100.005
	57.18		56.20		10.31			
	57.12		56.41		10.18			
	57.16		56.37		10.40			
1-2	57.05	56.99	55.80	56.07	10.79	10.78	34.44	103.5002
	56.91		56.30		11.24			
	56.99		56.13		10.63			
	57.02		56.06		10.45			
1-3	57.00	57.01	56.37	56.14	11.08	11.05	35.36	106.695
	57.04		56.02		11.10			
	56.97		56.18		11.02			
	57.04		55.98		10.99			
1-4	57.35	57.34	56.39	56.50	9.86	9.95	32.24	96.6292
	57.33		56.69		10.18			
	57.25		56.52		10.06			
	57.43		56.39		9.71			
1-5	57.57	57.57	56.94	56.78	8.45	8.71	28.45	84.5084
	57.55		56.63		8.48			
	57.55		56.67		8.82			
	57.59		56.87		9.07			
1-6	57.74	57.66	57.02	56.92	6.90	7.33	24.06	69.8201
	57.57		56.69		6.82			
	57.69		57.16		7.43			
	57.62		56.81		8.18			
2-1	57.57	57.35	52.30	52.33	11.30	11.28	33.83	99.7096
	57.25		52.40		10.99			
	57.39		52.28		11.15			
	57.17		52.34		11.66			
2-2	57.42	57.39	52.40	52.41	9.55	9.61	28.89	84.8486
	57.54		52.53		9.73			
	57.16		52.38		9.62			
	57.43		52.34		9.52			
2-3	57.32	57.43	52.73	52.57	10.33	10.37	31.29	91.6851
	57.64		52.49		10.36			
	57.25		52.56		10.47			
	57.49		52.50		10.30			
2-4	57.47	57.58	52.62	52.65	9.79	9.81	29.74	86.7227
	57.79		52.69		9.83			
	57.66		52.70		9.83			
	57.40		52.57		9.79			
2-5	57.53	57.68	52.85	52.75	9.90	9.86	29.98	87.779
	57.86		52.71		9.85			
	57.81		52.68		9.82			
	57.50		52.76		9.85			

Table B 1. Diabase Plate Dimensions (continued)

Sample ID	Length (mm)	Average Length (mm)	Width (mm)	Average Width (mm)	Height (mm)	Avgerage Height (mm)	Average Volume (cm^3)	M_{dry} (g)
2-6	57.79	57.86	52.80	52.84	12.78	12.82	39.19	116.1833
	58.04		52.92		12.68			
	57.88		52.81		12.81			
	57.71		52.82		13.01			
3-1	54.45	54.45	52.56	52.72	10.84	10.79	30.98	90.3073
	54.65		53.18		10.73			
	54.58		52.84		10.75			
	54.10		52.31		10.85			
3-2	54.23	54.27	52.09	52.38	10.08	9.96	28.31	82.9597
	54.45		52.86		9.91			
	54.37		52.57		9.87			
	54.04		52.01		9.97			
3-3	54.23	54.16	52.74	52.19	10.14	10.21	28.86	85.5951
	54.18		51.86		10.20			
	54.18		51.81		10.33			
	54.06		52.34		10.17			
3-4	54.53	54.38	53.05	52.59	10.26	10.31	29.47	85.7106
	54.39		52.32		10.21			
	54.13		52.26		10.35			
	54.46		52.72		10.40			
3-5	54.03	54.04	52.48	52.03	11.00	11.43	32.12	93.2788
	54.09		51.73		11.47			
	54.06		51.60		11.74			
	53.96		52.29		11.50			
4-1	56.80	56.53	55.50	55.47	9.81	9.70	30.42	89.5677
	56.38		55.35		9.96			
	56.29		55.48		9.57			
	56.65		55.54		9.47			
4-2	56.54	56.63	55.58	55.67	9.97	9.98	31.46	93.2327
	56.78		55.71		9.91			
	56.47		55.72		9.96			
	56.71		55.66		10.08			
4-3	56.72	56.63	56.09	56.09	12.19	12.05	38.26	113.1528
	56.60		55.98		12.00			
	56.51		56.08		11.95			
	56.70		56.20		12.04			
5-1	55.95	55.80	55.00	55.08	13.21	13.39	41.14	121.0564
	55.67		55.28		13.68			
	55.66		54.86		13.48			
	55.90		55.16		13.18			
5-2	56.13	56.05	55.33	55.13	10.75	10.88	33.62	99.2675
	55.97		54.96		10.77			
	55.97		55.31		10.99			
	56.12		54.90		11.01			

Table B 1. Diabase Plate Dimensions (continued)

Sample ID	Length (mm)	Average Length (mm)	Width (mm)	Average Width (mm)	Height (mm)	Average Height (mm)	Average Volume (cm^3)	M_{dry} (g)
5-3	56.18	55.98	55.26	55.06	10.62	10.47	32.27	95.2542
	55.81		54.91		10.52			
	55.85		55.20		10.36			
	56.09		54.85		10.38			
6-1	57.47	57.51	56.76	56.61	9.96	10.28	33.47	100.2838
	57.40		56.45		10.04			
	57.73		56.49		10.90			
	57.45		56.72		10.22			
8-1	55.28	54.75	51.22	51.39	10.41	10.30	28.98	85.5062
	54.31		51.53		10.35			
	54.68		51.37		10.19			
	54.71		51.43		10.25			
8-2	54.40	54.71	50.55	50.89	11.25	11.26	31.34	92.5374
	54.95		51.30		11.32			
	54.74		50.96		11.23			
	54.76		50.74		11.22			
10-1	56.47	56.74	57.12	56.74	10.87	11.09	35.70	104.62
	57.10		56.52		10.72			
	56.74		56.50		11.26			
	56.64		56.80		11.51			
10-2	56.55	56.70	56.25	56.40	11.27	10.95	35.02	101.2895
	57.04		56.75		11.23			
	56.82		56.46		10.91			
	56.39		56.13		10.39			
10-3	57.04	56.65	56.44	56.59	10.00	9.75	31.24	92.8918
	56.38		56.87		9.73			
	56.41		56.68		9.62			
	56.75		56.37		9.63			
10-4	56.55	56.75	56.84	57.30	12.20	11.94	38.83	113.6829
	57.11		57.69		11.89			
	56.79		57.38		11.79			
	56.53		57.27		11.89			
11-1	56.51	56.85	59.91	59.73	9.94	10.42	35.38	103.4353
	57.56		59.45		10.94			
	56.92		59.70		10.87			
	56.42		59.85		9.93			
11-2	55.58	56.01	58.04	58.40	10.30	10.23	33.44	98.4824
	56.40		58.90		10.37			
	56.15		58.58		10.26			
	55.90		58.06		9.97			
11-3	58.21	57.72	56.95	56.65	11.66	11.84	38.71	114.8228
	57.62		56.36		11.84			
	57.58		56.49		12.12			
	57.47		56.80		11.74			

Table B 1. Diabase Plate Dimensions (continued)

Sample ID	Length (mm)	Average Length (mm)	Width (mm)	Average Width (mm)	Height (mm)	Avgerage Height (mm)	Average Volume (cm^3)	M_{dry} (g)
11-4	57.29	56.98	56.56	56.84	9.55	9.42	30.50	91.2574
	56.68		57.27		9.33			
	56.5		57.04		9.32			
	57.45		56.47		9.47			
11-5	56.22	56.64	56.23	56.08	10.02	10.24	32.52	97.0731
	56.74		56.01		10.87			
	56.64		55.96		10.3			
	56.95		56.12		9.76			
11-6	56.1	56.59	56.99	57.28	9.16	9.31	30.19	89.3138
	57.09		57.53		9.23			
	56.76		57.48		9.59			
	56.4		57.13		9.27			
12-1	56.99	56.47	57.8	57.45	8.9	8.90	28.87	86.2507
	56.17		57.3		8.88			
	56.01		56.95		8.92			
	56.72		57.73		8.9			
12-2	58.14	57.85	56.65	56.43	10.01	10.15	33.14	97.8067
	57.6		55.89		10.16			
	57.74		56.65		10.38			
	57.91		56.54		10.06			
12-3	56.52	56.07	57.86	58.20	9.85	9.98	32.57	96.0968
	55.76		58.51		10.02			
	55.76		58.53		10.17			
	56.22		57.88		9.89			
12-4	56.26	56.17	56.81	56.63	11.03	11.14	35.44	106.7042
	56.03		56.44		10.89			
	56.06		56.48		11.03			
	56.34		56.79		11.62			
12-5	56.47	56.28	57.01	56.87	9.13	9.18	29.39	88.081
	56.11		56.67		9.24			
	56.24		56.83		9.25			
	56.28		56.98		9.11			
12-6	56.85	57.20	57.38	56.93	9.71	9.79	31.89	95.3544
	57.52		56.69		9.94			
	57.43		56.48		9.84			
	57		57.15		9.68			
12-7	56.45	56.37	56.69	56.95	9.49	9.30	29.84	88.9768
	56.15		57.2		9.08			
	56.32		57.03		9.15			
	56.54		56.86		9.47			

Table B 1. Diabase Plate Dimensions (continued)

Sample ID	Length (mm)	Average Length (mm)	Width (mm)	Average Width (mm)	Height (mm)	Avgerage Height (mm)	Average Volume (cm^3)	M_{dry} (g)
13-1	56.49	56.47	56.45	56.42	10.78	10.77	34.31	102.8915
	56.31		56.27		10.8			
	56.36		56.4		10.74			
	56.7		56.54		10.76			
13-2	55.71	55.85	56.82	56.62	7.72	7.76	24.53	72.0548
	55.93		56.59		7.47			
	55.9		56.61		7.59			
	55.87		56.44		8.25			
13-3	56.27	56.35	56.24	56.15	7.59	8.11	25.65	77.845
	56.5		55.95		7.61			
	56.36		56.22		8.39			
	56.26		56.17		8.84			
13-4	57.24	56.97	56.43	56.28	10.95	11.29	36.18	
	56.77		56.15		11.92			
	56.9		56.18		11.43			
	56.98		56.35		10.84			

Table B 2. Limestone Square Plate Dimensions

Sample ID	Length (mm)	Average Length (mm)	Width (mm)	Average Width (mm)	Height (mm)	Average Height (mm)	Average Volume (cm3)
LS-10	56.75	57.09	55.26	55.35	6.93	6.60	20.86
	57.39		55.29		6.31		
	57.30		55.28		6.36		
LS-11	56.91	57.22	55.58	55.33	6.81	7.17	22.68
	57.40		55.22		7.49		
	56.99		55.38		7.13		
	57.06		55.31		6.98		
LS-12	57.43	57.14	55.41	55.41	7.06	6.38	20.20
	57.19		55.26		6.30		
	56.96		55.47		6.51		
	57.04		55.45		6.42		
LS-13	57.35	57.29	55.46	55.33	6.29	7.02	22.26
	57.31		55.40		6.94		
	56.99		55.22		6.96		
	57.27		55.40		7.10		
LS-14	57.58	55.47	55.31	56.85	7.09	7.37	23.24
	55.63		57.09		7.36		
	55.38		56.70		7.36		
	55.34		56.77		7.37		
LS-15	55.52	56.74	56.82	55.58	7.39	7.60	23.96
	56.93		55.45		7.71		
	56.55		55.59		7.57		
	56.61		55.65		7.56		
	56.86		55.61		7.56		

Table B 3. Results of SEM/EDX Analyses

Aggregate	Element	Wt (%)	At (%)
Diabase	O	20.30	34.12
	Na	2.17	2.54
	Mg	2.62	2.90
	Al	12.13	12.09
	Si	33.58	32.15
	Ca	10.14	6.80
	Ti	2.80	1.57
	Fe	16.26	7.83
	Total	100.0	100.0
Limestone	C	9.39	19.73
	O	23.22	36.60
	Mg	0.00	0.00
	Al	1.30	1.21
	Si	3.14	2.82
	K	1.57	1.01
	Ca	61.37	38.62
	Total	100.00	100.00
Sandstone	C	3.62	8.08
	O	20.78	34.84
	Al	1.26	1.25
	Si	22.13	21.13
	K	1.02	0.70
	Ca	49.81	33.33
	Fe	1.39	0.67
	Total	100.00	100.00

Table B 4. *POTS* Results of Binders on Various Substrates

Binder	Substrate	*N*	Mean *POTS* (psi)	Standard Deviation (psi)
AAD	Glass	4	116	15.17
	Diabase	4	154	11.90
	Sandstone	4	137	4.08
	Limestone	4	123	5.32
AAK	Glass	4	210	16.90
	Diabase	4	214	11.09
	Sandstone	4	161	8.54
	Limestone	4	157	20.00
AAM	Glass	8	248	21.95
	Diabase	4	277	13.23
	Sandstone	4	226	12.39
	Limestone	4	223	15.81
PG70-22 (B6298)	Glass	3	411	48.17
	Diabase	4	343	14.43
	Sandstone	4	245	21.46
	Limestone	4	233	10.75

Table B 5. Analysis of Variance Results for Binders on Glass, Diabase, Sandstone and Limestone Substrates

AAD

Summary of Fit

Rsquare	0.73
Adj Rsquare	0.67
Root Mean Square Error	10.21
Mean of Response	132.63
Observations (or Sum Wgts)	16

Analysis of Variance

Source	DF	Sum of Squares	Mean Square	F Ratio	Prob > F
Substrate	3	3453.2500	1151.08	11.0460	0.0009
Error	12	1250.5000	104.21		
C. Total	15	4703.7500			

AAK

Summary of Fit

Rsquare	0.81
Adj Rsquare	0.76
Root Mean Square Error	14.85
Mean of Response	185.44
Observations (or Sum Wgts)	16

Analysis of Variance

Source	DF	Sum of Squares	Mean Square	F Ratio	Prob > F
Substrate	3	11252.688	3750.90	17.0157	0.0001
Error	12	2645.250	220.44		
C. Total	15	13897.938			

AAM

Summary of Fit

Rsquare	0.59
Adj Rsquare	0.51
Root Mean Square Error	17.87
Mean of Response	244.5
Observations (or Sum Wgts)	20

Analysis of Variance

Source	DF	Sum of Squares	Mean Square	F Ratio	Prob > F
Substrate	3	7397.375	2465.79	7.7212	0.0021
Error	16	5109.625	319.35		
C. Total	19	12507.000			

PG70-22 (B6298)

Summary of Fit

Rsquare	0.91
Adj Rsquare	0.89
Root Mean Square Error	25.22
Mean of Response	300.93
Observations (or Sum Wgts)	15

Analysis of Variance

Source	DF	Sum of Squares	Mean Square	F Ratio	Prob > F
Substrate	3	74722.267	24907.4	39.1701	<.0001
Error	11	6994.667	635.9		
C. Total	14	81716.933			

Table B 6. *POTS* Results of Binders on Diabase Substrate

Binder	Cure Time (hours)	*N*	Mean (psi)	Standard Deviation (psi)
AAD	0	4	155	11.90
	8	4	111	12.25
	24	4	122	10.50
	48	4	137	8.17
	72	4	129	13.05
	96	4	144	26.44
	120	4	152	14.72
	144	4	148	31.42
	168	4	137	7.07
	336	3	210	10.41
AAM	0	4	277	13.23
	8	4	229	4.50
	24	4	276	14.31
	48	4	258	61.44
	72	4	268	20.61
	96	4	280	7.55
	120	4	298	18.48
	144	4	296	4.79
	168	4	232	12.31
	336	3	315	8.66

Table B 7. ANOVA Results for Binders on Diabase Substrate for Various Cure Times

AAD

Summary of Fit

Rsquare	0.73
Adj Rsquare	0.64
Root Mean Square Error	16.60
Mean of Response	142.69
Observations (or Sum Wgts)	39

Analysis of Variance

Source	Degrees of Freedom	Sum of Squares	Mean Square	F Ratio	Prob > F
Dry Time at 25o C	9	21230.141	2358.90	8.5594	<.0001
Error	29	7992.167	275.59		
C. Total	38	29222.308			

AAM

Summary of Fit

Rsquare	0.62
Adj Rsquare	0.50
Root Mean Square Error	23.24
Mean of Response	271.67
Observations (or Sum Wgts)	39

Analysis of Variance

Source	Degrees of Freedom	Sum of Squares	Mean Square	F Ratio	Prob > F
Dry Time at 25o C	9	25529.167	2836.57	5.2497	0.0003
Error	29	15669.500	540.33		
C. Total	38	41198.667			

Table B 8. *POTS* Results for Binders on Diabase Substrate for Various Soak Times

Binder	Substrate	Submerged 25° C (hours)	POTS (psi)	Mean POTS (psi)	Std. Dev. (psi)	CV (%)	Failure location
AAD	Diabase	0	167	155	11.90	7.70	b
AAD	Diabase	0	142				b
AAD	Diabase	0	162				b
AAD	Diabase	0	147				b
AAD	Diabase	24	50	56	12.76	22.62	b
AAD	Diabase	24	50				b
AAD	Diabase	24	76				b
AAD	Diabase	24	50				b
AAD	Diabase	48	45	48	2.95	6.10	b
AAD	Diabase	48	50				b
AAD†	Diabase	48	40				c/z
AAD	Diabase	48	50				b
AAD	Diabase	72	45	52	8	15	b
AAD	Diabase	72	50				b
AAD	Diabase	72	60				b
AAM	Diabase	0	264	277	13.23	4.78	b
AAM	Diabase	0	279				b
AAM	Diabase	0	269				b
AAM	Diabase	0	294				b
AAM	Diabase	16	188	167	28.86	17.25	b
AAM†	Diabase	16	116				b/c
AAM	Diabase	16	147				b
AAM†	Diabase	16	127				b/c
AAM†	Diabase	24	86	183	n/a	n/a	b/c
AAM†	Diabase	24	132				b/c
AAM	Diabase	24	183				b
AAM†	Diabase	24	152				b/b/c
AAM	Diabase	48	132	99	36.20	36.44	b
AAM	Diabase	48	106				b
AAM	Diabase	48	60				b
AAM†	Diabase	48	96				c/z
AAM	Diabase	72	111	143	26.47	18.50	b
AAM	Diabase	72	167				b
AAM	Diabase	72	132				b
AAM	Diabase	72	162				b
AAM	Diabase	99	76	133	43.96	33.08	b
AAM	Diabase	99	121				b
AAM	Diabase	99	167				b
AAM	Diabase	99	167				b

† Sample discarded

Table B 9. Results for AAD on Diabase – Aggregate Soak

Binder	Substrate	Soak Time, 25° C (hours)	POTS (psi)	Mean POTS (psi)	Std. Dev. (psi)	CV (%)	Failure location
AAD	Diabase	8	157	135	26.21	19.42	b
AAD	Diabase	8	142				b
AAD	Diabase	8	106				b
AAD†	Diabase	8	60				b and b/c
AAD	Diabase	16	111	105	6.42	6.12	b
AAD	Diabase	16	106				b
AAD	Diabase	16	96				b
AAD	Diabase	16	106				b
AAD	Diabase	24	157	136	15.17	11.14	b
AAD	Diabase	24	136				b
AAD	Diabase	24	121				b
AAD	Diabase	24	131				b
AAD	Diabase	48	152	156	8.54	5.48	b
AAD	Diabase	48	157				b
AAD	Diabase	48	147				b
AAD	Diabase	48	167				b
AAD	Diabase	72	127	135	10.52	7.76	b
AAD	Diabase	72	147				b
AAD	Diabase	72	127				b
AAD	Diabase	72	142				b
AAD	Diabase	96	127	133	7.65	5.76	b
AAD	Diabase	96	142				b
AAD	Diabase	96	137				b
AAD	Diabase	96	127				b
AAD	Diabase	120	101	125	16.33	13.04	b
AAD	Diabase	120	137				b
AAD	Diabase	120	132				b
AAD	Diabase	120	132				b
AAD	Diabase	144	101	121	15.02	12.37	b
AAD	Diabase	144	127				b
AAD	Diabase	144	121				b
AAD	Diabase	144	137				b
AAD†	Diabase	168	<50	160	7.64	4.76	b
AAD	Diabase	168	162				b
AAD	Diabase	168	152				b
AAD	Diabase	168	167				b
AAD	Diabase	336	106	119	18.86	15.87	b
AAD	Diabase	336	127				b
AAD	Diabase	336	101				b
AAD	Diabase	336	142				b

† Sample discarded

Table B 10. Results for AAM on Diabase – Aggregate Soak

Binder	Substrate	Soak Time, 25° C (hours)	POTS (psi)	Mean POTS (psi)	Std. Dev. (psi)	CV (%)	Failure location
AAM	Diabase	8	233	247	13.11	5.31	b
AAM	Diabase	8	259				b
AAM	Diabase	8	249				b
AAM†	Diabase	8	80				b
AAM	Diabase	16	178	231	47.59	20.59	b
AAM	Diabase	16	213				b
AAM	Diabase	16	290				b
AAM	Diabase	16	244				b
AAM	Diabase	24	223	227	35.78	15.78	b
AAM	Diabase	24	269				b
AAM	Diabase	24	182				b
AAM	Diabase	24	233				b
AAM	Diabase	24	178	218	32.00	14.65	b
AAM	Diabase	24	244				b
AAM	Diabase	24	244				b
AAM	Diabase	24	208				b
AAM	Diabase	48	279	282	8.66	3.08	b
AAM	Diabase	48	279				b
AAM	Diabase	48	294				b
AAM	Diabase	48	274				b
AAM	Diabase	72	218	248	22.19	8.96	b
AAM	Diabase	72	244				b
AAM	Diabase	72	259				b
AAM	Diabase	72	269				b
AAM	Diabase	96	183	207	32.10	15.52	b
AAM	Diabase	96	244				b
AAM	Diabase	96	223				b
AAM	Diabase	96	178				b
AAM	Diabase	120	208	215	15.24	7.10	b
AAM	Diabase	120	218				b
AAM	Diabase	120	234				b
AAM	Diabase	120	198				b
AAM†	Diabase	144	157	237	33.97	14.33	y
AAM	Diabase	144	229				b
AAM	Diabase	144	208				b & a/b
AAM	Diabase	144	274				b
AAM	Diabase	168	264	255	28.99	11.35	b
AAM	Diabase	168	223				b
AAM	Diabase	168	279				b
AAM†	Diabase	168	203				b/c
AAM	Diabase	336	285	288	10.62	3.69	b
AAM†	Diabase	336	269				b & b/c
AAM	Diabase	336	280				b & a/b
AAM	Diabase	336	300				b

† Sample discarded

APPENDIX C

TEST METHOD FOR PULL-OFF STRENGTH OF BITUMINOUS MATERIALS USING PORTABLE ADHESION TESTERS

Test Method for Pull-off Strength of Bituminous Materials Using Portable Adhesion Testers[‡]

Prepared by: Audrey Copeland, Turner Fairbank Highway Research Center
6300 Georgetown Pike
McLean, VA 22101

Last update: June 7, 2007

1. Scope

This test method covers a procedure for evaluating the pull-off strength (commonly referred to as adhesion) of a bituminous material by determining the greatest perpendicular force (in tension) that a surface area can bear before a plug of material is detached. Failure occurs along the weakest plane within the system comprised of the test fixture, adhesive, porous disc, bituminous specimen, and substrate, and is exposed by the fracture surface. Pull-off strength measurements depend upon both material and instrumental parameters. Results for same bituminous specimens on different substrates or exposed to different conditions may not be comparable.

This test method uses an apparatus known as a portable pull-off adhesion tester. It is capable of applying a concentric load and counter load to a single surface so that bituminous specimens can be tested even though only one side is accessible. Measurements are limited by the strength of adhesion bonds between the loading fixture and the specimen surface or the cohesive strengths of the adhesive, bituminous specimen layers, and substrate.

The values stated in inch-pound units are the standard.

2. Referenced Documents

2.1 ASTM Standards:

D4541 Standard Test Method for Pull-off Strength of Coatings Using Portable Adhesion Testers

D2651 Guide for Preparation of Metal Surfaces for Adhesive Bonding

3. Apparatus

3.1 *Adhesion Tester*, commercially available self-aligning tester with a self-contained pressure source and a measuring system that controls a choice of different load range detaching assemblies or comparable apparatus. It is shown in Figure C 1(a)[1].

3.1.1 *Loading fixture*, a flat cylindrical base that is 0.5 in (12.5 mm) in diameter on one end with ground down, sandblasted cut faces to allow for attachment of a porous disc. The other end of the fixture has 3/8-16 UNC threads (e.g. Hex Grade 5 zinc plated steel cap screws).

3.1.2 A *pressurized gas* (i.e. Nitrogen) that enters the detaching assembly through a flexible hose connected to a pressurization rate controller and a pressure gage (or electronic sensor).

[‡] *NOTE: This test method is based on ASTM D 4541-95 Standard Test Method for Pull-off Strength of Coatings Using Portable Adhesion Testers*

3.2 *Detaching assembly* (adhesion tester), which includes the base, annular ring, and piston grip (Figure C 1(b)). The detaching assemblies are available in six standard ranges in multiples of two from 0 to 500 psi (3.5 MPa) to 10,000 psi (70 MPa). The base is uniformly pressed against the substrate and is aligned so that the resultant force is normal to the surface. Included in the base is an annular bearing ring (or gasket) that will move the piston grip away from the base in a smooth and continuous

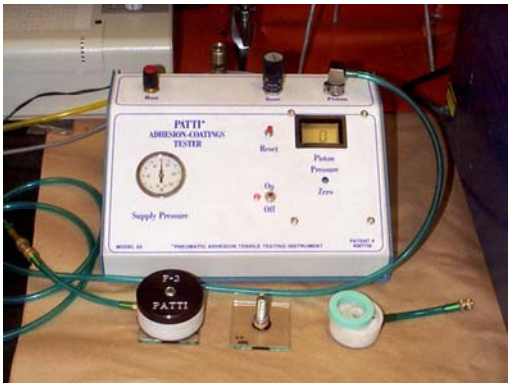

(a)

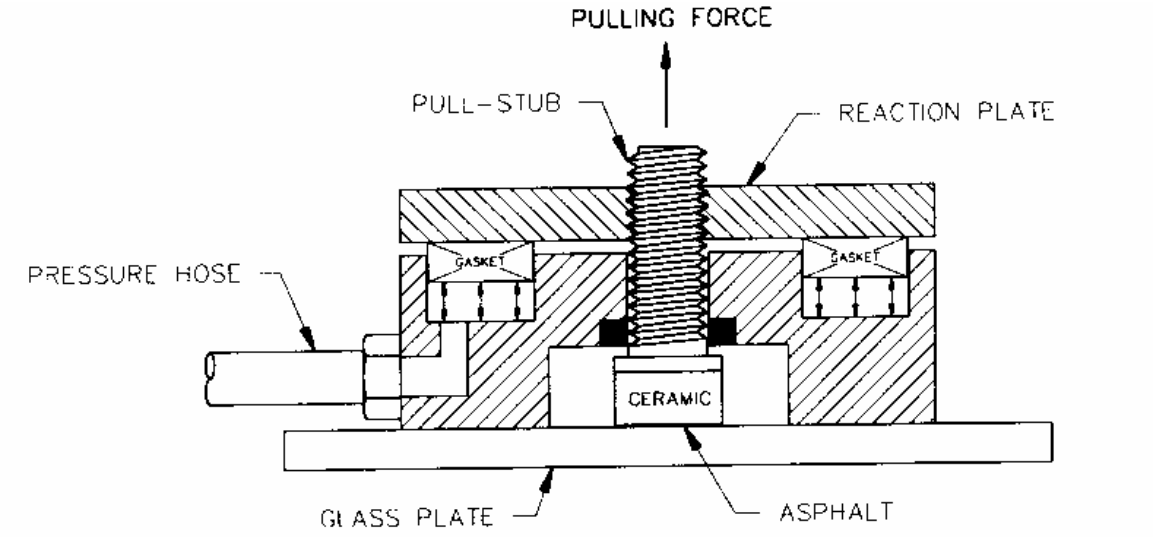

(b)

Figure C 1. Photograph (a) of self-alignment adhesion tester and (b) schematic of piston.

manner so that a torsion free, co-axial force results between them. A piston grip is a central threaded grip for engaging the loading fixture through the center of the detaching assembly that is forced away by the interaction of a self-aligning seal.

3.2.1 *Timer* or a means of limiting rate of stress to less than 150 psi/s (1 MPa/s) so that the maximum stress is obtained in less than about 100 s.

3.2.2 *Force indicator and calibration information,* for determining the actual force delivered to the loading fixture. An example is a strip chart recorder.

3.3 *Solvent,* or other means for cleaning the loading fixture surface.

3.4 *Porous discs,* or other means to provide a uniform means for water to reach the asphalt specimen. An example is ceramic disks (12.7 mm diameter) made of cordierite ($Mg_2Al_4Si_5O_{18}$).

3.5 *Adhesive,* for securing the ceramic frit to the fixture. Two component epoxies have been found to be most suitable.

3.6 *Substrate,* that serves as an adherend for bonding of binder (adhesive).

3.7 *Glass beads,* 200 μm in diameter to control the film thickness.

3.8 *Water bath,* that is temperature controlled.

4. Test Preparation

4.1 The method for selecting the substrate to be prepared for testing depends upon the objectives of the test. The following requirements apply to all substrates:

4.1.1 The selected substrate must be a flat surface large enough to accommodate the loading fixture. The surface may have any orientation with reference to gravitational pull. If one substrate is used for multiple tests, each test site must be separated by at least the distance needed to accommodate the detaching apparatus. The size of a test site is that of the secured loading fixture. At least three replications are required to characterize one sample.

4.1.2 The selected substrate must also have enough perpendicular and radial clearance to accommodate the apparatus, be flat enough to permit alignment, and be rigid enough to support the counter force. Measurements close to an edge may not be representative of the substrate as a whole.

4.1.3 Knowledge of the substrate thickness and composition should be reported for subsequent analysis and laboratory comparisons.

4.1.4 The substrate should be clean, dry, and free of debris and heated to 60^{o} C to make the pull-off specimen.

4.2 The method for adhering the porous disc to the loading fixture follows:

4.2.1 Clean the loading fixture surfaces in accordance with appropriate ASTM (e.g. D 2651 and D 3933) standard practice for preparing metal surfaces for adhesive bonding.

4.2.2 Prepare the adhesive in accordance with the adhesive manufacturer's recommendations. Apply adhesive to the fixture and one surface of the porous disc. Be certain to apply a thin layer of the adhesive across the entire surface to minimize excess adhesive. Position disc on the loading fixture.

4.2.3 Based on adhesive manufacturer's recommendations and environmental conditions, allow enough time for adhesive to set up and reach the recommended cure. Once the adhesive has cured, place the loading fixture with disc attached in an oven at 60^{o} C until it is used to make the pull-off specimen.

4.3 Prepare the bituminous specimen based on the following procedure:

4.3.1 Heat the bitumen to a temperature that facilitates pouring (e.g. 165^{o} C for thirty minutes) or producers recommended temperature and weigh out a sample of ten grams or less depending on the number of specimens that will be made. Record the weight.

4.3.2 Add glass beads in the amount of one percent by weight of the bitumen and mix thoroughly.

4.4 Prepare the pull-off test specimens accordingly:

4.4.1 Heat the bituminous-glass beads mixture to a workable condition (approximately 100° C). The mixture should be viscous enough to be applied to the disc but stiff enough to resist flowing.

4.4.2 Apply a small amount of the mixture to the entire surface of disc attached to the loading fixture. Position fixture on the substrate and press firmly with uniform pressure for approximately five seconds.

4.5 Allow the pull-off test specimen to cure for at least twenty-four hours at ambient conditions and longer in some cases depending on bituminous mixture's properties.

4.6 Note the approximate temperature and relative humidity during the time of curing.

5. Test Procedure

5.1 The general procedure for conducting pull-off tests is described in this section.

5.2 Select an adhesion-tester with a detaching assembly having a force calibration spanning the range of expected values along with its compatible loading fixture. Mid-range measurements are usually the best, but read the manufacturer's operating instructions before proceeding.

5.3 Position the annular detaching assembly over the fixture attached to the specimen and substrate to be tested. Carefully engage the loading fixture via the central threaded grip (piston) without bumping, bending or otherwise prestressing the sample. Leave at least 1/16-in. (1.6-mm) clearance between the detaching assembly and the bottom of the threaded grip so that the seal can protrude enough to align itself when pressurized.

5.4 Connect the detaching assembly to its control mechanism if necessary. Open the rate valve ¼ turn.

5.5 Align the device according to the manufacturer's instructions and zero the pressure measuring system.

5.6 Press the run button to control the gas flow to the detaching assembly and make final adjustment of rate valve so that rate of stress does not exceed 150 psi/s (1 MPa/s) yet reaches its maximum within 100 s. The rate on the PATTI device should be set at 6.

5.7 Record the maximum pressure attained (*BP*) and the specific detaching assembly. The *POTS* in psi for each specimen is determined as follows:

$$POTS = \frac{(BP * A_g) - C}{A_{ps}} \tag{2}$$

where A_g = contact area of the gasket with the reaction plate (sq in)
C = piston constant (lbs.)
A_{ps} = area of the pull-stub (sq in)
BP = burst pressure (psig).

Conversion to stress for ½-in. (12.7 mm) stud can be found in a table supplied for each detaching assembly.

5.8 If a plug of material is detached, qualify the failed surface in accordance with 6.2.

5.9 Report any departures from the procedure such as possible misalignment, hesitations in force application, etc.

6. Calculation and Interpretation of Results

6.1 Convert the maximum pressure attained to stress in psi using the tables supplied by the manufacturer for each detaching assembly.

6.2 For all tests to failure, estimate the percent of adhesive and cohesive failures in accordance to their respective areas and location within the test system comprised of coating and adhesive layers.

6.2.1 Describe the substrate as A, the bituminous specimen as B, the porous disc as C, the adhesive as Y, and the fixture as Z.

6.2.2 Designate cohesive failures by the layers within which they occur as A, B, C, etc., and the percent of each.

6.2.3 Designate adhesive failures by the interfaces at which they occur as A/B, B/C, C/Y, etc., and the percent of each.

6.3 A result that is very different from most of the results may be caused by a mistake in recording or calculating. If either of these is not the cause, then examine the experimental circumstances surrounding this run. In an irregular result can be attributed to an experimental cause, drop this result from the analysis. Do not discard a result unless there are valid nonstatistical reasons for doing so or unless the result is a statistical outlier. Valid nonstatistical reasons for dropping results include alignment of the apparatus that is not normal to the surface, poor definition of the area stressed due to improper application of the adhesive, poorly defined boundaries, holidays in the adhesive caused by voids or inclusions, improperly prepared surfaces, and sliding or twisting the fixture during the initial cure.

7. Report

7.1 Report the following information:

7.1.1. Brief description of the general nature of the test, such as, field or laboratory testing.

7.1.2. Temperature and relative humidity and any other environmental conditions during the cure and test period.

7.1.3. Description of the apparatus used, including: apparatus manufacturer and model number, loading fixture type and dimensions, and bearing ring type and dimensions.

7.1.4. Description of the test system, if possible, by the indexing scheme outlined above including: product identity and generic type for each specimen and any other information supplied, the substrate identity (thickness, type, geometry, etc.), porous disc and adhesive used.

7.1.5. Test results.

7.1.5.1 Date, test location, testing agent.

7.1.5.2 For test to failure, report all values computed along with the nature and location of the failures as specified above, or, if only the average strength is required, report the average strength along with the statistics.

8. Precision and Bias

8.1. Precision:

8.1.1. The within laboratory single operator standard deviation for dry pull-off tensile strength of binders on glass plates has been found to be 0.073 percent. Therefore, results of two properly conducted tests by the same operator in the same laboratory on the same type of binder sample should not differ by more than X.XX from each other.

8.1.2. The between laboratory standard deviation has not been determined.

8.2. Bias:

8.2.1. The bias of pull-off tests on bituminous material has not been determined.

[1] PATTI self-alignment adhesion tester is from SEMicro Corp., 15817 Crabbs Branch Way, Rockville, MD 20855.

REFERENCES

AASHTO. "Standard Practice for Accelerated Aging of Asphalt Binder Using a Pressurized Aging Vessel (PAV) Designation R 28." In: *Standard Specifications for Transportation Materials and Methods of Sampling and Testing, Part 1B: Specifications*. American Association of State Highway and Transportation Officials: 2002.

Anatomy of a Road. Website, http://www.mnh.si.edu/earth/text/3_1_1_1.html, Accessed on: March 8, 2007.

Ang, A.H-S., and Amin, M. *Studies of Probabilistic Safety Analysis of Structures and Structural Systems*. Structural Research Series No. 320, University of Illinois, Urbana, 1967.

ASCE. Infrastructure Report Card. Website, http://www.asce.org/reportcard/2005/page.cfm?id=30, Accessed on: March 9, 2005.

Aschenbrener, T. "Evaluation of Hamburg Wheel-Tracking Device to Predict Moisture Damage in Hot-Mix Asphalt." *Transportation Research Record*. 1492:193-201, 1995.

ASTM. "Standard Test Method for Pull-off Strength of Coatings Using Portable Adhesion Tester, Designation: D 4541-95." In: *Annual Book of ASTM Standards*. 06.01. Philadelphia, PA: American Society for Testing and Materials: 1995.

ASTM. "Designation D 8 - Standard Terminology Relating to Materials for Roads and Pavements." *American Society of Testing Materials*. 1997.

Bahia, H.U., D.I. Hanson, M. Zeng, et al. *Characterization of Modified Asphalt Binders in Superpave Mix Design*. National Cooperative Highway Research Program (NCHRP) 459. Transportation Research Board, Washington, D.C.: 2001.

Bhasin, A. and D.N. Little. "Characterization of aggregate surface energy using the universal sorption device." *Journal of Materials in Civil Engineering (ASCE)*. 2006.

Bhasin, A., D.N. Little, K.L. Vasconcelos and E. Masad. "Use of Surface Free Energy to Identify Moisture Sensitivity of Materials for Asphalt Mixes." 86th Annual Meeting of the Transportation Research Board, Washington, D.C., Transportation Research Board, 2007.

Bhasin, A., E. Masad, D.N. Little and R. Lytton. "Limits of Adhesive Bond Energy for Improved Resistance of Hot-Mix Asphalt to Moisture Damage." *Transportation*

Research Record: Journal of the Transportation Research Board. 1970:3-13, 2006.

Birgisson, B., R. Roque and G.C. Page. "Evaluation of Water Damage Using Hot-Mix Asphalt Fracture Mechanics." *Asphalt Paving Technology*. 72:424-462, 2003.

Birgisson, B., R. Roque and G.C. Page. "Performance-Based Fracture Criterion for Evaluation of Moisture Susceptibility in Hot-Mix Asphalt." *Transportation Research Record*. 1891:55-61, 2004.

Bradbury, M.H., D. Lever and D. Kinsey. "Aquaous Phase Diffusion in Crystalline Rock." In: *Scientific Basis for Radioactive Waste Management V. Proceedings of the Materials Research Society Fifth International Symposium on the Scientific Basis for Nuclear Waste*. 569-578, 1982.

Breitung, K. "Asymptotic Approximations for Multinormal Integrals." *Journal of Engineering Mechanics, ASCE*. 110:3; 357-366, 1984.

Cheng, D. *Surface free energy of asphalt-aggregate system and performance analysis of asphalt concrete based on surface free energy*. PhD Dissertation, Civil Engineering, Texas A&M University, College Station, 2002.

Cheng, D., D. Little, R. Lytton and J. Holste. "Surface Free Energy Measurement of Aggregates and Its Applications on Adhesion and Moisture Damage of Asphalt-Aggregate System." Ninth Annual Symposium of the International Center for Aggregate Research, 2001.

Cheng, D., D. Little, R. Lytton and J. Holste. "Surface Energy Measurement of Asphalt and Its Application to Predicting Fatigue and Healing in Asphalt Mixtures." *Transportation Research Record: Journal of the Transportation Research Board*. 1810:44-53, 2002a.

Cheng, D., D. Little, R. Lytton and J. Holste. "Use of Surface Free Energy Properties of the Asphalt-Aggregate System to Predict Moisture Damage Potential." *Asphalt Paving Technology: Association of Asphalt Paving Technologists-Proceedings of the Technical Sessions*. 71:59-88, 2002b.

Cheng, D., D. Little, R. Lytton and J. Holste. "Moisture Damage Evaluation of Asphalt Mixtures by Considering Both Moisture Diffusion and Repeated-Load Conditions." *Transportation Research Record: Journal of the Transportation Research Board*. 1832:42-49, 2003.

Claisse, P. "Transport Properties of Concrete." *Concrete International*. 27:1; 43-48, 2005.

Copeland, A., N. Kringos, T. Scarpas, J. Youtcheff and S. Mahadevan. "Determination of Bond Strength as a Function of Moisture Content at the Aggregate-Mastic Interface." 10th International Conference on Asphalt Pavements, Quebec City, Canada, International Society of Asphalt Pavements, 2006.

Copeland, A., J. Youtcheff and A. Shenoy. "Moisture Sensitivity of Modified Asphalt Binders: Factors Influencing Bond Strength." *Transportation Research Record: Journal of the Transportation Research Board*. to be published:2007.

Cornell, C.A. "Bounds on the Reliability of Structural Systems." *Journal of the Structural Engineering, ASCE*, Vol. 93, No. ST1, pp. 171-200, 1967.

Curtis, C.W., K. Ensley and J. Epps. *Fundamental Properties of Asphalt-Aggregate Interactions Including Adhesion and Absorption*. SHRP-A-341. Strategic Highway Research Program, National Research Council, Washington, DC: 1993.

D'Angelo, J. and R.M. Anderson. "Material Production, Mix Design, and Pavement Design Effects on Moisture Damage." Moisture Sensitivity of Aspalt Pavements: A National Seminar, San Diego, CA, Transportation Research Board, 2003.

DerKiureghian, A., H.Z. Lin and S.J. Hwang. "Second-Order Reliabilty Approximations." *Journal of Engineering Mechanics*. 113:8; 1208-1225, 1987.

Ditlevsen, O. "Narrow Reliability Bounds for Structural Systems." *Journal of Structural Mechanics*, Vol. 3, 453-472, 1979.

Elphingstone, G.M. *Adhesion and Cohesion in Asphalt-Aggregate Systems*. Ph.D. Dissertation, Chemical Engineering, Texas A&M University, College Station, 1997.

Epps, J.A., P.E. Sebaaly, J. Penaranda, et al. *Compatibility of a Test for Moisture-Induced Damage with Superpave Volumetric Mix Design*. NCHRP Report 444. National Cooperative Highway Research Council, Transportation Research Board, Washington, DC: 2000.

Fiessler, B., H.J. Neumann and R. Rackwitz. "Quadratic Limit States in Structural Reliability." *Journal of Engineering Mechanics, ASCE*. 1095:4; 661-676, 1979.

Griffith, A.A. "The Phenomena of Rupture and Flow in Solids." *Philosophical Transactions of the Royal Society of London. Series A, Containing Papers of a Mathematical or Physical Character*. 221:163-98, 1921.

Haldar, A. and S. Mahadevan. *Probability, Reliability, and Statistical Methods in Engineering Design*. New York: John Wiley & Sons, Inc.: 2000.

Harbitz, A. "An Efficient Sampling Method for Probability of Failure Calculation." *Structural Safety*. 3:2; 109-115, 1986.

Harvey, J.A.F. and D. Cebon. "Failure mechanisms in viscoelastic films." *Journal of Materials Science*. 38:1021-1032, 2003.

Hefer, A.W., A. Bhasin and D.N. Little. "Bitumen Surface Energy Characterization Using a Contact Angle Approach." *Journal of Materials in Civil Engineering*. 18:6; 759-767, 2006.

Hefer, AW, DN Little, and BE Herbert. "Bitumen Surface Energy Characterization by Inverse Gas Chromotography." *Journal of Testing and Evaluation*, 35:3; 2007.

Hicks, R.G., R.B. Leahy, M. Cook, J.S. Moulthrop and J. Button. "Road Map for Mitigating National Moisture Sensitivity Concerns in Hot-Mix Pavements." Moisture Sensitivity of Asphalt Pavements: A National Seminar, San Diego, CA, 2003.

Huang, Y. *Pavement Analysis and Design*. Englewood Cliffs, NJ: Prentice-Hall, Inc.: 1993.

Ishai, I. and J. Craus. "Effect of the Filler on Aggregate-Bitumen Adhesion Properties in Bituminous Mixtures." *Asphalt Paving Technology: Association of Asphalt Paving Technologists-Proceedings of the Technical Sessions*. 46:228-258, 1977.

Jones, D. *SHRP Materials Reference Library: Asphalt Cements: A Concise Data Compilation*. National Research Council, Washington, D.C.: 1993.

Kandhal, P. "Field and Laboratory Investigation of Stripping in Asphalt Pavements: State of the Art Report." *Transportation Research Record: Journal of the Transportation Research Board*. 1454:36-47, 1994.

Kandhal, P. and I. Rickards. "Premature failure of asphalt overlays from stripping: Case histories." *Asphalt Paving Technology: Association of Asphalt Paving Technologists-Proceedings of the Technical Sessions*. 70:301-351, 2002.

Kandhal, P.S. *Moisture Susceptibility of HMA Mixes: Identification of Problem and Recommended Solutions*. NCAT Report No. 92-1. National Center for Asphalt Technology (NCAT), Auburn University, Auburn: 1992.

Kanitpong, K. and H. Bahia. "Relating Adhesion and Cohesion of Asphalts to Effect of Moisture on Laboratory Performance of Asphalt Mixtures." *Transportation Research Record: Journal of the Transportation Research Board*. 1901:33-43, 2005.

Kanitpong, K. and H.U. Bahia. "Role of Adhesion and Thin Film Tackiness of Asphalt Binders in Moisture Damage of HMA." *Asphalt Paving Technology: Association of Asphalt Paving Technologists-Proceedings of the Technical Sessions*. 72:502-528, 2003.

Karamchandani, A., P. Bjerager and A.C. Cornell. "Adaptive Importance Sampling." Proceedings, International Conference on Structural Safety and Reliability (ICOSSAR), San Francisco, CA, 1989.

Kiggundu, B.M. and F.L. Roberts. *Stripping in HMA Mixtures: State-of-the-Art and Critical Review of Test Methods*. NCAT Report No. 88-2. National Center for Asphalt Technology (NCAT), Auburn University, Auburn: 1988.

Kim, N., R. Roque and D. Hiltunen. "Effect of Moisture on Low-Temperature Asphalt Mixture Properties and Thermal-Cracking Performance of Pavements." *Transportation Research Record: Journal of the Transportation Research Board*. 1454:82-88, 1994.

Kim, Y.-R., D. Little and R. Lytton. "Effect of Moisture Damage on Material Properties and Fatique Resistance of Asphalt Mixtures." *Transportation Research Record: Journal of the Transportation Research Board*. 1891:48-54, 2004.

Kringos, N. *Modeling of Combined Physical-Mechanical Moisture Induced Damage in Asphaltic Mixes*. PhD Dissertation, Delft University of Technology, Delft, The Netherlands, 2007.

Kringos, N. and A. Scarpas. "Development of a Finite Element Tool for Simulation of Raveling of Asphalt Mixes." 12th International Conference on Computational and Experimental Engineering and Sciences, 2004.

Kringos, N. and A. Scarpas. "Raveling of Asphaltic Mixes Due to Water Damage: Computational Identification of Controlling Parameters." *Transportation Research Record: Journal of the Transportation Research Board*. 1929:79-87, 2005a.

Kringos, N. and A. Scarpas. "Simulation of Combined Mechanical-Moisture Induced Damage in Asphaltic Mixes." International Workshop on Moisture Induced Damage of Asphaltic Mixes, Delft, The Netherlands, 2005b.

Little, D. and D. Jones. "Chemical and Mechanical Processes of Moisture Damage in Hot-Mix Asphalt Pavements." Moisture Sensitivity of Asphalt Pavements: A National Seminar, San Diego, CA, Transportation Research Board, 2003.

Lottman, R.P., R.P. Chen, K.S. Kumar and L.W. Wolf. "A Laboratory Test System for Prediction of Asphalt Concrete Moisture Damage." *Transportation Research Record: Journal of the Transportation Research Board*. 515:18-26, 1974.

Mahadevan, S. and P. Shi. "Multiple Linearization Method for Nonlinear Reliability Analysis." ASCE *Journal of Engineering Mechanics*, Vol. 127, No. 11, pp. 1165-1173, 2001.

Mack, C. "Physical properties of asphalts in thin films." *Ind. Engrg. Chem.* 10:422, 1957.

Majidzadeh, K. and M. Herrin. "Modes of Failure and Strength of Asphalt Films Subjected to Tensile Stresses." *Highway Research Record*. 67:98-121, 1965.

Masad, E., C. Zollinger, R. Bulut, D.N. Little and R.L. Lytton. "Characterization of HMA Moisture Damage Using Surface Energy and Fracture Properties." *Asphalt Paving Technology: Association of Asphalt Paving Technologists-Proceedings of the Technical Sessions*. 75:2006.

McClave, J.T., P.G. Benson and T. Sincich. *Statistics for Business and Economics*. 8th ed. Upper Saddle River, NJ: Prentice-Hall, Inc.: 2001.

Melchers, R.E. "Improved Importance Sampling Methods for Structural System Reliability Calculation." Proceedings, 5th International Conference on Structural Safety and Reliabilty, ICOSSAR, 1989.

Miknis, F.P., A.T. Pauli, A. Beemer and B. Wilde. "Use of NMR imaging to measure interfacial properties of asphalts." *Fuel*. 84:1041-1051, 2005.

Miller, J.S., R.B. Rogers, G.R. Rada and W.Y. Bellinger. *Distress Identification Manual for the Long-Term Pavement Performance Project*. SHRP-P-338. Strategic Highway Research Program, Washington, DC: 1993.

NCHRP. *Guide for Mechanistic-Empirical Design of New and Rehabilitated Pavement Structures Final Report*. 1-37A. National Cooperative Highway Research Program, Transportation Research Board, National Research Council, Washington, D.C.: 2004.

Nguyen, T., E. Byrd, D. Bentz and J. Seiler. *Development of a Method for Measuring Water-Stripping Resistance of Asphalt/Siliceous Aggregate Mixtures,*. NCHRP-ID-002. National Cooperative Highway Research Program, Transportation Research Board, National Research Council, Washington, D.C.: 1-31, 1996.

Nguyen, T., W.E. Byrd, D.P. Bentz and J. James Seiler. *Development of a Technique for In Situ Measurement of Water at the Asphalt/Model Siliceous Aggregate Interface*. NISTIR 4783. National Institute of Standards and Technology, Washington, DC: 1-62, 1992.

Ogunsola, O., J. Rozario and J. Youtcheff. *Comparison of Moisture Sensitivity Results from Pull-off Test with Mixture Test Results*. Internal Report, Deliverable 4.10. Turner Fairbank Highway Research Center, McLean: 1-8, Unknown Year.

Pauli, A.T., S.C. Huang, R.E. Robertson. "Surface Energy Studies of Asphalts by AFM." *Preprints - American Chemical Society. Division of Fuel Chemistry*, Vol. 48, Iss. 1, pp. 14-18, 2003.

Perera, D.Y. "On adhesion and stress in organic coatings." *Progress in Organic Coatings*. 28:21-23, 1996.

Perera, D.Y. "Effect of pigmentation on organic coating characteristics." *Progress in Organic Coatings*. 50:247-262, 2004.

Petersen, J.C., H. Plancher, E.K. Ensley, R.L. Venable and G. Miyake. "Chemistry of Asphalt-Aggregate Interaction: Relationship with Pavement Moisture-Damage Prediction Test." *Transportation Research Record*. 843:95-104, 1982.

Rackwitz, R. and B. Fiessler. "Structural Reliability Under Combined Random Load Sequences." *Computers and Structures*. 9:5; 484-494, 1978.

Rice, J.M. "Relationship of Aggregate Characteristics to the Effect of Water on Bituminous Paving Mixtures." In: *American Society of Testing and Materials STP 240*. Philadelphia, PA: American Society for Testing and Materials: 1958.

Robertson, R., J. Branthaver, P.M. Harnsberger, et al. *Fundamental Properties of Asphalts and Modified Asphalts, Volume 1, Interpretive Report*. Federal Highway Administration, FHWA-RD-99-212, 1-496, 2001.

Robl, T., D. Milburn, G. Thomas, et al. *The Strategic Highway Research Program (SHRP) Materials Reference Library Aggregates: Chemical, Mineralogical, and Sorption Analyses*. SHRP-A/UIR-91-509. National Research Council, Washington, DC: 1991.

Scarpas, A. *CAPA-3D Finite Element System Users Manual I-III*. Delft University of Technology, Delft: 2000.

Scholz, T.V., R.L. Terrel, A. Al-Joaib and J. Bea. *Water Sensitivity: Binder Validation*. SHRP-A-402. Strategic Highway Research Program (SHRP), National Research Council, Washington, D.C.: 1994.

Seville, E. and J. Metcalfe. *Developing a hazard risk assessment framework for the New Zealand State highway network. Land Transport New Zealand Research Report* 276. Wellington, New Zealand: 80 pp., 2005.

Shenoy, A. "Determination of the Temperature for Mixing Aggregates with Polymer-Modified Asphalts." *International Journal of Pavement Engineering*. 2:1; 33-47, 2001.

Solaimanian, M., J. Harvey, M. Tahmoressi and V. Tandon. "Test Methods to Predict Moisture Sensitivity of Hot-Mix Asphalt Pavements." Moisture Sensitivity of Asphalt Pavements: A National Seminar, San Diego, CA, Transportation Research Board, 2003.

Soltesz, U., E. Baudendistel and R. Schaefer. "Stress analyses of pull-off tests for strength measurements of coatings." *International Congress on Bioceramics and the Human Body*. 504, 1992.

St. Martin, J., L.A. Cooley, Jr. and H.R. Hainin. "Production and Construction Issues for Moisture Sensitivity of Hot-Mix Asphalt Pavements." Moisture Sensitivity of Asphalt Pavements: A National Seminar, San Diego, CA, Transportation Research Board, 2003.

Stuart, K. *Moisture Damage in Asphalt Mixtures - A State-of-the-Art Report*. FHWA-RD-90-019. Federal Highway Administration, Turner-Fairbank Highway Research Center, McLean, VA: 1990.

Stuart, K.D. *Understanding the Performance of Modified Asphalt Binders in Mixtures: High Temperature Characterization*. FHWA-RD-02-075. Turner Fairbank Highway Research Center, McLean, VA: 1-41, 2002.

Stuart, K.D. and W.S. Mogawer. *Understanding the Performance of Modified Asphalt Binders in Mixtures: Permanent Deformation Using a Mixture with Diabase Aggregate*. FHWA-RD-02-042. Federal Highway Administration, Turner-Fairbank Highway Research Center, McLean, VA: 1-57, 2002.

Stuart, K.D., J. Youtcheff and W.S. Mogawer. *Understanding the Performance of Modified Asphalt Binders in Mixtures: Evaluation of Moisture Sensitivity*. FHWA-RD-02-029. Federal Highway Administration, Turner-Fairbank Highway Research Center, McLean, VA: 2002.

Stuart, K.D. and J.S. Youtcheff. *Understanding the Performance of Modified Asphalt Binders in Mixtures: Low-Temperature Properties*. FHWA-RD-02-074. Federal Highway Administration, Turner-Fairbank Highway Research Center, McLean, VA: 2002.

Terrel, R.L. and S. Al-Swailmi. "Water Sensitivity of Asphalt Paving Mixtures." Serviceability and Durability of Construction Materials: Proceedings of the First Materials Engineering Congress, August 13-15, Denver, CO, 1990.

Terrel, R.L. and S. Al-Swailmi. *Water Sensitivity of Asphalt-Aggregate Mixes: Test Selection*. Strategic Highway Research Program Report A-403. Oregon State University, Corvallis, OR: 1994.

Thelen, E. "Surface energy and adhesion properties in asphalt-aggregate systems." *Highway Research Board Bulletin*. 192:1958.

Tunnicliff, D.G. and R.E. Root. *NCHRP Report 274 - Use of Antistripping Additives in Asphaltic Concrete Mixtures: Laboratory Phase*. NCHRP Report 274. Transportation Research Board, Washington, D.C.: 1-50, 1984.

Tvedt, L. "Distribution of Quadratic Forms in Normal Space-Application to Structural Reliabilty." *Journal of Engineering Mechanics, ASCE*. 116:6; 1183-1197, 1990.

Washington, U.o. http://training.ce.washington.edu/WSDOT/Modules/09_pavement_evaluation/09-7_body.htm#transverse_cracking. Accessed on: March 9, Accessed March 9, 2005.

WRI. *Fundamental Properties of Asphalts and Modified Asphalts*. FHWA Contract No. DTFH61-99C-00022. Western Research Institute, Laramie, WY: 2004.

Wu, Y.T. "An Adaptive Importance Sampling Method for Structural System Reliability Analysis, Reliability Technology 1992." In: *ASME Winter Annual Meeting*. AD-28. Anaheim, CA: 217-231, 1992.

Youtcheff, J. and V. Aurilio. "Moisture Sensitivity of Asphalt Binders: Evaluation and Modeling of the Pneumatic Adhesion Test Results." 42nd Annual Conference of Canadian Technical Asphalt Association, Ottawa, Ontario, Polyscience Publications Inc., 1997.

Zollinger, C. *Application of Surface Energy Measurements to Evaluate Moisture Susceptibility of Asphalt and Aggregates*. Masters Thesis, Texas A&M University, College Station, 2005.

VITA

Audrey Rebecca Copeland was born in Birmingham, Alabama and grew up in Brentwood, Tennessee. She earned her Bachelor of Science (BS) in December 1999 and Master of Science (MS) in May 2001 in Civil Engineering from Tennessee Technological University. While studying for her MS, she worked as a graduate research and teaching assistant. Her research project was funded by the Tennessee Department of Transportation and her thesis is titled "Air Void Content of Compacted Bituminous Mixtures".

In August 2001, Miss Copeland continued her studies at Vanderbilt University pursuing a Doctor of Philosophy (PhD) in Civil Engineering. At Vanderbilt University, she was part of the National Science Foundation (NSF) Integrative Graduate Education and Research Traineeship (IGERT) Multidisciplinary Program for Risk and Reliability Engineering and Management. As an IGERT Fellow, she completed an internship at FedEx Express World Headquarters in Memphis, Tennessee where she developed an initial reliability analysis for express shipment air networks. She was invited to present the findings at the National Air and Space Administration's (NASA) Langley Research Center in Hampton, Virginia and briefly worked on a project funded by NASA entitled "Probabilistic Multidisciplinary Optimization Methods for the Next Generation Reusable Launch Vehicle". She also worked as a teaching assistant while at Vanderbilt University.

In fall of 2004, Miss Copeland received an Eisenhower Transportation Fellowship to develop a risk-based framework to assess moisture damage in asphalt pavements which resulted in the topic of her PhD dissertation research. Since November 2004, she

has been a Graduate Research Fellow at the Federal Highway Administration (FHWA) Turner Fairbank Highway Research Center in McLean, Virginia. She received her PhD in August 2007.